BioMed Research International

# Incidental Thoracic and Abdominal Findings in Diagnostic Imaging

Guest Editors: Arnaldo Scardapane, Giuseppe Angelelli, and Luca Macarini

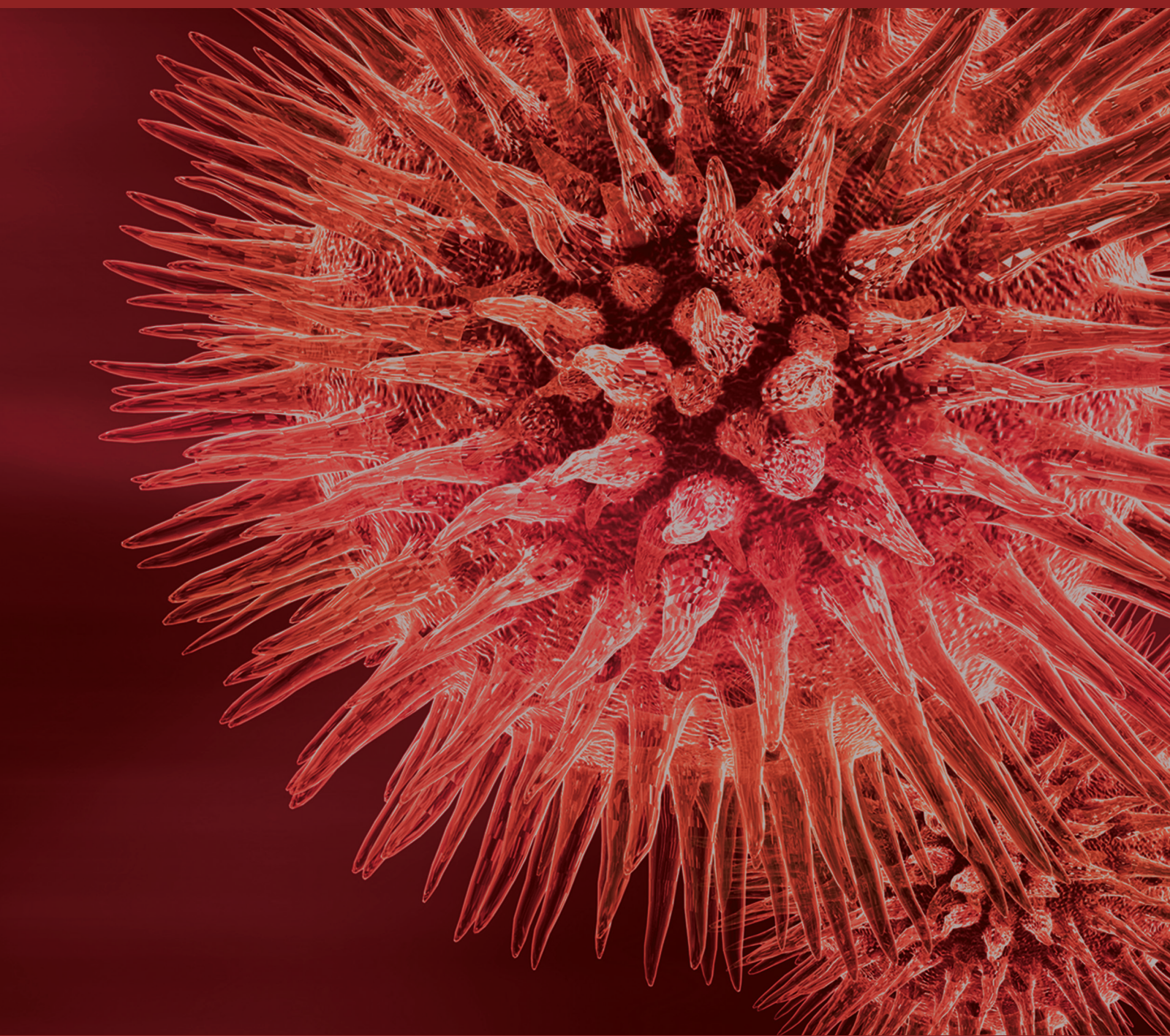

# Incidental Thoracic and Abdominal Findings in Diagnostic Imaging

BioMed Research International

# Incidental Thoracic and Abdominal Findings in Diagnostic Imaging

Guest Editors: Arnaldo Scardapane, Giuseppe Angelelli, and Luca Macarini

# Contents

Hindawi
BioMed Research International
Volume 2018, Article ID 4051606, 2 pages
https://doi.org/10.1155/2018/4051606

*Editorial*

# Incidental Thoracic and Abdominal Findings in Diagnostic Imaging

**Arnaldo Scardapane**,[1] **Giuseppe Angelelli**,[1] **and Luca Macarini**[2]

[1]*Interdisciplinary Department of Medicine, Section of Diagnostic Imaging, Bari Medical School, Bari, Italy*
[2]*Radiology Department, University of Foggia, Foggia, Italy*

Correspondence should be addressed to Arnaldo Scardapane; arnaldo.scardapane@uniba.it

Received 16 January 2018; Accepted 17 January 2018; Published 12 February 2018



In recent years the rapid diffusion of advanced imaging studies such as magnetic resonance and multidetector computed tomography has resulted in a considerable increase of asymptomatic and unexpected findings. A recent meta-analysis by Lumbreras et al. showed that incidental findings are commonly encountered in diagnostic imaging with a mean frequency of 23.6% across all imaging modalities [1]. Therefore, the radiologist has more and more frequently the task of correctly interpreting these lesions and giving comprehensive information to the patients about their clinical relevance. The ability to correctly detect likely benign findings may help reduce unnecessary imaging studies, although the lack of established follow-up guidelines for many nonunivocal interpretation results suggests that further studies are needed.

This special issue of BioMed Research International reviews the most common incidental thoracic and abdominal findings recognized by any imaging technique (X-ray, ultrasound, MDCT, MRI, and interventional radiology procedures).

The use of cross-sectional cardiac imaging for the diagnosis of cardiovascular disease is continuing to increase [2–4]. Cardiac magnetic resonance imaging (cMRI) was recently proposed as a new noninvasive imaging modality that allows higher structural and functional assessment of the heart in any desired plane without radiation. A typical cMRI exam includes several structures besides the cardiovascular system, such as parts of lungs, thorax, and upper abdomen. In this special issue, M. Gravina et al. analyse retrospectively the prevalence and the nature of incidental extracardiac findings (IEFs) in a large series of patients referred for cMRI. The incidences of IEFs as well as their clinical management are discussed in detail.

In this issue, M. A. Mazzei et al. describe the prevalence, as incidental findings, and the underreporting rate of pleural plaques (PPs) in chest CT scans. As we know, PPs represent a risk factor for mortality from lung cancer in asbestos-exposed workers and they are often underreported in absence of clinical suspicion. This study shows that knowledge of the typical appearance and location of PPs is crucial for their correct recognition and their differential diagnosis.

Incidental renal masses are frequently encountered. In fact, it has been estimated that over half of patients over the age of 50 years harbour at least one renal mass, and often several are found during one radiologic examination [5, 6]. Most of these are benign simple cysts that can be definitely diagnosed as benign on the basis of cross-sectional imaging and do not require treatment. However, complex cystic and solid renal masses are also discovered, many of which are clearly malignant and need to be surgically removed, while others may not require surgical intervention. The original research report authored by S. Mazziotti et al. provides a practical guide to identify and classify the main incidental renal findings and their correct management is well detailed.

Incidental gastrointestinal findings are commonly detected on MDCT exams performed for various medical indications. As pointed out by the comprehensive review by G. Di Grezia et al. on the radiological appearances' spectrum of several gastrointestinal acute conditions in this issue, MDCT exam plays a crucial rule since an appropriate differential diagnosis is needed. Lastly the prevalence of

incidental peritracheal cysts in association with lung fibrosis is discussed in a paper by H. Y. Kim et al.

In conclusion, the present special issue offers useful guides for the correct interpretation and management of the main incidental thoracic and abdominal findings encountered using cross-sectional imaging. Furthermore, on the basis of these considerations, these articles also emphasize the role of the radiologist as the only figure with the appropriate professional background for the interpretation of all the findings that can be unexpectedly encountered in complex and organ-tailored examinations and to provide the clinicians and patients with the right recommendations.

*Arnaldo Scardapane*
*Giuseppe Angelelli*
*Luca Macarini*

## References

[1] B. Lumbreras, L. Donat, and I. Hernandez-Aguado, "Incidental findings in imaging diagnostic tests: a systematic review," *British Journal of Radiology*, vol. 83, no. 988, pp. 276–289, 2010.

[2] J. Gaztanaga and M. J. Garcia, "New noninvasive imaging technologies in coronary artery disease," *Current Cardiology Reports*, vol. 11, no. 4, pp. 252–257, 2009.

[3] J. A. C. Lima and M. Y. Desai, "Cardiovascular magnetic resonance imaging: Current and emerging applications," *Journal of the American College of Cardiology*, vol. 44, no. 6, pp. 1164–1171, 2004.

[4] J. Vogel-Claussen, E. K. Fishman, and D. A. Bluemke, "Novel cardiovascular MRI and CT methods for evaluation of ischemic heart disease," *Expert Review of Cardiovascular Therapy*, vol. 5, no. 4, pp. 791–802, 2007.

[5] J. M. Kissane, "Congenital malformations," in *Pathology of the Kidney*, R. H. Hepinstall, Ed., pp. 69–119, Little, Brown and Company, Boston, Mass, USA, 1974.

[6] S. Tada, J. Yamagishi, H. Kobayashi, Y. Hata, and T. Kobari, "The incidence of simple renal cyst by computed tomography," *Clinical Radiology*, vol. 34, no. 4, pp. 437–439, 1983.

Hindawi
BioMed Research International
Volume 2017, Article ID 2423546, 8 pages
https://doi.org/10.1155/2017/2423546

*Research Article*

# Incidental Extracardiac Findings and Their Characterization on Cardiac MRI

**Matteo Gravina,[1] Luca Pio Stoppino,[1] Grazia Casavecchia,[2] Angelo Pio Moffa,[1] Roberta Vinci,[1] Natale Daniele Brunetti,[2] Matteo Di Biase,[2] and Luca Macarini[1]**

[1]*Radiology Department, University of Foggia, Foggia, Italy*
[2]*Cardiology Department, University of Foggia, Foggia, Italy*

Correspondence should be addressed to Matteo Gravina; matteogravina@inwind.it

Received 20 February 2017; Revised 28 July 2017; Accepted 20 August 2017; Published 3 October 2017

Academic Editor: Enzo Terreno



*Background*. Cardiac magnetic resonance imaging (cMRI) has recently emerged as a new noninvasive imaging modality that offers superior structural and functional assessment of the heart. cMRI benefits from a large field of view but, consequently, may capture incidental extracardiac findings (IEFs). We aimed to evaluate the frequency and significance of IEFs reported from clinically indicated cMRI scans. *Methods*. 742 consecutive patients (402 males and 340 females) referred to the Cardiac Magnetic Resonance Center of our University Hospital between January 2015 and December 2016 for clinically indicated cMRI were retrospectively enrolled for the evaluation of IEF prevalence and relevance. The median age of the subjects was 51 years (range: 5–85 years). *Results*. A significant number of patients who underwent cMRI had incidental and clinically significant IEFs (2% of the population, 11.4% of cases). cMRI allowed a correct diagnosis in 116/131 cases with a diagnostic accuracy value of 88.5%. *Conclusions*. IEFs on cMRI are not uncommon and lesions with mild or no clinical significance represent the most frequent findings. cMRI can characterize incidental findings with high accuracy in most cases.

## 1. Background

Cardiac magnetic resonance imaging (cMRI) has recently emerged as a new noninvasive imaging modality capable of providing high-resolution images of the heart in any desired plane view, without radiation exposure. cMRI consists of several techniques that can be performed separately or in various combinations during a patient's examination. Most frequent indications for cMRI are myocarditis/cardiomyopathies, risk stratification in suspected coronary artery disease/ischemia, and assessment of myocardial viability [1, 2] and congenital heart disease.

Significant parts of neck, thorax, and upper abdomen are imaged at the time of routine clinical cMRI, particularly in the initial multislice axial and coronal images. A careful observation of the surrounding structures may therefore often identify during cMRI incidental extracardiac findings (IEFs) [3]. IEFs can represent unsuspected important diseases or benign findings, carrying several ethical, medicolegal, and financial implications [4]. Extracardiac findings during cMRI may also significantly modify clinical management of patients assessed by cMRI. Studies in literature showed different rates of prevalence of IEFs, ranging between 3 and 31% [3]. Moreover, cMRI differs from computed tomography (CT) in its use of several sequences which allows the recognizing of many differences in the appearance and conspicuity of IEFs [5]. The aim of this study was therefore to analyze retrospectively the prevalence and the nature of IEFs in a recent large series of patients referred for cMRI.

## 2. Methods

*2.1. Patients.* 742 consecutive patients (402 males and 340 females) referred to the Cardiac Magnetic Resonance Center of our University Hospital (Foggia, Italy) between January 2015 and December 2016 for clinically indicated cMRI (Table 1) were enrolled retrospectively in this study for the evaluation of IEFs prevalence and relevance.

Table 1: Clinical indications for cardiac magnetic resonance imaging studies ($n$ = 742).

| Indication for CMR | Number of cases |
|---|---|
| Myocarditis/cardiomyopathies | 356 (47.9%) |
| Coronary artery assessment | 168 (22.6%) |
| Cardiac masses | 60 (8%) |
| Valvular disease | 56 (7.5%) |
| Congenital heart disease | 42 (5.6%) |
| Pericardial disease | 31 (4.2%) |
| Myocardial viability | 26 (3.5%) |
| Others | 3 (0.4%) |

CMR examinations were all interpreted by both a radiologist and cardiologist experienced in cMRI. The diagnosis of IEF was made upon images and always included in the report.

All incidental findings discovered on cMRI were characterized by means of additional imaging techniques: ultrasound (US), computed tomography (CT), dedicated MR examination, bone scintigraphy with technetium 99m-methylene diphosphonate (99mTC-MDP), and positron emission tomography-computed tomography (PET-CT).

IEFs were classified into three categories: (1) findings with mild or no clinical significance, (2) findings with possible clinical significance, and (3) clinically significant findings. The overall prevalence and the sites of extracardiac findings were evaluated and reported.

Written informed consent was obtained from all patients; the study was held according to the principles of the Declaration of Helsinki.

*2.2. CMR Protocol.* CMR protocols were based on standardized protocols recommended by the Society for Cardiovascular Magnetic Resonance (SCMR) and the European Society of Cardiology (ESC) Working Group EuroCMR, respectively [6].

CMR was performed using a 1.5 T magnet (Achieva, Philips Healthcare, Best, Netherlands) with a cardiac phased-array receiver coil with cardiac gating. The standard protocol included multiplane steady-state free precession (SSFP) localizers, transversal T1-TSE black blood, sequences cine steady-state free precession (SSFP) oriented 2, 3, 4 chamber and short axis for the study of the kinetics of the right and left ventricles, T2 short-tau inversion recovery (STIR) black blood for the study of myocardial oedema in short axis and 4 chamber, dynamic sequence T1-TFE in short axis, Phase-contrast to study valvular flow, Phase Sensitive Inversion Recovery (PSIR) sequences for the study of late gadolinium enhancement (LGE) performed after 10–15 minutes after intravenous administration of gadolinium (0.1 mmol/kg). Field of view (FOV) of CMR sequences is the determining factor for the highlight of the exhibits around the heart and it is standard according to the international protocols.

*2.3. Statistical Analysis.* Continuous variables were reported as mean ± standard deviation or median and interquartile range, dichotomic as percentages.

## 3. Results

The median age of the subjects was 51 years (range: 5–85 years). Incidental findings were found in 109/742 (14.7%) of examined patients for a total of 131 IEFs; of these, 52 (40%) were intrathoracic and the remaining 79 (60%) were located in upper abdomen. 15 out of 131 incidental findings (11%) were confirmed to be clinically significant, while in the remaining 116 findings 87 were considered to be of mild or no clinical significance (66%); 29 were considered to be of possible clinical significance (22%) based on patient's clinical condition (Table 2).

Of the 131 collateral findings, 15 in 15 patients (prevalence: 2%) were classified as significant and deserving further diagnostic work-up: mediastinal lymphadenopathy/mass (6/15), lung nodule/mass (3/15), aortic coarctation (2/15), breast nodule (1/15), complex renal cyst (1/15), hepatic mass (1/15), and solid renal mass (1/15). Findings with possible clinical significance (29/131) were present in 22 patients (prevalence: 3%): pleural effusion/thickening (9/29), thyroid goitre (6/29), gallbladder lithiasis (5/29), airspace disease (4/29), splenomegaly (2/29), hydronephrosis (2/29), and adrenal nodule (1/29). IEFs with mild or no clinical significance were found in 72 patients (prevalence: 9.7%): simple renal cyst (31/87), hepatic cyst (24/87), hiatal hernia (8/87), hepatic haemangioma (8/87), thyroid nodule < 1 cm (7/87), bone haemangioma (3/87), paraspinal cyst (2/87), and splenic cyst (1/87) (Table 3).

The most common site of IEFs' localization was the kidney (35/131, 26.7%), followed by liver (33/131, 25.2%), lung (19/131, 14.5%), and thyroid (13/131, 9.9%). The lesions found in spleen, pleura, and gallbladder resulted to be with mild or possible clinical significance in all cases and no further diagnostic work-up was deemed necessary. Lung lesions resulted to be malignant in all cases including metastases in 2/3 and lung cancer in 1/3 of cases. Only one of 33 (3%) focal liver lesions resulted to be a metastatic hepatic mass. Two out of 35 (6.7%) kidney lesions resulted to be malignant including 1 case of complex renal cyst and 1 case of renal cell cancer. In two other cases of kidney lesions (6.7%), we observed unilateral hydronephrosis caused by kidney stones, as confirmed by additional imaging. Comparing MR findings with the additional definitive imaging tools, cMRI allowed a correct diagnosis in 116/131 cases with a diagnostic accuracy value of 88.5%. In particular, a lung mass was misdiagnosed as a cancer by cMRI, while it was shown to be a pulmonary atelectasis on chest CT examination.

A new/previously unknown diagnosis was made in 74% of cases with IEFs. The most informative sequences for IEFs were surveys (Balanced-TFE), that is, the initial locating sequences in the three planes of space which allow a global view of neck, chest, and abdomen, 90% of IEFs. Further relevant sequences for details were morphological sequences T1-TSE and T1-Fat Sat before and after contrast imaging (5%) and T2-STIR (5%).

Table 2: Prevalence of incidental extracardiac findings at cardiac magnetic resonance imaging.

| Category | Number of cases | Patients | Prevalence |
|---|---|---|---|
| Mild or no clinical significance | 87 | 72 | 9.7% |
| Possible clinical significance | 29 | 22 | 3% |
| Clinically significant | 15 | 15 | 2% |
| Total | 131 | 109 | 14.7% |

Table 3: Frequency of incidental extracardiac findings at cardiac magnetic resonance imaging.

| Mild or no clinical significance | | Possible clinical significance | | Clinically significant | |
|---|---|---|---|---|---|
| Simple renal cyst | 31 | Pleural effusion | 9 | Mediastinal lymphadenopathy/mass | 6 |
| Hepatic cyst | 24 | Thyroid goitre | 6 | Lung nodule/mass | 3 |
| Hiatal hernia | 8 | Gallbladder lithiasis | 5 | Aortic coarctation | 2 |
| Liver haemangioma | 8 | Airspace disease | 4 | Breast nodule | 1 |
| Thyroid nodule < 1 cm | 7 | Splenomegaly | 2 | Complex renal cyst | 1 |
| Pleural thickening | 3 | Hydronephrosis | 2 | Hepatic mass | 1 |
| Paraspinal cyst | 2 | Adrenal nodule | 1 | Solid renal mass | 1 |
| Splenic cyst | 1 | | | | |
| *Total* | 87 | | 29 | | 15 |
| | | Recommendation | | | |
| *No further work-up is necessary* | | *Further work-up is recommended depending on specific clinical scenario* | | *Further diagnostic work-up is mandatory* | |

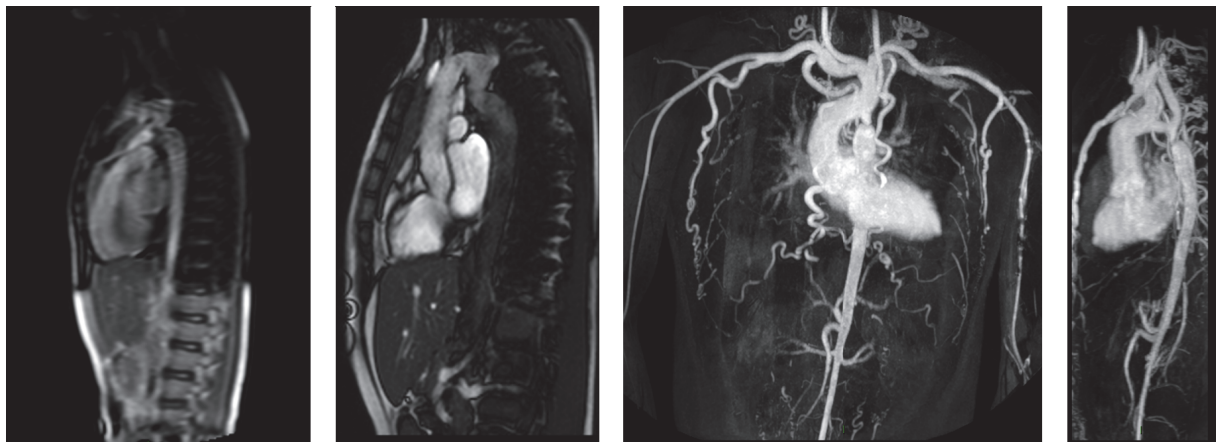

Figure 1: Sagittal localizers, SSFP 2 chamber, and 3D-CE-MRA images of aortic coarctation.

## 4. Discussion

cMRI is a highly reproducible tool to assess myocardial morphology as well as global and regional heart function. It also provides relevant information regarding tissue characteristics such as viability, myocardial perfusion, storage diseases, and inflammation. cMRI is thus increasingly used in daily practice [7].

In cMRI examinations, a careful assessment of noncardiac structures may also detect relevant noncardiac diseases. The wide FOV used to perform axial/coronal SSFP and BB-FSE sequences at the beginning of the CMR examination

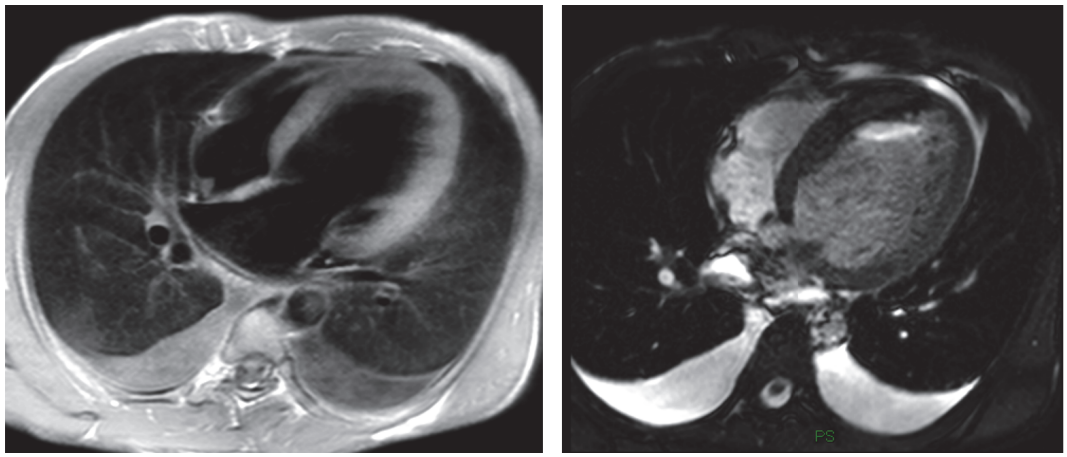

Figure 2: Bilateral pleural effusion.

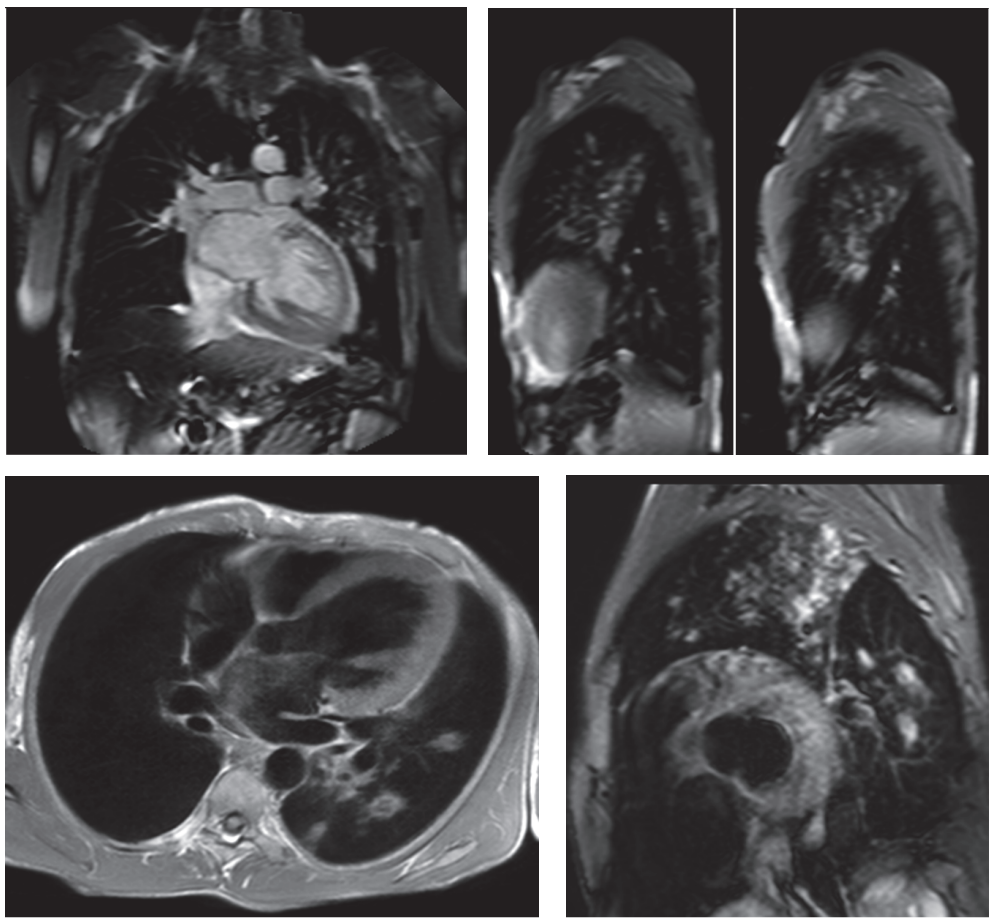

Figure 3: Coronal and sagittal localizer SSFP, Transverse T1-TSE, and short axis STIR-T2 images showing pulmonary irregular opacities in the upper lobe and apical segment of the lower lobe of the left lung compatible with a diagnosis of secondary tuberculosis.

allows exploring surrounding cardiac structures including the lungs, upper abdomen, and thoracic spine. This enables detecting possible IEFs that could be clinically significant or require further diagnostic work-up [8]. Few studies are reported in literature concerning the prevalence and the nature of IEFs on cMRI; their comparison is difficult because of different study design (i.e., cohort studied, "clinical setting," sequences applied, and reading session format). Indeed, IEFs based on CMR reports' review were reported by some authors [9], while others, as in the current study, performed

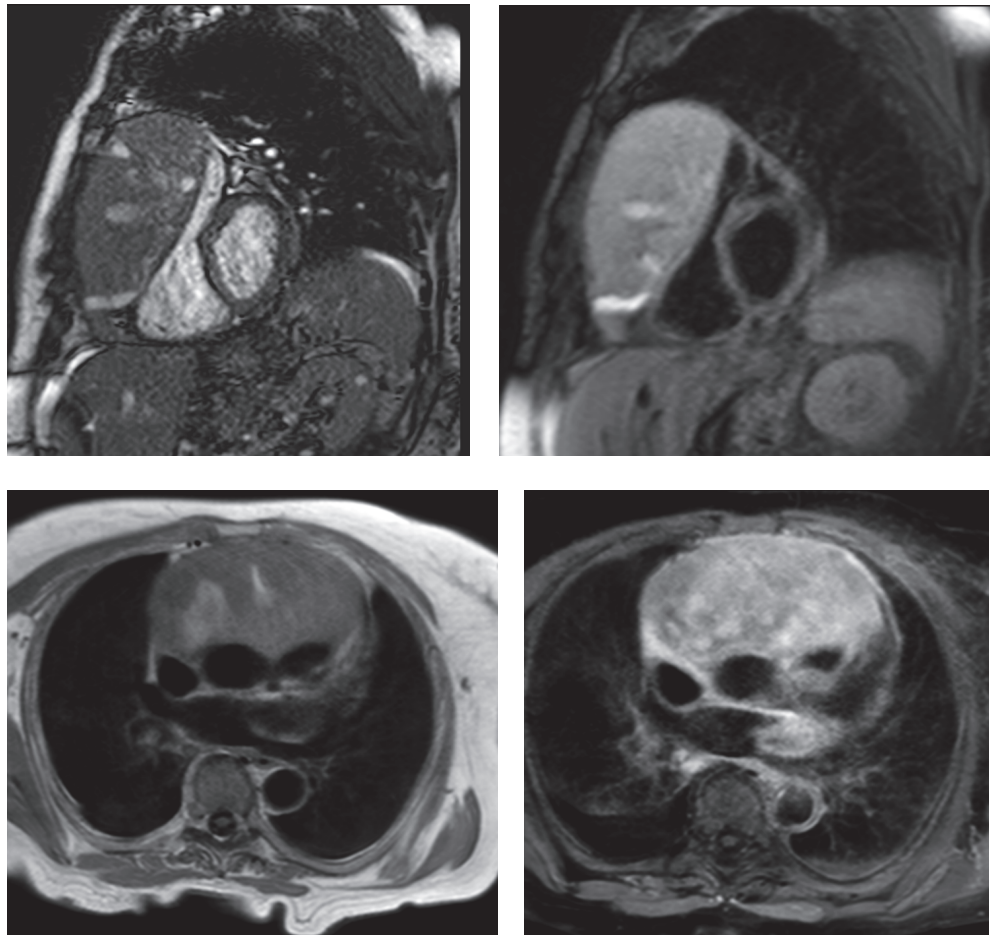

Figure 4: Cine-SSFP short axis and T2-STIR short axis and T1-TSE without gadolinium and T1-TSE-SPIR images with gadolinium showing a voluminous mass in the anterior mediastinum compressing right heart chambers.

an extensive image analysis [10]. In our series, IEFs were encountered in 109 (14.7%) of the 742 examined patients. The prevalence of IEFs in our study population is slightly higher than that previously observed: about twofold greater than Chan et al. [11] in 1534 consecutive clinically indicated cMRI studies (15% versus 7.6%) and almost threefold greater than Ulyte et al. [12] (15% versus 5.3%) in a review of 4165 cMRI reports. Sohns et al. [10] reported in 234 cMRI studies a slightly higher rate of extracardiac findings (26% of 854 patients), almost comparable with the prevalence in Irwin et al.'s work [9] (21.4% of 714 patients). A recent systematic review and meta-analysis of 12 studies including data from 7,062 patients demonstrated pooled prevalence of incidental extracardiac findings of 35% [13].

In the present study, images (and not cMRI reports) were analyzed in order to assess the incidence of IEFs. According to Klysik et al. [14], in our study, IEFs were classified into three categories: findings with mild or no clinical significance, findings with possible clinical significance, and clinically significant findings. Most of findings with mild or no clinical significance could generally be ignored without consequence for the patient's outcome. Findings with possible clinical significance may require additional imaging depending on patients' clinical condition or due to their nondedicated imaging. Finally, the clinically significant findings need immediate evaluation or treatment and further diagnostic work-up should be mandatory. In our study, we found two cases of aortic coarctation; sequences dedicated cine-MRI type allowed a detailed study of the anomalies (Figure 1); further CT scan examinations were therefore considered unnecessary. Vascular abnormalities (such as a case of abnormal pulmonary venous return undiagnosed earlier), mild and severe pleural effusions (Figure 2), consolidative pulmonary parenchymal phenomena (Figure 3), and both benign and malignant pulmonary nodules were found (Figure 4). Extracardiac mediastinal masses were also revealed with an accurate analysis of the relationship with the cardiac structures and of mediastinal adenopathy. A case of Takotsubo cardiomyopathy is noteworthy with an adrenal mass characterized by an intense enhancement at first pass; a pheochromocytoma was confirmed at following histological examination [15, 16] (Figure 5).

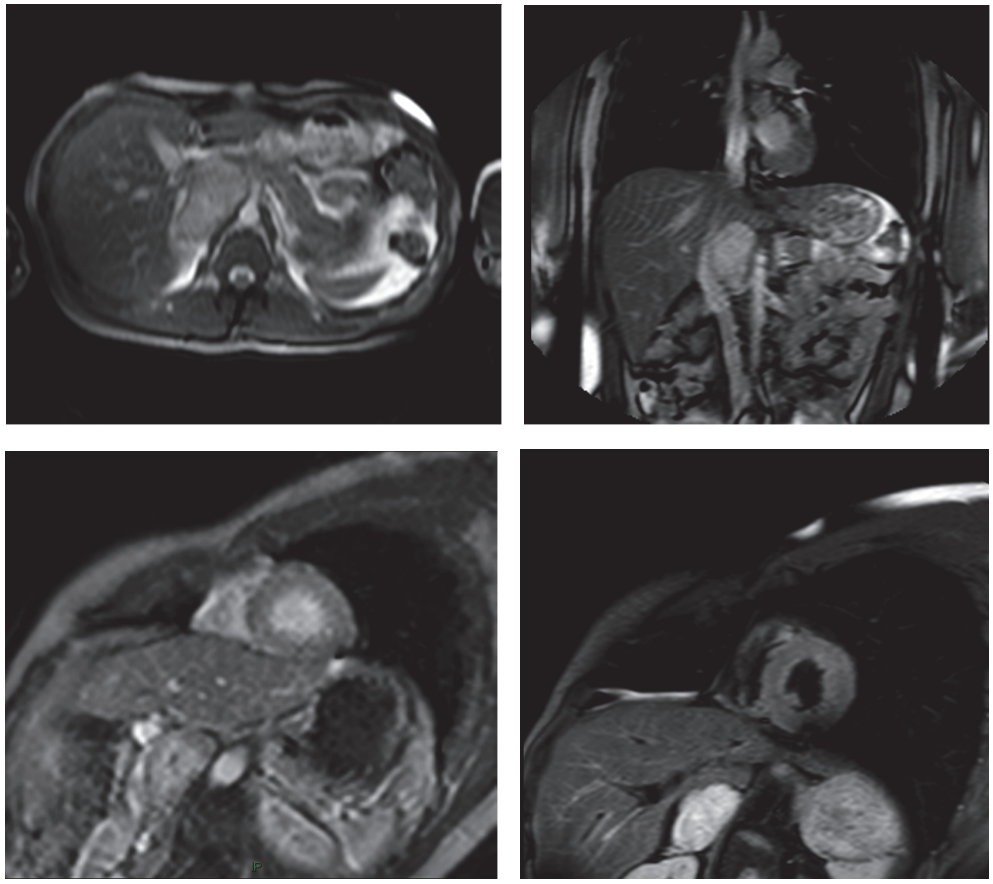

Figure 5: Axial and coronal localizer SSFP, short axis perfusion, and STIR-T2 short axis images showing an adrenal mass compatible with a diagnosis of pheochromocytoma confirmed at histology.

In the present study, clinically significant extracardiac findings were observed in 2% of the population (11.4% of cases), which is consistent with previous studies that reported similar prevalence for "major" IEFs during cMRI (range: 1–27%) [10]. The most frequent clinically significant IEF was mediastinal lymphadenopathy/mass (defined as >1 cm in the short axis), which was encountered in 6 patients. However, the majority of IEFs were less important and were associated with a benign diagnosis. In fact, in 65% of cases, extracardiac lesions detected on CMR were benign. The most common site of IEFs' localization was the kidney (26.7%), followed by the liver (25.2%) (Figure 6), the lung (14.5%), and thyroid (9.9%). The results of this study demonstrate that a significant number of patients who underwent cMRI may present IEFs. However, a small percentage of these occasional findings actually have a clinical relevance and deserve further diagnostic investigation.

cMRI may be extremely useful in characterizing these incidental findings, with an excellent diagnostic accuracy (88.5%), although further imaging techniques are often necessary to precisely define incidental findings. In particular, CT and fluorodeoxyglucose PET-CT (FDG PET-CT) scan are the first choice to characterize and discriminate the nature of incidental lung parenchymal lesions. Ultrasound (US) or dedicated MRI may be used to further evaluate abdominal and breast lesions. Finally, in all cases of incidental bony lesions, MR with dedicated sequences or bone scintigraphy may improve the characterization of IEFs.

## 5. Conclusions

A significant number of IEFs can be detected during cMRI, with high accuracy. It is therefore extremely important that whoever reports cMRI should be able to properly assess normal and abnormal thorax and superior abdominal findings. IEFs should be searched, for potentially modifying the clinical management of patients with such findings.

## Conflicts of Interest

The authors have no potential conflicts of interest to disclose.

## Authors' Contributions

All authors have read and approved the manuscript.

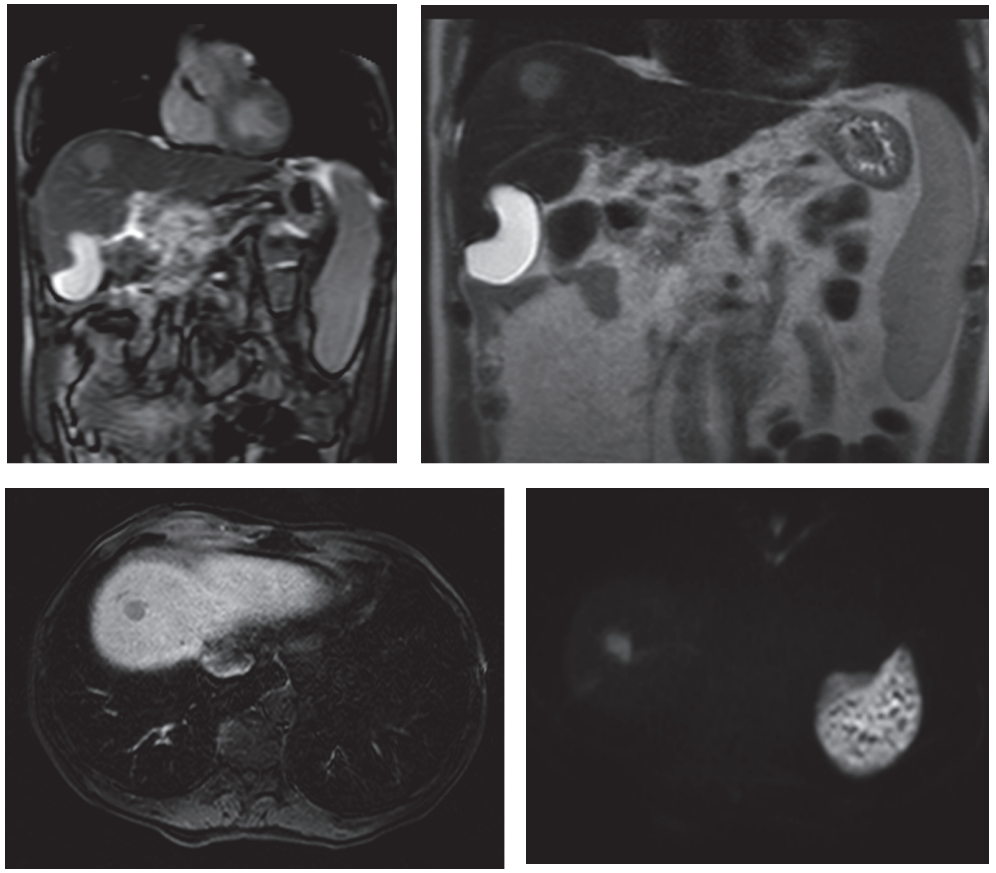

Figure 6: Coronal localizer SSFP, coronal T2-TSE, and Transverse Thrive images with gadolinium and diffusion weighted images of a case of hemochromatosis with a liver nodular hepatocellular carcinoma.

## References


[1] O. Bruder, S. Schneider, D. Nothnagel et al., "EuroCMR (European Cardiovascular Magnetic Resonance) Registry. Results of the German Pilot Phase," *Journal of the American College of Cardiology*, vol. 54, no. 15, pp. 1457–1466, 2009.

[2] O. Bruder, A. Wagner, M. Lombardi et al., "European cardiovascular magnetic resonance (EuroCMR) registry—multi national results from 57 centers in 15 countries," *Journal of Cardiovascular Magnetic Resonance*, vol. 15, pp. 1–9, 2013.

[3] V. Dunet, H. Barras, X. Boulanger et al., "Impact of extracardiac findings during cardiac MR on patient management and outcome," *Medical Science Monitor*, vol. 21, pp. 1288–1296, 2015.

[4] F. Khosa, B. P. Romney, D. N. Costa, N. M. Rofsky, and W. J. Manning, "Prevalence of noncardiac findings on clinical cardiovascular MRI," *American Journal of Roentgenology*, vol. 196, no. 4, pp. W380–W386, 2011.

[5] M. K. Atalay, E. A. Prince, C. A. Pearson, and K. J. Chang, "The prevalence and clinical significance of noncardiac findings on cardiac MRI," *The American Journal of Roentgenology*, vol. 196, no. 4, pp. W387–W393, 2011.

[6] C. M. Kramer, J. Barkhausen, S. D. Flamm, R. J. Kim, and E. Nagel, "Standardized cardiovascular magnetic resonance imaging (CMR) protocols, society for cardiovascular magnetic resonance: board of trustees task force on standardized protocols," *Journal of Cardiovascular Magnetic Resonance*, vol. 10, no. 1, 35 pages, 2008.

[7] C. M. Kramer, J. Barkhausen, S. D. Flamm, R. J. Kim, and E. Nagel, "Society for cardiovascular magnetic resonance board of trustees task force on standardized protocols. standardized cardiovascular magnetic resonance (CMR) protocols 2013 update," *Journal of Cardiovascular Magnetic Resonance*, vol. 15, no. 91, 2013.

[8] P. S. Douglas, M. Cerqueria, G. D. Rubin, and A. S.-L. Chin, "Extracardiac Findings: What Is a Cardiologist to Do?" *JACC: Cardiovascular Imaging*, vol. 1, no. 5, pp. 682–687, 2008.

[9] R. B. Irwin, T. Newton, C. Peebles et al., "Incidental extracardiac findings on clinical CMR," *European Heart Journal Cardiovascular Imaging*, vol. 14, no. 2, pp. 158–166, 2013.

[10] J. M. Sohns, A. Schwarz, J. Menke et al., "Prevalence and clinical relevance of extracardiac findings at cardiac MRI," *Journal of Magnetic Resonance Imaging*, vol. 39, no. 1, pp. 68–76, 2014.

[11] P. G. Chan, M. P. Smith, T. H. Hauser et al., "Noncardiac Pathology on Clinical Cardiac Magnetic Resonance Imaging," *JACC: Cardiovascular Imaging*, vol. 2, no. 8, pp. 980–986, 2009.

[12] A. Ulyte, N. Valeviciene, D. Palionis, S. Kundrotaite, and A. Tamosiunas, "Prevalence and clinical significance of extracardiac findings in cardiovascular magnetic resonance," *Hellenic Journal of Cardiology*, vol. 57, no. 4, pp. 256–260, 2016.

[13] V. Dunet, J. Schwitter, R. Meuli, and C. Beigelman-Aubry, "Incidental extracardiac findings on cardiac MR: Systematic review and meta-analysis," *Journal of Magnetic Resonance Imaging*, vol. 43, no. 4, pp. 929–939, 2016.

[14] M. Klysik, D. Lynch, N. Stence, and K. Garg, "Incidental non-cardiovascular, non-pulmonary findings identified in a low-dose CT lung cancer screening population: prevalence and clinical implications," *International Journal of Radiology and Imaging Technology*, 1:002, 2015.

[15] M. Gravina, G. Casavecchia, N. D'Alonzo et al., "Pheochromocytoma behind takotsubo(stress)-cardiomyopathy: The great pretender," *American Journal of Emergency Medicine*, vol. 35, no. 3, p. 514, 2017.

[16] M. Gravina, G. Casavecchia, N. D'Alonzo et al., "Pheochromocytoma mimicking Takotsubo cardiomyopathy and hypertrophic cardiomyopathy: A cardiac magnetic resonance study," *American Journal of Emergency Medicine*, vol. 35, no. 2, pp. 353–355, 2017.

Hindawi
BioMed Research International
Volume 2017, Article ID 6797826, 8 pages
https://doi.org/10.1155/2017/6797826

*Research Article*

# Incidental and Underreported Pleural Plaques at Chest CT: Do Not Miss Them—Asbestos Exposure Still Exists

**Maria Antonietta Mazzei,[1,2] Francesco Contorni,[3] Francesco Gentili,[1,2] Susanna Guerrini,[1] Francesco Giuseppe Mazzei,[2,4] Antonio Pinto,[2,5] Nevada Cioffi Squitieri,[1] Antonietta Gerardina Sisinni,[6] Valentina Paolucci,[6] Riccardo Romeo,[6] Pietro Sartorelli,[6,7] and Luca Volterrani[1]**

[1]*Department of Medicine, Surgery and Neuroscience, Unit of Diagnostic Imaging, Azienda Ospedaliera Universitaria Senese, University of Siena, Siena, Italy*
[2]*Italian College of Ethics and Forensic Radiology, Italian Society of Medical Radiology (SIRM), Milan, Italy*
[3]*University of Siena, Siena, Italy*
[4]*Unit of Diagnostic Imaging, Azienda Ospedaliera Universitaria Senese, University of Siena, Siena, Italy*
[5]*Department of Radiology, Cardarelli Hospital, Naples, Italy*
[6]*Unit of Occupational Medicine, Azienda Ospedaliera Universitaria Senese, University of Siena, Siena, Italy*
[7]*Department of Medical Biotechnology, Unit of Occupational Medicine, Azienda Ospedaliera Universitaria Senese, University of Siena, Siena, Italy*

Correspondence should be addressed to Maria Antonietta Mazzei; mariaantonietta.mazzei@unisi.it

Received 3 February 2017; Accepted 10 April 2017; Published 5 June 2017

Academic Editor: Giuseppe Angelelli



Pleural plaques (PPs) may be a risk factor for mortality from lung cancer in asbestos-exposed workers and are considered to be a marker of exposure. Diagnosing PPs is also important because asbestos-exposed patients should be offered a health surveillance that is mandatory in many countries. On the other hand PPs are useful for compensation purposes. In this study we aimed to evaluate the prevalence, as incidental findings, and the underreporting rate of PPs in chest CT scans (CTs) performed in a cohort of patients (1512) who underwent chest CT with a slice thickness no more than 1.25 mm. PPs were found in 76 out of 1482 patients (5.1%); in 13 out of 76 (17,1%) CTs were performed because of clinical suspicion of asbestos exposure and 5 of them (38%) were underreported by radiologist. In the remaining 63 cases (82.9%) there was no clinical suspicion of asbestos exposure at the time of CTs (incidental findings) and in 38 of these 63 patients (60.3%) PPs were underreported. Reaching a correct diagnosis of PPs requires a good knowledge of normal locoregional anatomy and rigorous technical approach in chest CT execution. However the job history of the patient should always be kept in mind.

## 1. Introduction

Asbestos is a general term for a heterogeneous group of hydrated magnesium silicate minerals that have in common a tendency to separate into fibres [1]. It has long been used in roofing, insulators, brake pads, and gaskets, and in various workplaces and construction sites. Asbestos has been the largest single cause of occupational cancer in the United States and a significant cause of disease and disability from nonmalignant disease [2]. In Italy, the asbestos epidemic continues and is even increasing because of the country's industrial history. Up to the end of the 1980s, Italy was the second largest asbestos producer in Europe after the Soviet Union and the largest in the European Community, with a peak between 1976 and 1980 [3]. Furthermore asbestos imports to Italy reached a peak when they were already falling in the UK and US and the consumption curve of asbestos shows a lag time of about 10 years compared to many

industrialized countries [4]. Asbestos fibres, inhaled and displaced by various means to lung tissue, may cause a spectrum of diseases including cancer (especially mesothelioma and lung cancer) and nonmalignant asbestos-related disease that refer to the following conditions: asbestosis, pleural thickening or asbestos-related pleural fibrosis (plaques or diffuse fibrosis), "benign" (nonmalignant) pleural effusion, and airflow obstruction [5, 6]. Pleural plaques (PPs) are usually asymptomatic and cause slight impairment of lung function only when they are extended in size [7–9]. However, they are the most common form of the pleuropulmonary abnormality consistent with asbestos exposure and are considered to be a marker of exposure, indicating an increased risk of pulmonary fibrosis or asbestos-related malignancies versus the general population [10]. In fact PPs may be a risk factor for mortality from lung cancer in asbestos-exposed workers, particularly in either smokers or former/ex-smokers [11]. Moreover the presence of PPs may help in considering asbestosis as a cause of interstitial lung disease predominating in the subpleural area of the lower lobes [12]. A recent Japanese study even found that in lung cancer patients the plaque extent had a significant positive relationship with the asbestos body concentration in lung tissue that represents a biomarker of past exposure [13]. However even if for certain types of asbestos the development of PPs is statistically correlated with malignant disease, the evidence is consistent with the hypothesis that PPs without other pleural disease are a marker of exposure, rather than an independent risk factor [14]. Diagnosing PPs is also important as asbestos-exposed patients should be offered a health surveillance that is mandatory in many countries. On the other hand PPs are useful for compensation purposes. In Italy PPs notification by physicians is required by law. From 2016 it is also mandatory to send the first medical certificate of PPs diagnosis to the Italian National Insurance Institute (INAIL). Doctors who fail to comply with these obligations may be fined. From a diagnostic point of view, in most screenings for pneumoconiosis, a chest radiograph is used as the standard method, but this procedure has important limitations in the detection of early subtle PPs, whereas a CT scan enables diagnosis of thin or tiny noncalcified plaques [10, 15–17]. Experienced CT readers can diagnose PPs with high confidence in most cases, which show the typical findings of bilateral, multiple, localised, pleural thickenings sparing the costophrenic angles. However, the CT features of PPs are sometimes equivocal in challenging cases and if the radiologists are not skilled in occupational diseases PPs could be underreported [18].

In this study we aimed to evaluate the prevalence, as incidental findings, and the underreporting rate of PPs in chest CT scans (CTs) performed in a cohort of patients who underwent chest CT with a slice thickness no more than 1.25 mm (high resolution protocol) at our department.

## 2. Material and Method

*2.1. Study Design.* This retrospective study was approved by the institutional review board of each participating centre, and the requirement for patient approval or informed consent for the retrospective analysis of anonymous images was waived. The study cases were identified by reviewing the radiological databases of the Diagnostic Imaging Unit at the Azienda Ospedaliera Universitaria Senese from January 2016 to June 2016. 1512 CTs fulfilled technical eligibility criteria (see CT scanning protocols section). All the CTs were independently reviewed by two radiologists in order to search for pleural thickening or asbestos-related pleural fibrosis (plaques or diffuse fibrosis); the presence of "benign" (nonmalignant) pleural effusion and asbestosis was also investigated.

*2.2. Scanning Protocols.* All CTs were performed using a 64-detector row CT scanner (Discovery 750 HD, GE Healthcare, Milwaukee, WI, USA). The field of view (FOV) of all eligible chest CTs had to include the rib cage. Since CT slice thickness varied according to the clinical indication, only the exams with a slice thickness no greater than 1.25 mm for pulmonary embolism detection or cancer evaluation (total number 960) and 1.25 mm for high resolution CT (HRCT, total number 552) were considered eligible for this study. In all patients chest CTs were performed without contrast medium administration; in oncological patients or patients with clinical suspicion of pulmonary embolism, a CT scan after administering contrast medium was also performed, and in the latter cases both scans (with and without contrast medium administration) were provided for review. Eligible HRCTs were acquired using a volumetric technique; in 273 out of 552 HRCTs, the scan was performed with the patient in a prone position because of the clinical suspicion of interstitial lung disease, to avoid possible parenchymal dysventilation in the dependent portions of the lung, mimicking lung fibrosis. Finally all CTs provided for review were reconstructed at window settings optimised for the assessment of the mediastinum.

*2.3. Image Evaluation.* Each CT examination, from which patient personal information has been removed, was analysed by two radiologists (with 16 and 8 years' experience in chest CT, resp., and 5 years of experience each as CT readers for asbestos-related thoracic diseases) who were blind to subjects' job history and possible history of asbestos exposure. The two readers independently assessed the pulmonary and pleural lesions as consistent with asbestos exposure and reached a conclusion by consensus. Image analysis was performed at both mediastinal (window level, 40 Hounsfield units [HU]; window width, 400 HU) and lung window settings (window level, 700 HU; window width, 1500 HU), using a dedicated workstation. The radiologists were permitted to adjust the window settings if necessary. PPs were defined as variable-size localised pleural thickening of soft tissue, or calcific densities attached along the pleura of the chest wall, diaphragm, and mediastinum on the CTs. The following findings were recorded: number, presence of calcification, maximum width and length, location (chest wall, diaphragm, and mediastinal pleura), and extent score of PPs. The maximum width was measured from the thickest plaque in the subjects and defined as the maximum vertical distance from the parietal pleura to the interface between the plaque and lung. The maximum length was measured in the largest plaque in the subjects and defined as the longest

diameter of the plaque in coronal or sagittal 2D multiplanar reconstruction. For the evaluation of plaque location, the chest wall was divided into right and left, ventral (anterior to the mid-axillary line) and dorsal, and upper (upper 1/2 of the thorax) and lower parts. Finally the extent scores were measured in each hemithorax according to the International Classification of HRCT for Occupational and Environmental Respiratory Diseases (ICOERD) classification system [19]. In particular, the involvement of the circumference of the lung, excluding the mediastinum, was calculated by combining maximum lengths of pleural plaques on axial image at the mid-thoracic level as follows: 0 = no plaques; 1 = up to 1/4; 2 = 1/4–1/2; and 3 > 1/2 of the circumference of the chest wall. The total extent score was defined as the sum of the extent scores of the right and left hemithorax (min. 1, max 6). The thickening score was assessed by measuring the thickest plaque of each hemithorax assigning the score as follows: 0 = no plaques; 1 = 1–5 mm; 2 = 5–10 mm; 3 > 10 mm. The total thickening score was defined as the sum of the scores of the right and left hemithorax (min. 1, max 6). ICOERD classification was also used to report parenchymal findings and in particular the presence of well-defined rounded opacities, irregular and/or linear opacities, ground glass opacities, honeycombing, emphysema, and large opacities.

*2.4. Statistical Analysis.* The pleural findings detected by the readers were collected, and the results expressed as mean +/− standard deviation (SD). A descriptive statistical analysis was performed and variables were expressed as percentages. Student's $t$-test for paired samples was used to compare the maximum width of reported and underreported PPs. A $p$ value of less than 0.05 was considered to indicate a significant difference. The statistical review of the study was performed by a biomedical statistician. The analysis was performed using Stata version 8.0 (Stata Corp., College Station, Texas).

## 3. Results

Thirty out of 1512 CTs (2%) examinations were excluded because of motion artefacts ($n = 10$), insufficient image resolution ($n = 6$), or partially explored lung ($n = 14$). The remaining 1482 chest CTs represent the final cohort of the study. PPs were found in 76 out of 1482 patients (5.1%); in thirteen out of 76 (17.1%) CTs were performed because of clinical suspicion of asbestos exposure and 5 of them (38%) were underreported by radiologist. In the remaining 63 cases (82.9%) there was no clinical suspicion of asbestos exposure at the time of CTs (incidental findings). Among these 63 cases, a history of asbestos exposure was established in 53 (84.1%) by recording their work history, analysing clinical reports, and acquiring information from the patients, after our blinded image analysis. In thirty-eight of these 63 patients (60.3%) PPs were not mentioned in the final report of CTs (underreported) (Figure 1). After consensus all the 76 patients with PPs at CTs (56 men, mean age 67 years, range 55–84, and 2 women of 63 and 72 years of age, resp.) were scored by the study reviewers as showing at least one pleural plaque. The jobs features of patients with history of asbestos exposure (66/76, 86.8%) are summarised in Table 1 whereas all PPs features are summarised in Tables 2 and 3, respectively. Among the 66 cases with history of asbestos exposure, 65 had multiple and bilateral PPs whereas 1 had two monolateral PPs. The 10 cases of PPs without a history of occupational asbestos exposure had a single and unilateral plaque in 8 cases and multiple and bilateral plaques in 2 cases. There were less than 5 plaques in 17 cases (22.4%), uncalcified

Table 1: Jobs' features of patient with history of asbestos exposure.

| | |
|---|---|
| *Industrial sector* | |
| Metal workers | 9 |
| Asbestos sheets producers | 2 |
| Asbestos insulation removers | 7 |
| *Construction sector* | |
| Bricklayer | 21 |
| Plumber | 5 |
| Aqueduct technician | 3 |
| Boiler technician | 3 |
| *Transport sector* | |
| Shipyard workers | 5 |
| Dockers | 3 |
| Mechanics | 3 |
| *Craftsmanship* | |
| Shoemaker | 2 |
| Glassworkers | 3 |
| *Total* | 66 |

Table 2: PPs distribution.

| Chest wall | |
|---|---|
| *Upper versus lower* | 45 (59.2%) versus 60 (78.9%) |
| Upper | 11 (14.5%) |
| Lower | 26 (34.2%) |
| Both | 34 (44.73%) |
| *Total* | 71 (93.4%) |
| Upper ventral versus upper dorsal | 24/45 (53.3%) versus 18/45 (40%) |
| Both | 3/45 (6.7%) |
| Lower ventral versus lower dorsal | 16/60 (35.5%) versus 37/60 (61.7%) |
| Both | 7/60 (2.8%) |
| Diaphragm | |
| Right | 15 (19.7%) |
| Left | 7 (9.2%) |
| Both | 21 (27.6%) |
| *Total* | 43 (56.5%) |
| Mediastinum | |
| Right | 3 (3.9%) |
| Left | 9 (11.8%) |
| Both | 0% |
| *Total* | 12 (15.7%) |

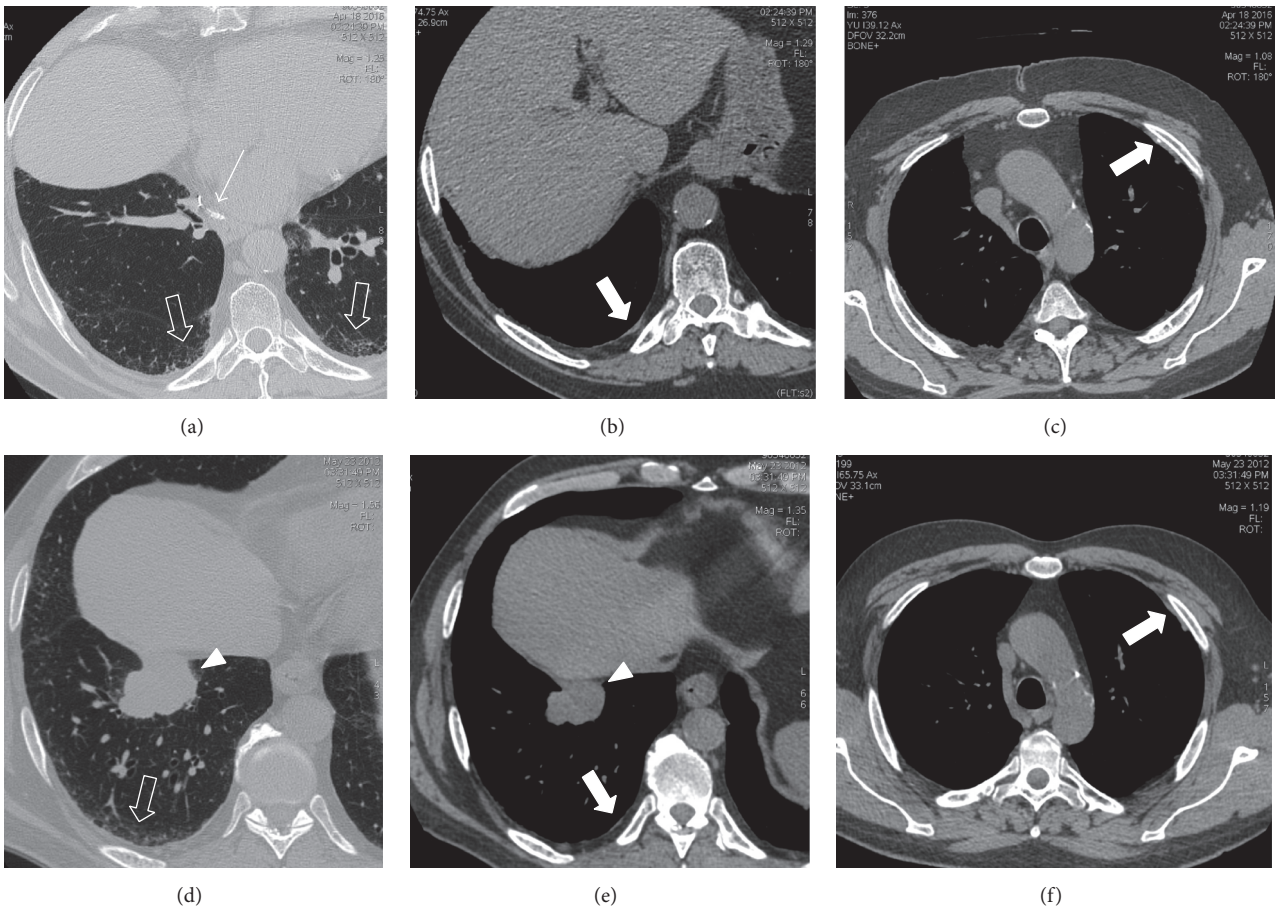

Figure 1: (a–f) Follow-up CT in a 65-year-old man 4 years after lower right lobectomy for lung cancer (arrow in (a)) demonstrates asbestosis (white open arrows in (a)) and bilateral PPs (white solid arrows in (b) and (c)). These CT findings were present since 2012 as showed by the presurgical staging CT (lung cancer, arrowhead in (d) and (e); asbestosis, white open arrows in (d); PPs, white solid arrows in (e) and (f)).

in 23 (30.3%), partially calcified in 38 (50%), and completely calcified in 15 (19.7%). With regard to the distribution on the pleural surface, the chest wall was the most common location (71/76, 93.4%), followed by the diaphragm (43/76, 56.5%) and the mediastinum (12/76, 15.7%). Chest wall PPs had a particular distribution along the craniocaudal and anteroposterior directions: the lower half was more commonly involved than the upper one (26/76, lower half, 34.2%; 11/76, upper half, 14.5%; 34/76, both the regions, 44.73%) and in the upper half there was a slight ventral predominance (24/45, upper ventral, 53.3%; 18/45, upper-dorsal, 40%; 3/45, both the regions, 6.7%), whereas in the lower half there was a clear dorsal predominance (37/60, lower-dorsal, 61.7%; 16/60, lower-ventral, 35.5%; 7/60, both the regions, 2.8%). Diaphragmatic pleurae were bilaterally involved in 21 cases (27.6%), only on the right side in 15 cases (19.7%) and only on the left side in 7 (9.2%). Mediastinal pleura had no cases with bilateral involvement and the left side had more plaques than the right side (9, 11.8%, versus 3, 3.9%). Among the 10 cases of PPs without a history of occupational asbestos exposure, six out of 8 cases with a single plaque were attributable to pleuritis, caused by previous episodes of pneumonia, and the other 2 were probably caused by the hemothorax due to previous trauma. In the remaining 2 cases of bilateral and multiple plaques it is plausible that there was environmental asbestos exposure. PPs mean width of all 76 cases was 5.5 ± 2.96 mm (range 1–12.2) and mean length was 62.9 ± 49.1 mm (range 2–178). According to the ICOERD classification, extent and width scores were as follows: *extent score* (mean): right hemithorax 1.5 ± 0.7; left hemithorax 1.6 ± 0.8; total mean score 3.1 ± 1.5 (range 1–6); width score (mean): right hemitorax 1.4 ± 0.6; left hemitorax 1.3 ± 0.6; total mean score 2.7 ± 1.2 (range 1–6). The other findings resulting from ICOERD classification are summarised in Table 4. Furthermore there was not a significant difference in PPs mean width between reported and underreported PPs (5.4 ± 2.7 mm versus 5.5 ± 3.3 mm, $p > 0.05$).

## 4. Discussion

Incidental findings on radiographic examinations have been available since the beginning of diagnostic radiology. With the introduction of cross-sectional imaging, the detection of such findings became more common, and their recognition was typically believed to be useful by leading to

Table 3: PPs characteristics.

| | |
|---|---|
| *Number of plaques* | |
| Less than 5 | 17 (22.4%) |
| 5 or more | 59 (77.6%) |
| *Calcification* | |
| Uncalcified | 23 (30.3%) |
| Partially calcified | 38 (50%) |
| Completely calcified | 15 (19.7%) |
| *Involvement of hemithorax* | |
| Unilateral | 9 (11.8%) |
| Bilateral | 67 (88.2%) |
| *Maximum width* | |
| Range | 1–12.2 mm |
| Mean | 5.5 mm |
| *Maximum length* | |
| Range | 2–178 mm |
| Mean | 62.9 mm |
| *Extent score (mean)* | |
| Right | 1.5 |
| Left | 1.6 |
| *Total* | 3.1 |
| *Width score (mean)* | |
| Right | 1.4 |
| Left | 1.3 |
| *Total* | 2.7 |

early detection of subclinical disease, and probably to better outcomes [20]. Incidental abnormalities of the pleura are most commonly pleural effusions, followed by focal abnormalities such as noncalcified or calcified PPs. Clinically significant incidental pleural abnormalities, namely, indeterminate pleural masses, were rarely reported among lung cancer screening studies in less than 1% of subjects [21]. Our study highlights that PPs, that are considered to be indicators of asbestos exposure and the most common manifestation of inhalation, retention, and biological effect of asbestos fibres, can be detected, as incidental findings, on chest CTs, even if there is no specific suspicion, and that radiologists tend to underreport them. Underreporting and undercompensation of occupational diseases, especially asbestos-related ones, is a widespread phenomenon in many countries, so that various authors identified the need for action to reduce underestimation and to improve current reporting practices and compensation policies [22]. The explanations for this phenomenon could be found in different reasons. First of all, it is necessary to recognise five main scenarios: (1) the radiologist is not aware of the clinical suspicion of asbestos exposure; (2) the radiologist is aware of the clinical suspicion of asbestos exposure and he is sufficiently familiar with CT findings in occupational diseases; (3) the radiologist is aware of the clinical suspicion of asbestos exposure but his experience in the field of occupational diseases is not sufficient; (4) the radiologist is aware of the patient's job history but is not aware of possible asbestos exposure in that job (e.g., not all radiologists are aware of possible asbestos exposure in plumbers!); (5) the CT technique is not sufficiently adequate to demonstrate PPs. Regarding the first two points, the underreporting of PPs could be due to observer or perceptual errors and in particular to both scanning and alliterative error. In the former (scanning or perceptual error) error is the result the radiologist's failure to fixate on the area of the lesion, in these cases the pleurae. Scanning or perceptual errors, in general, are related to multiple psychophysiological factors, including level of observation alertness, observer fatigue, duration of the observation task, any distracting factors, conspicuity of the abnormality, and many other factors, such as the absence of a specific clinical suspicion when searching PPs in the first clinical scenario [23–26]. In an MDCT examination, the high number of CT images substantially contributes to the perceptual error; however, the reduction in the number of images (i.e., image retroreconstruction with a thicker slice) should be discouraged because of the reduction of the CT diagnostic capabilities [27]. Alliterative error, that could also occur in the third scenario, is a perceptual error that results from the influence a radiology report has over another radiologist. This type of perceptual error occurs because the radiologist reads the old report before looking at the images; if the first radiologist missed it, the next radiologist is likely to miss it as well [28]. In our case history, among the 63 patients with PPs as incidental findings, 43 patients have at least one previous CT, with a negative report for pleural findings and in particular PPs. In the third and fourth clinical scenarios (the radiologist is aware of the clinical suspicion of asbestos exposure but his experience in the field of occupational diseases is not sufficient or the radiologist is aware of the patient's job history but is not aware of possible asbestos exposure in that job) the error could also be attributed to mistaken exam interpretation or cognitive error. A cognitive error is the result of a failure to correctly interpret a perceived radiological abnormality because of insufficient experience or knowledge or an underestimation of one or more signs that would have prompted the correct diagnosis. It is a common condition as occupational diseases are a niche field in radiology and also due to the variety of CT findings in environmental and occupational exposure, although this type of error could be reduced if the correct diagnostic predictions based on clinical information are suggested. In cognitive error the radiologists' awareness of PPs and focal pleural thickening mimicking PPs on chest CTs could also be considered. In fact even if the diagnosis of PPs is commonly straightforward, numerous causes of focal pleural thickening may nevertheless be seen and misinterpreted in routine practice, producing both false positive and false negative results that may lead to medicolegal consequences or can cause underreporting and undercompensation of occupational diseases. Reaching a correct diagnosis of PPs requires a good knowledge of normal locoregional anatomy (transversus thoracic muscle, subcostal muscle, extrapleural fat, etc.), different features of PPs, and common pitfalls in their diagnosis (focal dependent pleural thickening, pseudoplaques in sarcoidosis and silicosis) [18, 29, 30]. Last but not least, in order to reduce underestimation and to improve current reporting practices of PPs, technical approaches in chest CT execution should

Table 4: Additional lung ICOERD findings.

| Lung ICOERD features | Patients | Abnormalities significance (number of cases) |
|---|---|---|
| *Normal lung parenchyma* | 21<br>27.6% | |
| *Well defined rounded opacities* | 18<br>23.7% | (i) Postinflammatory (8)<br>(ii) Silicosis (2)<br>(iii) Metastasis (3)<br>(iv) Sarcoidosis (1)<br>(v) Uncertain significance (4) |
| *Irregular and/or linear opacities* | 20<br>29.3% | (i) Lung fibrosis with UIP consistent pattern (2)<br>(ii) Organizing pneumonia (1)<br>(iii) Hypersensibility pneumonia (1)<br>(iv) Sarcoidosis (1)<br>(v) Asbestosis (6)<br>(vi) Pulmonary infarction (2)<br>(vii) Uncertain significance (7) |
| *Ground glass opacities* | 8<br>10.5% | (i) Lung cancer (3 cases)<br>(ii) Desquamative interstitial pneumonia (2)<br>(iii) Uncertain significance (3) |
| *Honeycombing* | 4<br>5.2% | (i) Lung fibrosis with UIP consistent pattern (3)<br>(ii) Hypersensibility pneumonia (1) |
| *Emphysema* | 16<br>21% | |
| *Large opacities* | 5<br>6.8% | (i) Lung cancer (2 cases)<br>(ii) Rounded atelectasis (1)<br>(iii) Mesothelioma (1)<br>(iv) Hamartoma (1) |

also be rigorous. Thin-section CT acquisition (≤1.25 mm) in full inspiration is recommended for scanning the thorax, in order to avoid missing tiny, thin, and uncalcified PPs. Furthermore, considering the fact that PPs more commonly involve lower pleura than the upper, the dorsal regions of basal thoracic wall and the diaphragm, and that asbestosis also prefers the dorsal regions of the lower lobes, the patient should be placed in a prone position during CTs. However, if the CTs are performed with the patient in a supine position, the presence of pleural thickening in the dorsal regions, in the absence of PPs in other regions of the pleura, requires an additional acquisition in prone position. This approach will differentiate a real plaque from reversible dependent pleural thickening [29]. According to a recent study by Kim et al. [31], an interesting distribution of PPs was found, in particular: *diaphragmatic plaques* were distributed more commonly on the right side, since the right diaphragmatic dome has a large interface with the lung; *mediastinal plaques* were distributed more commonly on the left side due to anatomical and mechanical factors such as larger interface with the lung and the pulsating left ventricle pushing the left mediastinal pleura against the adjacent left lung with more mechanical stress than the right mediastinal pleura; *chest wall pleural* plaques more commonly involved both the basal sides due to combination of high ventilation and gravity in these lung regions. Inferior pleura is more frequently involved than the upper; basal thoracic wall and diaphragm localisations generally prefer dorsal regions; on the contrary apices of the thoracic cavity show a prevalent ventral distribution. Furthermore, in our case history, PPs mean thickness and extension were, respectively, 5.5 ± 2.96 mm (range 1–12.2) and 62.9 ± 49.1 mm (range 2–178). At these sizes their CT identification should be easy, if the pleura is carefully and systematically analysed on all chest images, even if clinical suspicion of asbestos exposure is not present. This study has some limitations. Firstly the size of this case population may still be not sufficiently comprehensive to fully understand whether and how radiologists report the pleural findings on standard chest CTs. Nevertheless, the observed prevalence of PPs highlights the importance of looking carefully at the pleura, which is more assessable nowadays with the use of thin slice thickness on CTs.

## 5. Conclusions

In conclusion, this study shows that PPs can be detected on CTs even in absence of clinical suspicion of asbestos exposure, but regardless of their potential relevance, they are often underreported. Knowledge of the typical appearance and location of PPs is crucial for their correct recognition and their differentials. However the patient's job history should always be kept in mind and the associated findings carefully looked at.

## Conflicts of Interest

The authors declare that they have no conflicts of interest.

## References


[1] Committee on Nonoccupational Health Risks of Asbestiform Fibers Board of Toxicology and Enviromental Health Hazard and National Research Council, *Asebstiform Fibers: Nonoccupational Health Risks*, National Academies Press, Washington, DC, USA, 1984.

[2] American Thoracic Society, "Diagnosis and initial management of nonmalignant disease related to asbestos," *American Journal of Respiratory and Critical Care Medicine*, vol. 170, no. 6, pp. 691–715, 2004.

[3] A. Marinaccio, A. Binazzi, D. D. Marzio et al., "Pleural malignant mesothelioma epidemic: incidence, modalities of asbestos exposure and occupations involved from the Italian National Register," *International Journal of Cancer*, vol. 130, no. 9, pp. 2146–2154, 2012.

[4] A. Marinaccio, F. Montanaro, M. Mastrantonio et al., "Predictions of mortality from pleural mesothelioma in Italy: a model based on asbestos consumption figures supports results from age-period-cohort models," *International Journal of Cancer*, vol. 115, no. 1, pp. 142–147, 2005.

[5] J. C. McDonald, A. D. McDonald, B. Armstrong, and P. Sebastien, "Cohort study of mortality of vermiculite miners exposed to tremolite," *British Journal of Industrial Medicine*, vol. 43, pp. 436–444, 1986.

[6] M. Artvinli and Y. I. Baris, "Malignant mesotheliomas in a small village in the anatolian region of turkey: an epidemiologic study," *Journal of the National Cancer Institute*, vol. 63, no. 1, pp. 17–22, 1979.

[7] R. N. Jones, T. McLoud, and S. D. Rockoff, "The radiographic pleural abnormalities in asbestos exposure: relationship to physiologic abnormalities," *Journal of Thoracic Imaging*, vol. 3, no. 4, pp. 57–66, 1988.

[8] T. C. Larson, M. Lewin, E. B. Gottschall, V. C. Antao, V. Kapil, and C. S. Rose, "Associations between radiographic findings and spirometry in a community exposed to Libby amphibole," *Occupational and Environmental Medicine*, vol. 69, no. 5, pp. 361–366, 2012.

[9] B. Clin, C. Paris, J. Ameille et al., "Do asbestos-related pleural plaques on HRCT scans cause restrictive impairment in the absence of pulmonary fibrosis?" *Thorax*, vol. 66, no. 11, pp. 985–991, 2011.

[10] D. W. Cugell and D. W. Kamp, "Asbestos and the pleura: a review," *Chest*, vol. 125, no. 3, pp. 1103–1117, 2004.

[11] J.-C. Pairon, P. Andujar, M. Rinaldo et al., "Asbestos exposure, pleural plaques, and the risk of death from lung cancer," *American Journal of Respiratory and Critical Care Medicine*, vol. 190, no. 12, pp. 1413–1420, 2014.

[12] H. Arakawa, T. Kishimoto, K. Ashizawa et al., "Asbestosis and other pulmonary fibrosis in asbestos-exposed workers: high-resolution CT features with pathological correlations," *European Radiology*, vol. 26, no. 5, pp. 1485–1492, 2016.

[13] T. Yusa, K. Hiroshima, F. Sakai et al., "Significant relationship between the extent of pleural plaques and pulmonary asbestos body concentration in lung cancer patients with occupational asbestos exposure," *American Journal of Industrial Medicine*, vol. 58, no. 4, pp. 444–455, 2015.

[14] L. D. Maxim, R. Niebo, and M. J. Utell, "Are pleural plaques an appropriate endpoint for risk analyses?" *Inhalation Toxicology*, vol. 27, no. 7, pp. 321–334, 2015.

[15] A. C. Friedman, S. B. Fiel, M. S. Fisher, P. D. Radecki, A. S. Lev-Toaff, and D. F. Caroline, "Asbestos-related pleural disease and asbestosis: a comparison of CT and chest radiography," *American Journal of Roentgenology*, vol. 150, no. 2, pp. 269–275, 1987.

[16] D. R. Aberle, G. Gamsu, C. S. Ray, and I. M. Feuerstein, "Asbestos-related pleural and parenchymal fibrosis: detection with high-resolution CT," *Radiology*, vol. 166, no. 3, pp. 729–734, 1988.

[17] M. Elshazley, E. Shibata, N. Hisanaga et al., "Pleural plaque profiles on the chest radiographs and ct scans of asbestos-exposed Japanese construction workers," *Industrial Health*, vol. 49, no. 5, pp. 626–633, 2011.

[18] K. M. Alfudhili, D. A. Lynch, F. Laurent, G. R. Ferretti, V. Dunet, and C. Beigelman-Aubry, "Focal pleural thickening mimicking pleural plaques on chest computed tomography: tips and tricks," *British Journal of Radiology*, vol. 89, no. 1057, Article ID 20150792, 2015.

[19] N. A. Jarad, P. Wilkinson, M. C. Pearson, and R. M. Rudd, "A new high resolution computed tomography scoring system for pulmonary fibrosis, pleural disease, and emphysema in patients with asbestos related disease," *British Journal of Industrial Medicine*, vol. 49, no. 2, pp. 73–84, 1992.

[20] L. L. Berland, "The American College of Radiology Strategy for Managing Incidental Findings on Abdominal Computed Tomography," *Radiologic Clinics of North America*, vol. 49, no. 2, pp. 237–243, 2011.

[21] J. B. Alpert and D. P. Naidich, "Imaging of incidental findings on thoracic computed tomography," *Radiologic Clinics of North America*, vol. 49, no. 2, pp. 267–289, 2011.

[22] S. Porru, A. Carta, E. Toninelli, G. Bozzola, and C. Arici, "Reducing the underreporting of lung cancer attributable to occupation: outcomes from a hospital-based systematic search in Northern Italy," *International Archives of Occupational and Environmental Health*, vol. 89, no. 6, pp. 981–989, 2016.

[23] A. G. Pitman, "Perceptual error and the culture of open disclosure in Australian radiology," *Australasian Radiology*, vol. 50, no. 3, pp. 206–211, 2006.

[24] A. Pinto and L. Brunese, "Spectrum of diagnostic errors in radiology," *World Journal of Radiology*, vol. 2, pp. 377–383, 2010.

[25] A. Pinto, L. Brunese, F. Pinto, R. Reali, S. Daniele, and L. Romano, "The concept of error and malpractice in radiology," *Seminars in Ultrasound, CT and MRI*, vol. 33, no. 4, pp. 275–279, 2012.

[26] A. Pinto, F. Caranci, L. Romano, G. Carrafiello, P. Fonio, and L. Brunese, "Learning from errors in radiology: a comprehensive review," *Seminars in Ultrasound, CT and MRI*, vol. 33, no. 4, pp. 379–382, 2012.

[27] M. A. Mazzei and L. Volterrani, "Errors in multidetector row computed tomography," *Radiologia Medica*, vol. 120, no. 9, pp. 785–794, 2015.

[28] L. Berlin, "Malpractice issues in radiology. Alliterative errors," *American Journal of Roentgenology*, vol. 174, no. 4, pp. 925–931, 2000.

[29] M. Claude-Desroches, G. Bierry, D. Touitou-Gottenberg, J.-L. Golmard, P. A. Grenier, and C. Beigelman-Aubry, "Focal dependent pleural thickening at MDCT: pleural lesion or functional abnormality?" *Diagnostic and Interventional Imaging*, vol. 93, no. 5, pp. 360–364, 2012.

[30] V. Paolucci, R. Romeo, AG. Sisinni, D. Bartoli, MA. Mazzei, and P. Sartorelli, "Silicosis in workers exposed to artificial quartz conglomerates: does it differ from chronic simple silicosis?" *Arch Bronconeumol*, vol. 51, no. 12, pp. e57–e60, 2015.

[31] Y. Kim, J.-P. Myong, J. K. Lee, J. S. Kim, Y. K. Kim, and S.-H. Jung, "CT characteristics of pleural plaques related to occupational or environmental asbestos exposure from South Korean asbestos mines," *Korean Journal of Radiology*, vol. 16, no. 5, pp. 1142–1152, 2015.

Hindawi
BioMed Research International
Volume 2017, Article ID 1854027, 15 pages
https://doi.org/10.1155/2017/1854027

*Review Article*

# Imaging and Management of Incidental Renal Lesions

**Silvio Mazziotti, Giuseppe Cicero, Tommaso D'Angelo, Maria Adele Marino, Carmela Visalli, Ignazio Salamone, Giorgio Ascenti, and Alfredo Blandino**

*Department of Biomedical Sciences and Morphological and Functional Imaging, University of Messina, Policlinico "G. Martino", Via Consolare Valeria 1, 98100 Messina, Italy*

Correspondence should be addressed to Alfredo Blandino; ablandino@unime.it

Received 22 February 2017; Accepted 4 May 2017; Published 31 May 2017

Academic Editor: Luca Macarini



The increased use of imaging modalities in the last years has led to a greater incidence in depicting abdominal incidental lesions. In particular, "incidentalomas" of the kidney are discovered in asymptomatic patients or patients who suffer from diseases not directly related to the kidneys. The aim of this paper is to provide the radiologist with a useful guide to recognize and classify the main incidental renal findings with the purpose of establishing the correct management. First we describe the so-called "pseudotumors" which are important to recognize in order to avoid a misdiagnosis. Afterwards we categorize true renal lesions into cystic and solid types, reporting radiological signs helpful in differentiating between benign and malignant nature.

## 1. Introduction

The majority of renal masses are found incidentally as a result of the widespread use of ultrasonography (US) and computed tomography (CT) as well as magnetic resonance imaging (MRI) performed for problems often unrelated to the kidneys. Furthermore, technological improvements have increased the spatial, contrast, and temporal resolution of these imaging modalities allowing for higher rates of detection.

Therefore, so often, these incidental renal masses are recognized in patients without symptoms directly ascribable to the kidneys.

In an aging population, the incidence of renal incidentalomas is rising because the prevalence of both renal cysts and renal cell carcinoma (RCC) increases with the age. Autopsy results have shown that almost half of people older than 50 years have one or more renal masses. Most of these represent simple cysts that can be easily diagnosed as benign on the basis of imaging and do not require treatment. However, complex cystic and solid renal masses are also discovered, many of which are clearly malignant and need to be surgically removed, while others may not require surgical intervention.

In any case, despite the most frequent benign nature of the incidental renal lesions, their discovery often produces a cascade of costly examinations also determining patient's anxiety and unnecessary radiation exposure.

In this context, whenever an incidental renal mass is found, it is important (a) to establish the most likely diagnosis on the basis of imaging findings and (b) to set the correct management for possible malignant lesions (e.g., close follow-up, change imaging technique, percutaneous biopsy, surgery, or ablation).

The aim of this paper is to provide the radiologist with a useful guide for the most correct interpretation of incidental renal findings in order to distinguish surgical from nonsurgical lesions.

Initially, we describe pseudotumors, a common pitfall in the radiological approach to renal incidentalomas. Afterwards, we categorize true renal lesions into cystic and solid types, reporting radiological signs helpful in differentiating their behavior, from benign to potentially serious, including malignant.

## 2. Pseudotumors

"*Pseudotumors*" are common findings which can mimic a mass for their appearance; the most common ones are the hypertrophied column of Bertin and the lobar dimorphisms (like the "dromedary hump" or the persistent fetal lobulations).

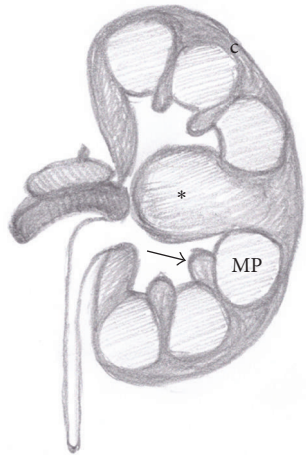


Figure 1: Anatomical drawing of a hypertrophied column of Bertin (asterisk). Normal renal column (arrow); medullary pyramid (MP); renal cortex (c).

The *hypertrophied column of Bertin* (also known as "septa of Bertin") is a common anatomical variant consisting in a "mass-like" enlargement of the cortical tissue normally present between the renal pyramids. It is usually located in the middle third of the kidney, more commonly on the left side (Figure 1) [1].

Sonography can easily recognize this condition, characterized by the same echogenicity of renal parenchyma, smooth renal contour, and lack of acoustic posterior enhancement (Figure 2(a)) [2]. Moreover, on Doppler US, septa of Bertin show arterial and venous flow pattern similar to the renal parenchyma [3].

Contrast-enhanced US (CEUS) can be a useful tool to confirm the normal cortical tissue interposed between medullary pyramids (Figures 2(b) and 2(c)).

Sometimes an atypical appearance may require further evaluation with cross-sectional imaging. Hypertrophic column of Bertin is isodense at CT and isointense at MRI to the normal renal parenchyma.

Contrast-enhanced imaging (US, CT, and MR) will show the same enhancement pattern of the surrounding renal parenchyma (Figures 3(a), 3(b), and 4) allowing the differential diagnosis between pseudotumors and infiltrative solid renal lesion (Figure 5) [2, 4, 5].

*Dromedary hump* or *splenic hump* appears as a focal bulge on the lateral border of the left kidney, caused by the splenic impression on its superolateral contour. It can be easily diagnosed with sonography due to the same echogenicity of the renal parenchyma and normal blood flow at color Doppler and CEUS [4, 5]. At unenhanced and contrast-enhanced CT and MRI it shows the same features of the normal renal parenchyma.

*Persistent fetal lobulation (lobation)* is a normal variant diagnosed in 4% of children and 10% of adult population. It consists of an indentation of the renal surface in between the renal pyramids, caused by an incomplete fusion of the renal lobules during early childhood (Figures 6, 7(a), and 7(b)) [5, 6]. When depicted in adult kidneys, it can be misdiagnosed with a tumor or a renal scar.

Postpyelonephritic renal scars can be easily distinguished because they usually overlay the medullary pyramids with calyceal clubbing due to the retraction of the papilla from the scar (Figure 8).

*Infectious processes* (pyelonephritis, abscesses) or *traumatic injuries* were excluded from this topic because of the symptoms and the clinical history of the patient.

## 3. Cystic Lesions

The majority of cystic lesions incidentally discovered at imaging are simple cysts which are easily diagnosed and do not require further follow-up or treatment. However, complex cysts that need a more careful evaluation are not so rare [7].

The Bosniak classification is an evaluating system of cystic renal masses, originally based only on contrast-enhanced CT findings but then commonly applied to US and MRI. It is used to categorize a cystic renal mass according to the risk of malignancy into one of five categories (I, II, IIF, III, and IV) and to suggest the consequent follow-up or treatment [7, 8].

In particular, a correct Bosniak classification of a cystic renal lesion requires the i.v. administration of contrast medium, in order to evaluate the enhancement of septa, walls, or nodules.

In this regard contrast-enhanced multiphasic evaluation at cross-sectional imaging, composed of corticomedullary, early and delayed nephrographic phases, is usually performed.

A further help in depicting even small amounts of intralesional contrast medium enhancement can also come from CEUS, dual-energy CT, and dynamic contrast-enhanced subtraction MRI [7, 9–12].

Sometimes *vascular anomalies* (such as renal artery aneurysm or arteriovenous fistula) may also mimic a cystic renal lesion on US. When an anechoic lesion is depicted within the renal sinus or in the central part of the kidney it is mandatory to complete the examination with Doppler evaluation (Figure 9). Contrast-enhanced CT or contrast-enhanced MRI can also easily demonstrate the fake cystic nature of the vascular anomaly [7, 9].

*3.1. Benign Cysts (Categories I and II).* At US examination a simple renal cyst is defined as a rounded, anechoic lesion with a posterior acoustic enhancement, although this last finding is not specific.

At MRI simple cysts are hypointense on T1-weighted sequences and strongly hyperintense at T2-weighted images [7, 9].

According to the Bosniak classification, a benign simple cyst *(category I)* typically shows water attenuation values at CT-scan (<20 HU) without enhancement after i.v. contrast medium administration and a hairline-thin wall and does not contain septa, calcifications, or solid components.

There is no enhancement if the attenuation increases by less than 10 HU [8, 9, 13]. Enhancement is considered unequivocal when the attenuation of the mass increases over

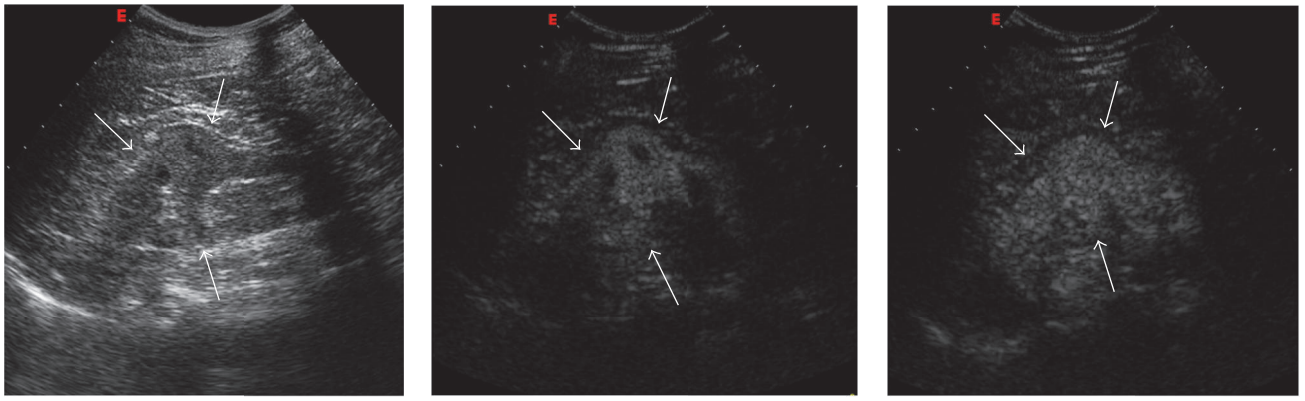

(a) (b) (c)

Figure 2: Hypertrophied column of Bertin. Gray scale US (a); CEUS (b, c). Gray scale US shows a "mass-mimicking" unfolding of cortical renal tissue (arrows) between renal medullary pyramids. After contrast medium administration, the enhancement is similar to the surrounding cortical parenchyma.

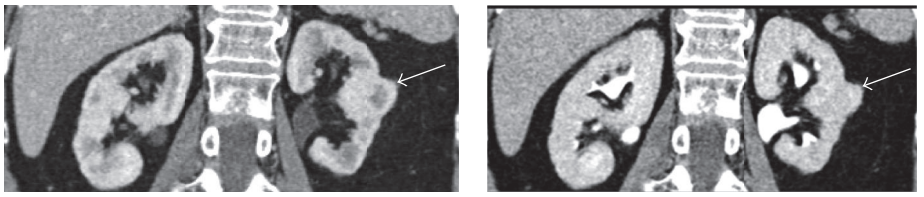

(a) (b)

Figure 3: Hypertrophied column of Bertin. Coronal reformatted contrast-enhanced CT images in corticomedullary (a) and nephrographic phase (b) well demonstrate the enlarged column of Bertin (arrows) characterized by the same pattern of enhancement of the normal renal cortex.

20 HU and ambiguous between 10 and 20 HU (the so-called "pseudoenhancement") [9].

*Category II* cyst is a benign lesion that may contain a few hairline-thin septa in which perceived (not measurable) enhancement may be appreciated; fine calcification or a short segment of slightly thickened calcification may be present in the wall or septa [7].

This category also includes uniformly high-attenuating lesions smaller than 3 cm, sharply marginated, considered as benign (hemorrhagic or proteinaceous) cysts. It is already known that a renal mass with homogeneous attenuation greater than 70 HU on an unenhanced CT has a greater than 99% probability of being benign (Figure 10) [14].

MRI is helpful in clarifying hemorrhagic cysts found on ultrasound and CT, showing increased signal intensity on T1-weighted and decrease on T2-weighted images, with lack of enhancement after contrast medium injection.

Renal masses included in Bosniak categories I and II are considered benign; therefore they do not require further follow-up or intervention [7].

Although the size is not considered a parameter of Bosniak classification, renal lesions measuring less than 1 cm with simple cysts appearance are statistically likely to represent benign renal cysts. However, the real nature of these masses remains unclear due to their small dimensions.

*3.2. Low and Medium Risk of Malignancy (Categories IIF and III).* *Category IIF* lesions may contain multiple hairline-thin septa. The wall and the septa could be thickened and may contain calcifications, with perceived (not measurable) contrast enhancement [7]. There are no soft tissue enhancing nodules inside (Figure 11).

Nonenhancing high-attenuating renal lesions (<70 HU) that measure more than 3 cm are also included in this category.

These lesions are generally benign but require follow-up imaging ("F" is for follow-up) for morphologic and structural changes, such as development of septa, wall thickening, or new areas of enhancement, suggestive of malignancy [7, 9].

The recommended follow-up consists in a first CT-scan or MRI at 6–12 months, followed by yearly examinations for a minimum of 5 years [9].

*Category III* cysts show thickened irregular or smooth walls or septa manifesting measurable enhancement. This category also includes complicated hemorrhagic or infected cysts, multilocular cystic nephroma, and cystic neoplasms.

These masses are considered indeterminate, because a malignant neoplasm cannot be excluded. Therefore, a histologic diagnosis and, in many cases, also surgical intervention are required (Figure 12) [7].

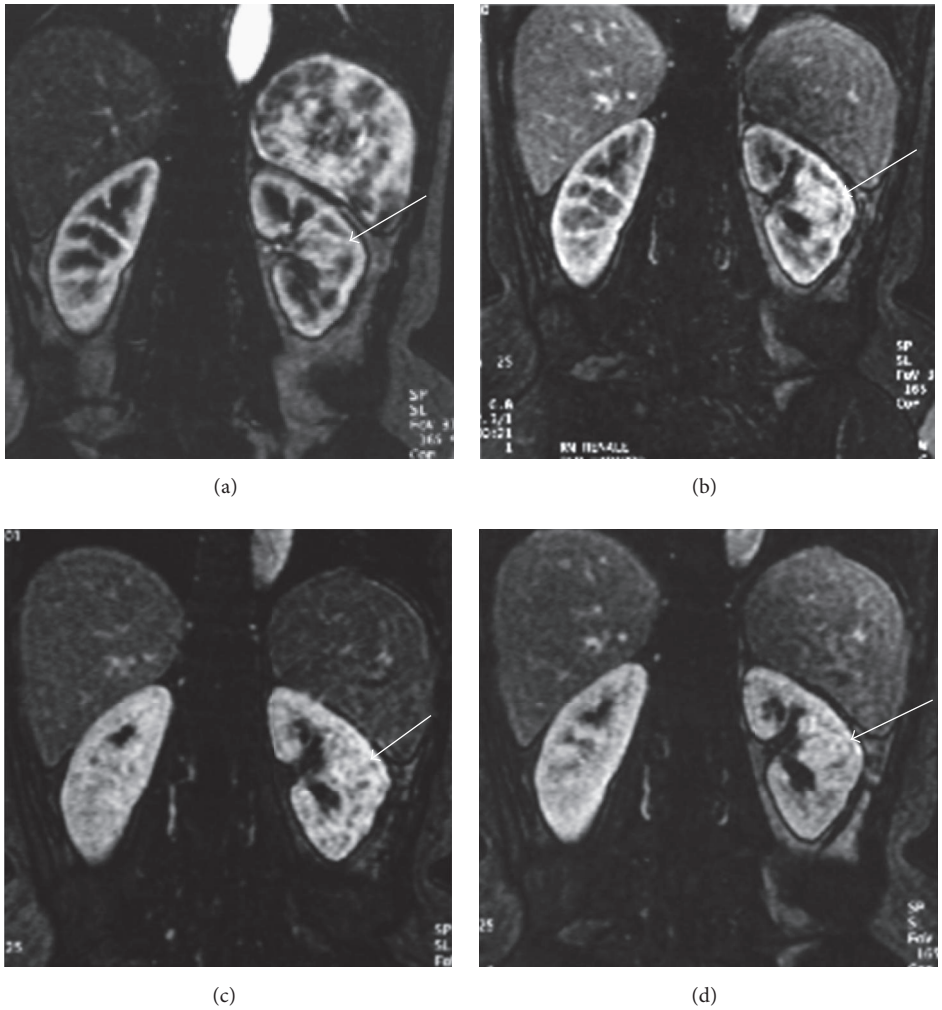

(a) (b)

(c) (d)

Figure 4: Hypertrophied column of Bertin. Coronal GE T1-weighted fat-sat gadolinium enhanced images (a–d) showing a mass-like finding in the left kidney (arrow). The prominent column of Bertin is in continuity with the renal cortex and manifests the same enhancement of the renal parenchyma in all contrastographic phases.

Differentiation between category IIF and category III can be challenging, due to the variable appearance and the radiologists' experience, and often require more than one imaging modality (Figure 13).

However, it is always extremely important to define in order to establish the correct management.

Contrary to the common opinion, it should be considered that a small percentage of category III masses can be benign (the range of malignancy is between 31% and 100%). Despite this consideration, surgery is the treatment of choice in order to avoid a misdiagnosis.

*3.3. High Risk of Malignancy (Category IV).* *Category IV* includes cystic masses with the same characteristics of category III with a distinct enhancing of soft tissue components independent of the wall or septa.

These lesions are clearly malignant and need to be surgically removed (Figure 14) [7, 9].

## 4. Solid Renal Masses

Solid renal masses are structurally characterized by little or no fluid components usually containing predominantly enhancing tissue. Although a mass-like renal abnormality with these appearances could be a consequence of infarction and infection as well as trauma, clinical history is usually indicative of these illnesses.

Depending on the final treatment, solid renal masses can be distinguished in surgical and nonsurgical lesions.

Lymphoma and renal metastases were excluded from this topic because of their less frequent discovery as incidental lesions, due to the clinical history of the patient (e.g., extrarenal primary malignancy) and the frequent involvement of other anatomical districts.

*4.1. Nonsurgical Lesions.* *Renal angiomyolipomas* (AMLs) are the most common benign renal tumors, now considered

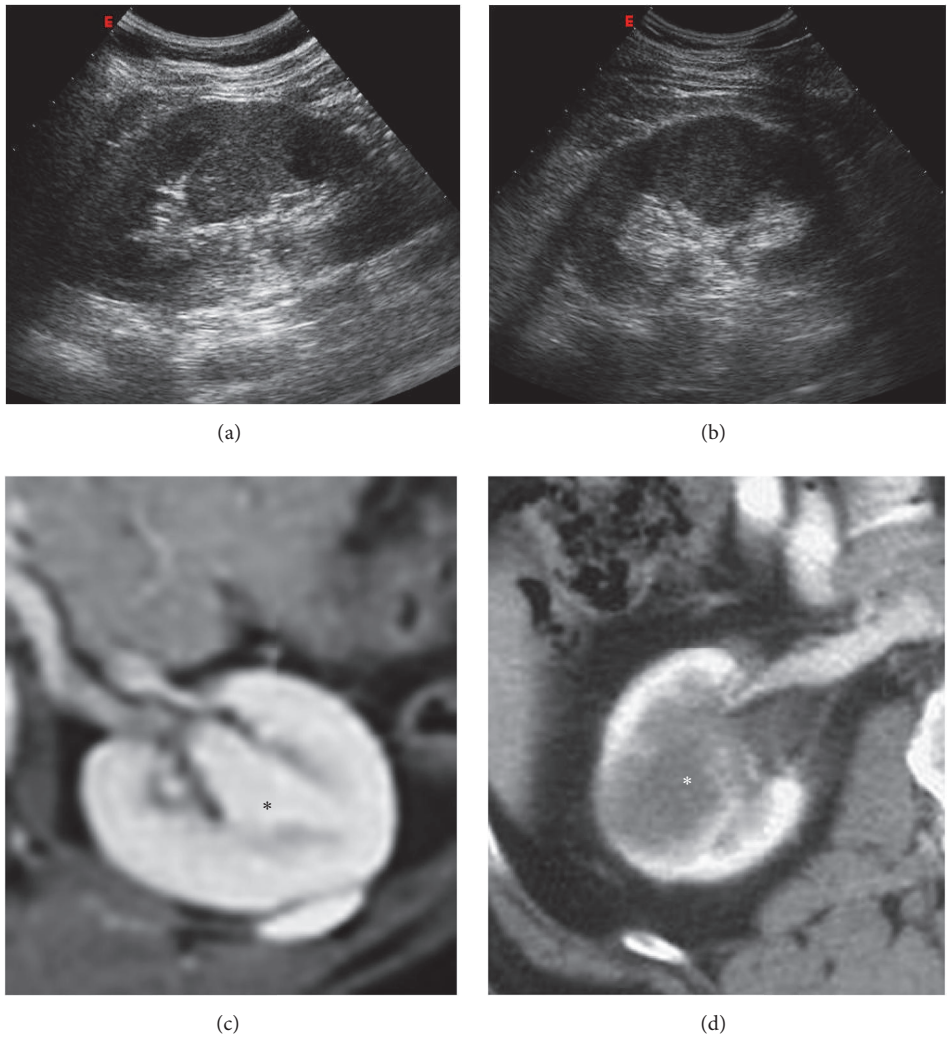


Figure 5: Pseudotumor versus true solid renal lesion. Gray scale US (a, b) and contrast-enhanced CT (c, d). Renal incidentalomas in two different patients with similar echogenicity pattern (a, b). Contrast-enhanced CT reveals a hypertrophied column of Bertin in the first case (black asterisk in (c)) and a solid hypovascular mass in the second case (white asterisk in (d)).

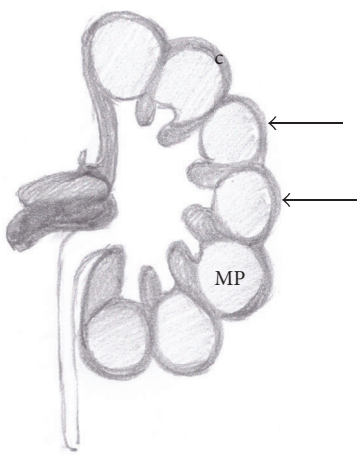


Figure 6: Anatomical drawing of persistent fetal lobulations (arrows). Medullary pyramid (MP); renal cortex (c).

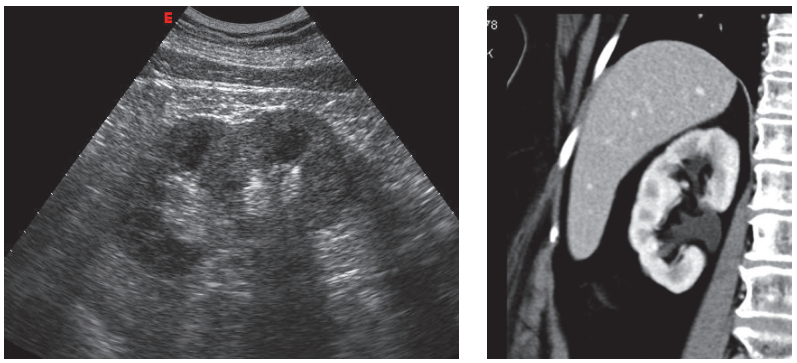

(a) (b)

Figure 7: Persistent fetal lobulations. US image (a) and multiplanar coronal contrast-enhanced CT obtained in corticomedullary phase (b). The typical appearance of the normal congenital variant is depicted on both US and contrast-enhanced CT.

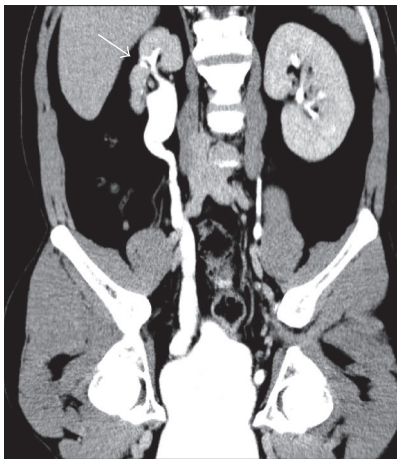

Figure 8: Postpyelonephritic scar. Coronal reformatted contrast-enhanced CT (excretory phase) shows a focal postpyelonephritic scar (arrow) in the upper-third of the right kidney with dilatation of ipsilateral renal pelvis and ureter.

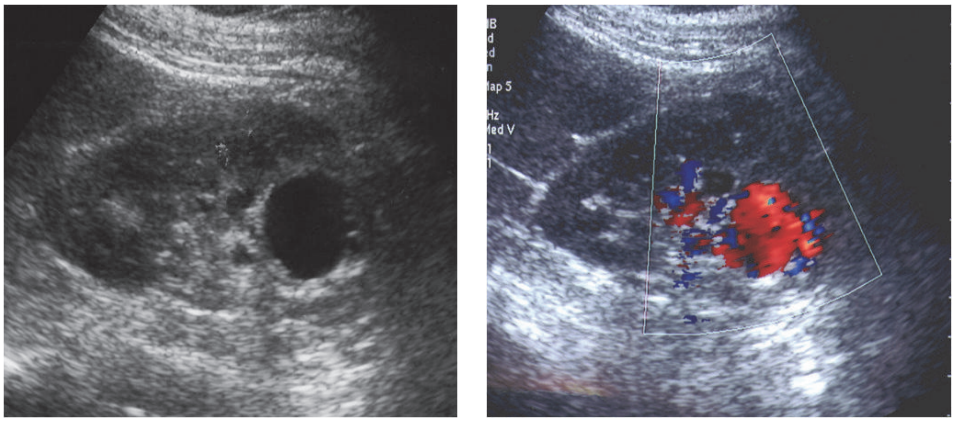

(a) (b)

Figure 9: Vascular malformation. Longitudinal gray scale US (a); color Doppler US (b). Gray scale US of the right kidney shows an anechoic renal lesion. At color Doppler vascular flow is depicted within the lesion allowing the diagnosis of a vascular malformation.

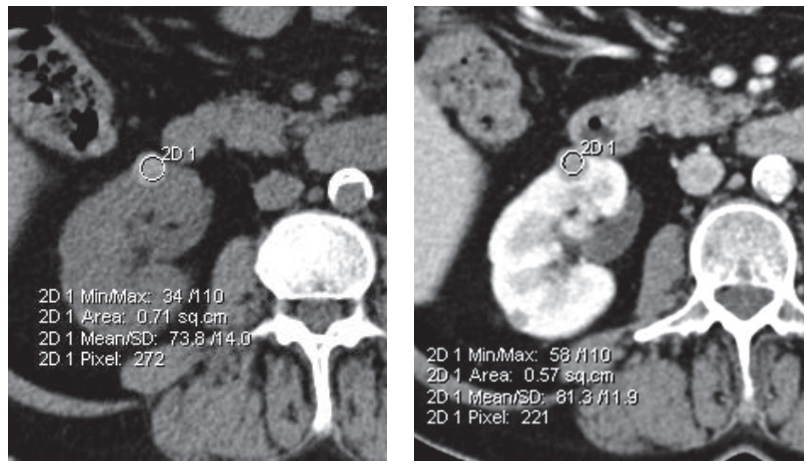


(a) (b)

Figure 10: Benign hyperdense renal cyst. Axial CT-scan before (a) and after contrast medium administration (b). The region of interest (ROI) positioned on the small exophytic renal cyst shows high-density content (73 HU) without any significant increase in postcontrastographic study.

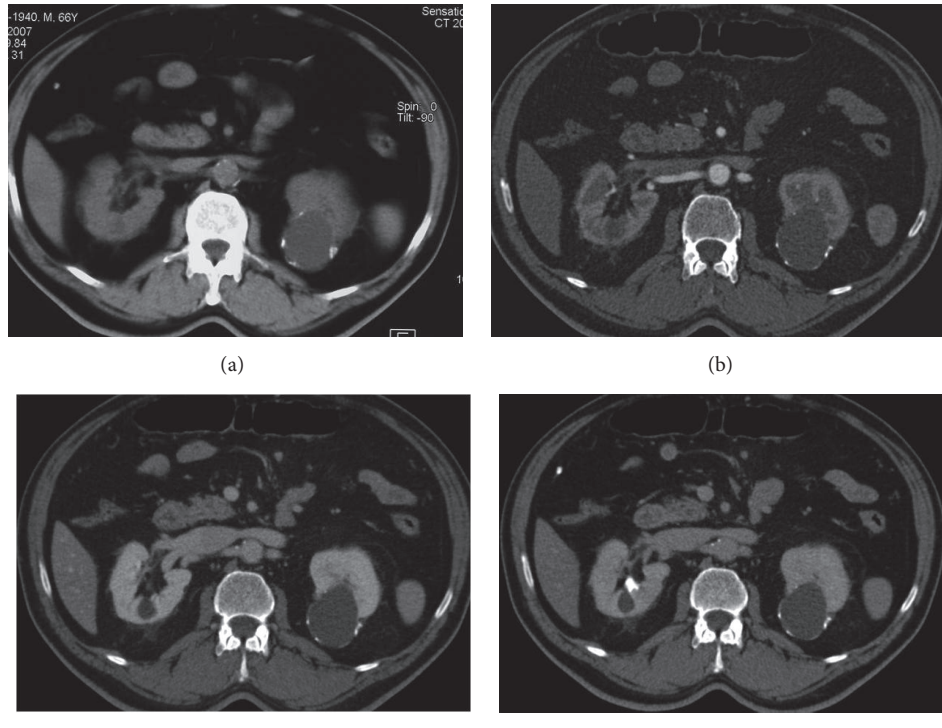

(a) (b)

(c) (d)

Figure 11: Bosniak category IIF cyst. Axial unenhanced (a) and enhanced CT-scans performed at corticomedullary (b), nephrographic (c), and excretory phase (d). The images show a large hypodense cyst in the left kidney with wall calcifications. A small simple cyst is also visible in the third middle of the right kidney.

among the family of perivascular epithelioid cell tumors (PEComa) and divided into two histological categories: triphasic AMLs and monotypic epithelioid AMLs [15].

While the latter ones represent an extremely rare and potentially malignant type, containing few or no fat cells, triphasic AMLs are the most common, with variable amount of vascular, muscular, and adipose components, and further categorized into classic and fat-poor lesions.

The frequent hyperechogenicity of AML at US is not specific and requires further evaluations to rule out a RCC.

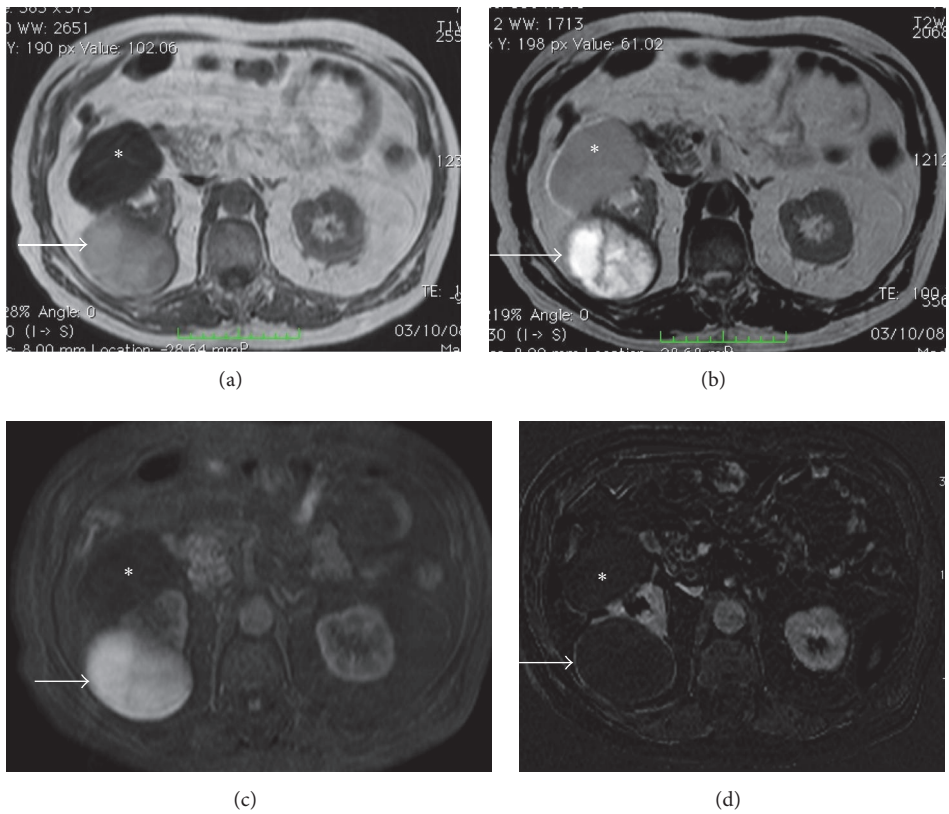


Figure 12: Hemorrhagic cyst. MRI GE T1-weighted (a), TSE T2-weighted (b), contrast-enhanced GE T1-weighted fat-sat (c), and subtracted postcontrastographic (d) image. A large cystic lesion is detectable on the right kidney (arrows), characterized by mild hyperintensity on GE T1-weighted images and inhomogeneous hyperintensity on T2-weighted and on contrast-enhanced GE T1-weighted fat-sat images. On subtracted postcontrastographic image (d) the lesion shows a regular thin wall with mild enhancement. The final histological diagnosis was hemorrhagic cyst. Note also an anterior huge simple cyst (asterisk) in the same kidney.

Although CEUS can potentially add diagnostic value, frequently showing a peripheral enhancement pattern, cross-sectional imaging is needed [10, 16].

In fact detection of macroscopic fat in a renal lesion is a specific finding of *Classic AMLs*, which are typically hypodense at CT-scan (<10 HU), hyperintense on T1- and T2-weighted sequences at MRI, and with loss of signal following frequency-selective fat-saturation technique; other typical MRI features include high signal intensity on T1-weighted GE in-phase (IP) and opposed-phase sequences (OP) with signal dropout on opposed-phase at the interface of the lesion with the normal parenchyma ("India-ink" artifact) (Figure 15) and high signal intensity on fat-only reconstruction from Dixon-based acquisitions.

Fat-poor AMLs (5% of all AMLs) without detectable fat on imaging cannot be differentiated from other renal masses, due to the lack of a typical appearance.

In particular, depending on fat-cell distribution and amount, fat-poor AMLs can appear as hyperattenuating (>45 HU) or isoattenuating (−10 to 45 HU) at CT-scan [15].

Moreover, MRI features overlap with RCCs; indeed, the typical T2-weighted low signal intensity of fat-poor AMLs can almost exclude a clear cell RCC but not a papillary RCC (although a small proportion of clear cell RCCs and chromophobe RCCs also had low signal intensity on T2-weighted images).

Furthermore, a signal loss in opposed-phase images cannot be used to accurately distinguish minimal fat AMLs from clear cell RCCs, which may present intracytoplasmic lipid-containing vacuoles.

Additionally, it should be noticed that the presence of necrosis virtually excludes the diagnosis of AML [16].

Other considerations were made about contrast-enhancement pattern and DWI in order to differentiate AMLs from RCCs, but the literature's data are not always univocal.

According to Sasiwimonphan et al. [17] the so-called arterial/delayed enhancement ratio (defined as the difference in signal intensity between arterial and precontrast phase divided by the difference between delayed and precontrast phase) can be helpful in differentiating poor fat AMLs from RCCs with values greater than 1.5 favoring the first [15]. However, more recently, Hakim et al. demonstrated that the contrast-enhancement pattern cannot be reliable due to overlap with the clear cell RCC enhancement [18].

Even DWI showed ambiguous results in differentiating AMLs from malignant masses.

Indeed, though some authors described a possible differential diagnosis between AMLs and RCCs depending on

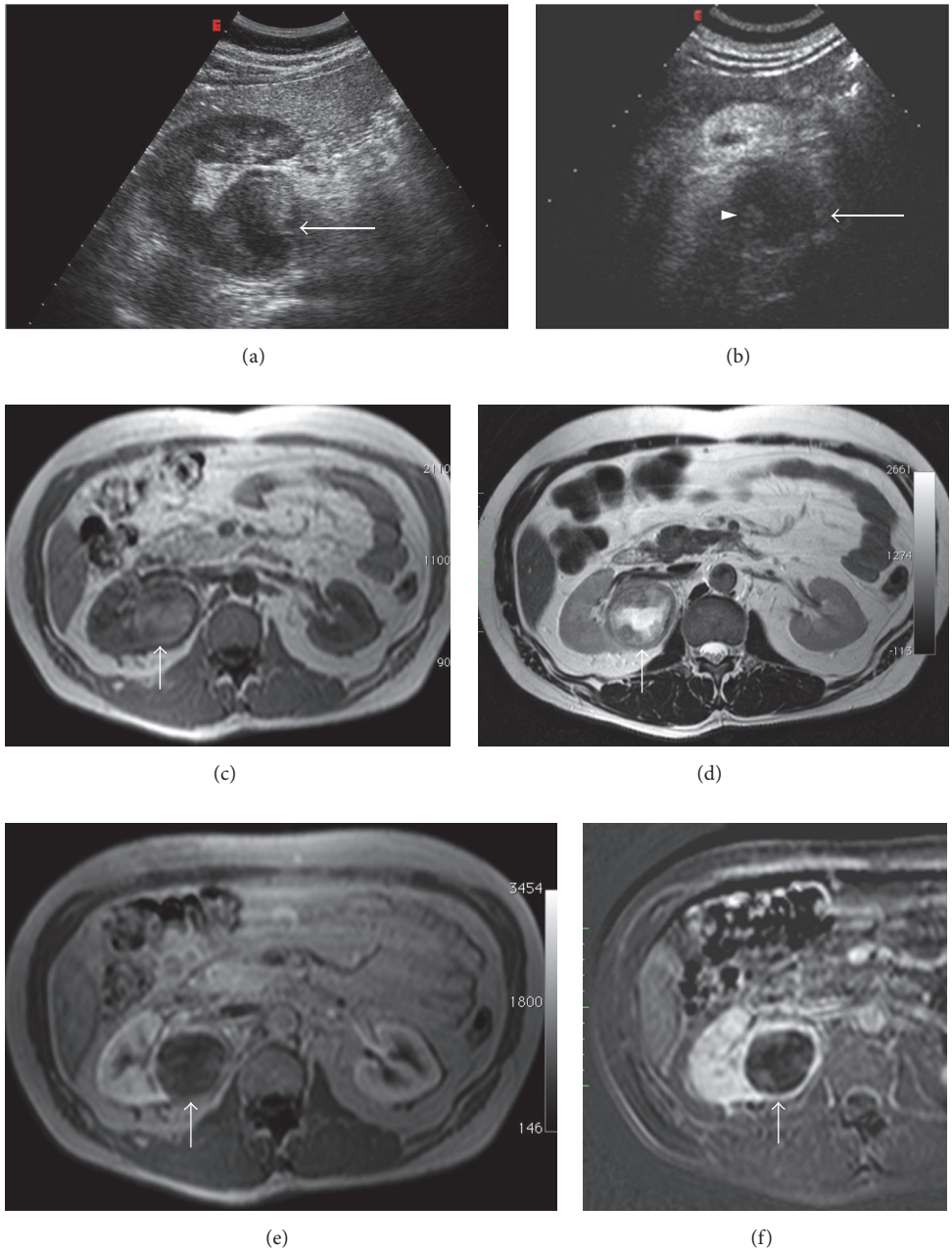


Figure 13: Cystic neoplasm (Bosniak category III). US examination shows a large inhomogeneous hypoechoic mass (arrow) in the third middle of the right kidney (a). At CEUS, enhancement of intralesional septa and nodulations (arrowhead) is also detectable (b). MRI in the same patient (c–f). The mass (arrow) is characterized by an inhomogeneous mild hyperintensity on axial GE T1-weighted image (c) and a central area of hyperintensity on axial T2-weighted TSE image (d). Axial contrast-enhanced GE T1-weighted fat-sat image (e) and subtracted image (f): enhancement of the small solid peripheral component is better depicted on the subtracted image, with similar CEUS appearance.

ADC map [19], up to now these data are not sufficiently reliable due to the great variability of the *b* values used, the MR field strength of the scanner, and even between individual readers picking the region of interest (ROI) [15].

*Oncocytoma* is the second benign renal tumor (3–9% of all primary renal neoplasms), hypo- or isoechoic solid mass at US, with homogeneous CT-attenuation values if small (<3 cm) and heterogeneous if large (>3 cm) and a T1-hypointensity and a T2-hyperintensity at MRI.

More typical features of oncocytoma, when present, are the central scar and the arterial spoke-wheel pattern of enhancement; moreover, at CT, in small oncocytomas (<4 cm) the "segmental inversion enhancement pattern" was recently described that is based on the presence of two

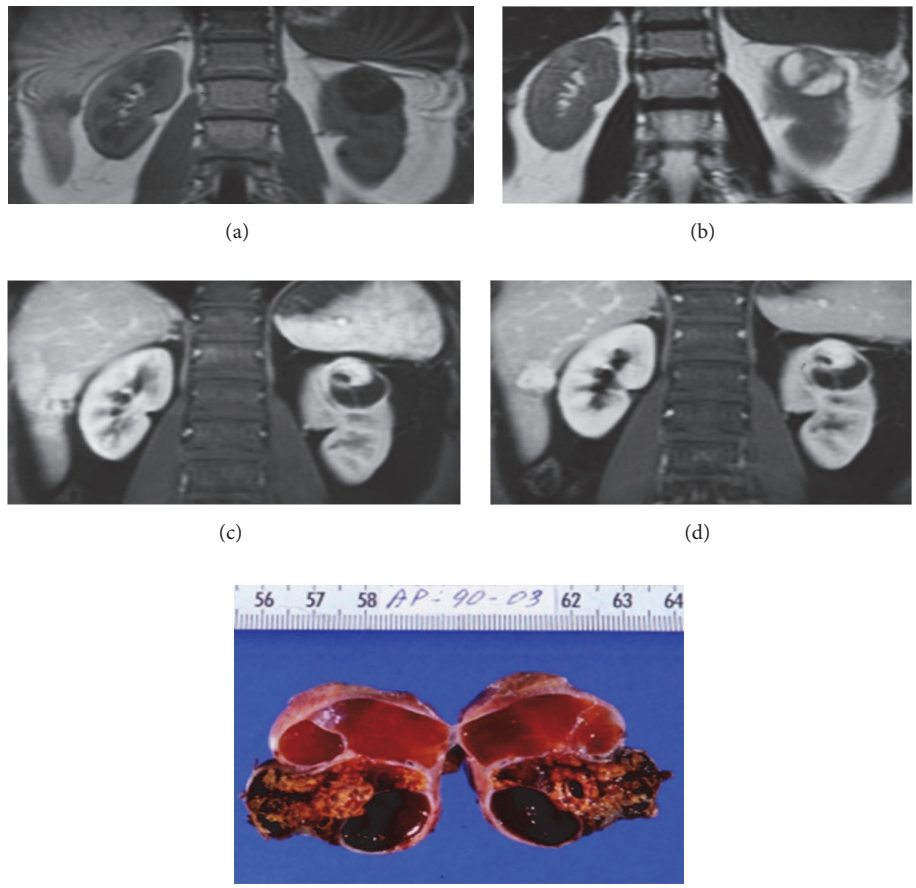


Figure 14: Bosniak IV type cystic lesion. Coronal GE T1-weighted image (a); coronal TSE T2-weighted image (b); contrast-enhanced coronal GE-T1 weighted image in corticomedullary (c) and nephrographic (d) phases. The cystic lesion with huge high enhanced solid parietal nodule is well depicted. Note also the good anatomoradiological correlation between the MR examination and histologic specimen (d). Note also a small liver hemangioma.

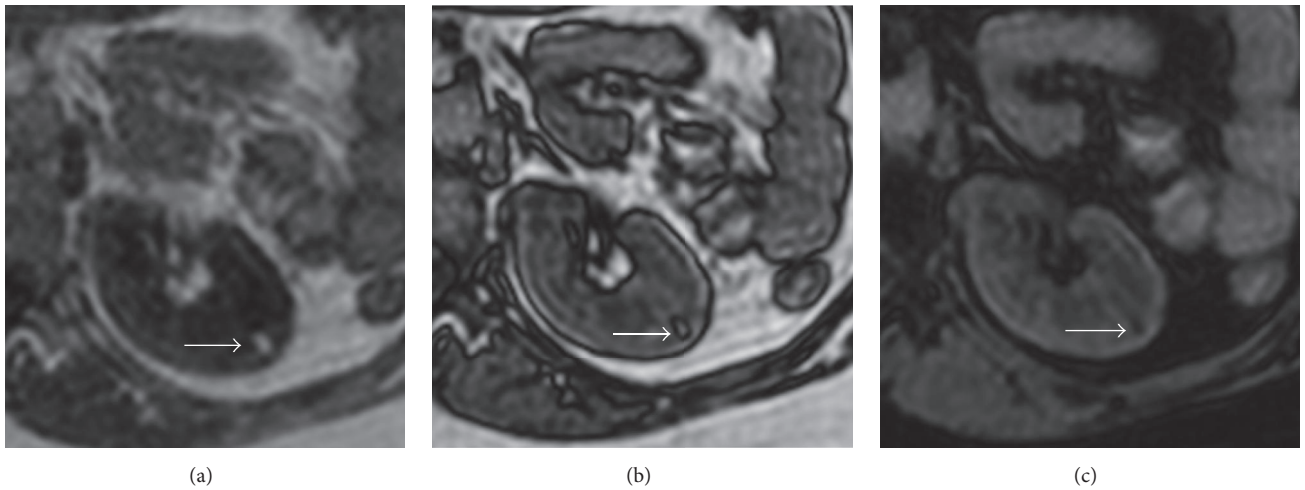


Figure 15: Small left kidney typical AML. Axial GE T1-weighted IP image (a); axial GE T1-weighted OP image (b); axial GE T1-weighted fat-sat image. A small renal AML with typical appearance (arrow): high signal intensity on T1-weighted IP image, "India-ink" artifact on T1-weighted OP image, and loss of signal intensity on T1-weighted fat-sat image.

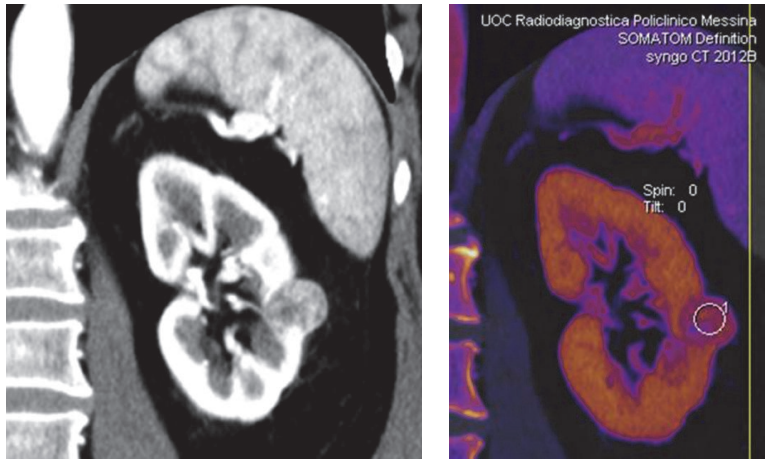


(a) (b)

Figure 16: Small cc-RCC. Coronal reformatted DE arterial-phase CT image (a); coronal color-coded iodine overlay image (b). High enhanced solid renal mass with an high iodine content (2.4 mgI on ROI).

distinct regions of enhancement in the corticomedullary phase (30–40 s) in which its degree reverses in the nephrographic phase (120–180 s) [9, 13, 20].

Unfortunately, all the imaging findings described up to now are not specific for oncocytoma and the final diagnosis is generally reached with biopsy [13].

However, recently, some authors evaluated if DWI can play a role in distinguishing oncocytoma from malignant lesions, reporting a significant difference with higher ADC values for the first ones [15, 16, 21, 22].

*4.2. Surgical Lesions.* RCC is the eighth most common tumor in the adulthood (2-3% of adult cancers) and the first tumor in the urinary tract (90%) [9, 23].

The most common histological subtypes are clear cell (cc-RCC, 75%), papillary (p-RCC, 10–15%), and chromophobe (ch-RCC, 5%) RCCs, with a better outcome for the last two [16, 24].

At US, RCCs are usually depicted as hypoechoic or isoechoic masses; Doppler and CEUS may be useful in depicting renal vein or inferior vena cava thrombosis [13] and in evaluating the vascularization of the mass but did not show a sufficient accuracy in differentiating the histological subtypes of RCCs [16, 25–27].

On noncontrast CT, RCCs are usually characterized by a soft tissue attenuation, except for larger lesions that can show heterogeneous content. Enhanced CT may be helpful in differentiating the tumor subtypes, magnifying the histological characteristics. Indeed, due to its rich vascular network, clear cell RCC manifests stronger enhancement in both the corticomedullary and excretory phases, while papillary and chromophobe tumors, which are less vascularized, tend to manifest a lower, homogeneous, and more peripheral enhancement.

Moreover, on dual-energy CT, the determination of iodine content on color-coded iodine overlay dual-energy images can allow an earlier recognition of clear cell histotype, which is the most aggressive RCC, with a significant improvement of patient's outcome (Figure 16) [28–31].

At MRI all RCCs are fundamentally hyperintense at T2-weighted sequences except for the papillary subtype, because of its hypovascularity (Figure 17). T1 signal intensity is always variable, depending on the presence of intralesional degeneration areas (hemorrhagic, cystic, or necrotic). After contrast medium administration, MRI shows the same enhancement patterns described for contrast-enhanced CT and can be useful in depicting renal vein and inferior vena cava involvement.

Although several recent studies have evaluated the use of DWI in RCCs, showing higher ADC values in cc-RCCs than papillary and chromophobic types, up to now it cannot be used in distinguishing among the different histotypes [32, 33].

However, imaging differentiation of the histological subtypes of RCCs may be unnecessary, considering that the characterization is reached by biopsy and the treatment is anyway surgical intervention.

## 5. Conclusions

Despite the substantial advances in the imaging-based diagnosis of the last decades, the characterization of incidental renal lesions still remains one of the most challenging topics for the radiologist.

Although cross-sectional imaging can confidently distinguish almost all large masses, the major critic point concerns the correct stratification of complex cysts and the characterization of small solid lesions.

Based on the probability of malignancy, active surveillance or biopsy can be suggested in order to avoid useless and more invasive treatments (like percutaneous ablation or surgical intervention) (Tables 1 and 2) (Figure 18).

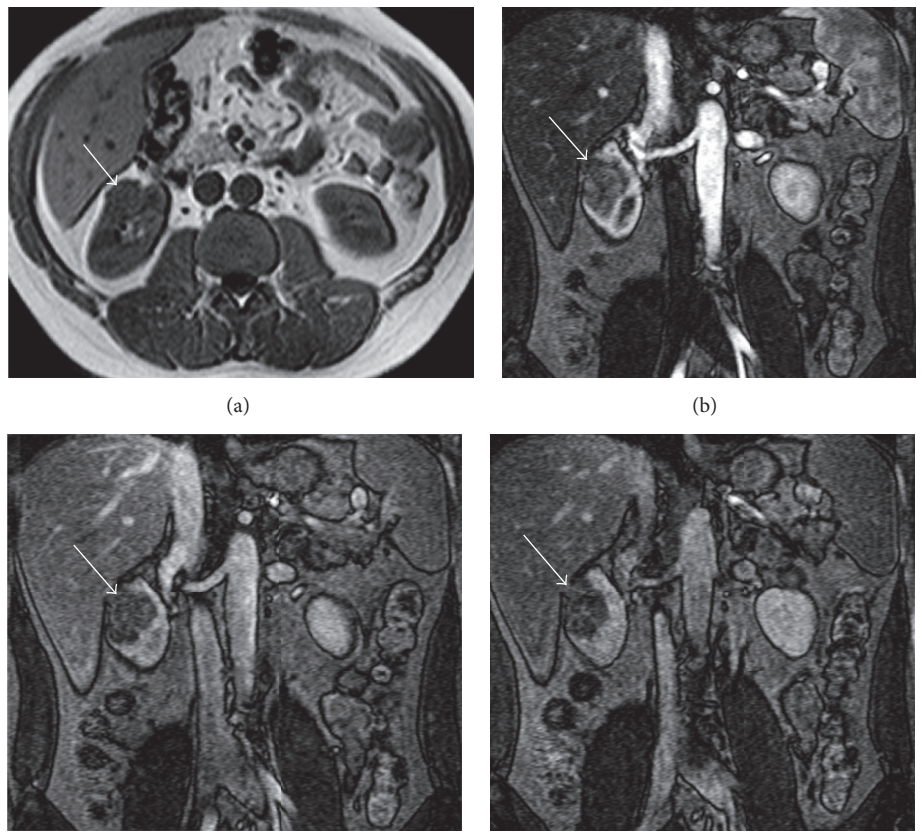


Figure 17: P-RCC. Axial GE T1-weighted image (a); coronal GE T1-weighted dynamic contrast-enhanced MR scans (b–d). Exophytic isointense nodule (arrow) in the right kidney with poor enhancement in multiphasic study.

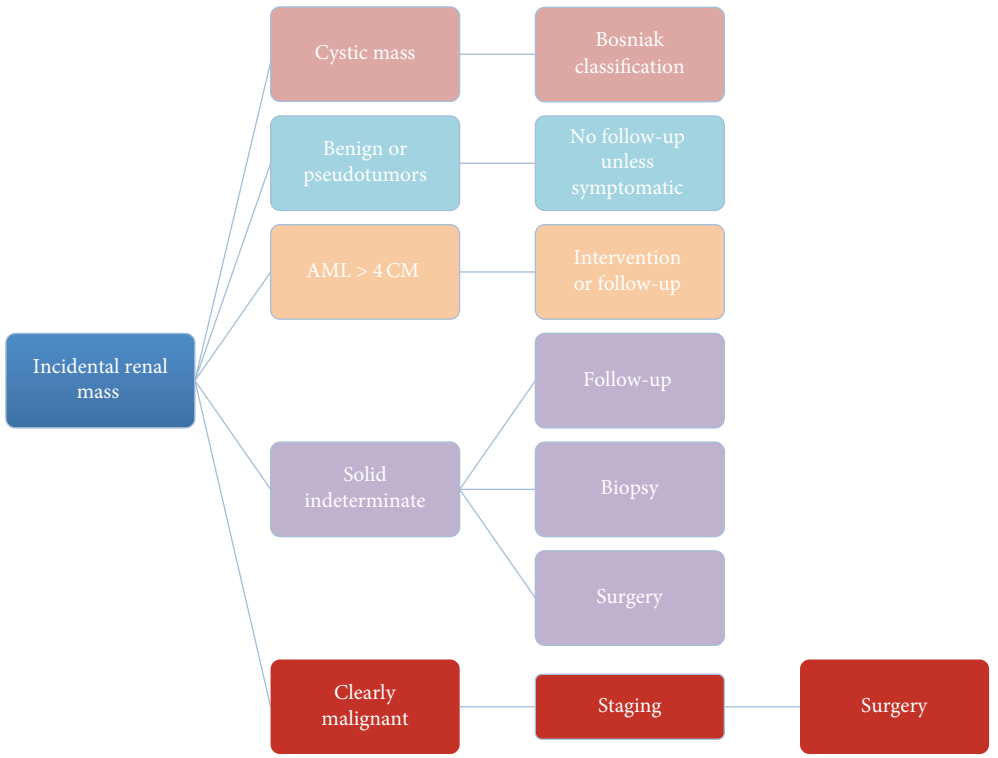


Figure 18: Management diagram.

Table 1: Cystic renal lesions.

| Type | Definition | US | CT | MRI | Percentage of malignancy | Management |
|---|---|---|---|---|---|---|
| Benign | *Bosniak class I*<br>simple cyst not containing septa or calcification; no enhancement | (i) Anechoic<br>(ii) Thin, smooth walls<br>(iii) Posterior acoustic enhancement | (i) Near water density (<10 HU)<br>(ii) Homogeneous density<br>(iii) No enhancement | (i) Sharp, well-defined walls<br>(ii) Signal characteristics of water<br>(iii) No enhancement | ~0% | No intervention |
| | *Bosniak class II*<br>cystic lesion containing thin septa or fine calcifications; no enhancement | (i) Hypoechoic<br>(ii) Iso- or hyperechoic < 3 cm | (i) Hypodense<br>(ii) Hyperdense < 3 cm | (i) T1 hypointense T2 hyperintense<br>(ii) T1 hyperintense T2 hypointense (<3 cm) | | |
| Minimally complex | *Bosniak class IIF*<br>(i) Multiple septa<br>(ii) Perceived (not measurable) enhancement<br>(iii) Calcifications | (i) Hypoechoic<br>(ii) Iso- or hyperechoic > 3 cm | (i) Hypodense<br>(ii) Hyperdense > 3 cm | (i) T1 hypointense T2 hyperintense<br>(ii) T1 hyperintense T2 hypointense (>3 cm) | 5% | Follow-up |
| Indeterminate and malignant | *Bosniak class III*<br>(i) Thickened irregular wall or septa<br>(ii) Thick calcifications<br>(iii) Measurable enhancement | | | | 55% | Histologic diagnosis and eventual surgical removal |
| | *Bosniak class IV*<br>(i) Bosniak class III parameters and solid nodular components | | | | 100% | Surgical removal |

Table 2: Nodular solid lesions ("ball" type).

| Type | Common diagnosis | CT | MRI |
|---|---|---|---|
| Benign | AML | (i) Macroscopic fat tissue at unenhanced CT<br>(ii) No calcifications | (i) T1 hyperintense<br>(ii) T2 hypointense<br>(iii) India-ink artifact at the interface between the mass and the renal parenchyma (intracellular fat) |
| Indeterminate | Oncocytoma | (i) Homogeneous intravascular pattern<br>(ii) Central scar<br>(iii) Segmental inversion enhancement pattern | (i) Not specific: usually T1-hypointensity and T2-hyperintensity<br>(ii) Scar: T2 hyperintense<br>(iii) High signal on ADC |
| Malignant | RCC | (i) Hypervascularity (cc-RCC)<br>(ii) Hypovascularity (p-RCC, ch-RCC)<br>(iii) Homogeneous peripheral enhancement (p-RCC)<br>(iv) Moderate enhancement (ch-RCC) | (i) T1 isointense and T2 hyperintense (cc-RCC)<br>(ii) T1 hyperintense and T2 hypointense (p-RCC and ch-RCC) |

In conclusion, the decision about the management of incidental renal lesions cannot simply result from depicting of radiological findings but should be focused on the patient, considering his anamnestic data (comorbidities, life expectancy) and clinical history.

## Conflicts of Interest

The authors declare that they have no conflicts of interest.

## References

[1] S. G. Silverman, G. M. Israel, B. R. Herts, and J. P. Richie, "Management of the incidental renal mass," *Radiology*, vol. 249, no. 1, pp. 16–31, 2008.

[2] M. Lafortune, A. Constantin, G. Breton, and C. Vallee, "Sonography of the hypertrophied column of Bertin," *American Journal of Roentgenology*, vol. 146, no. 1, pp. 53–56, 1986.

[3] O. Algin, E. Ozmen, and M. Gumus, "Hypertrophic columns of Bertin: imaging findings," *Eurasian Journal of Medicine*, vol. 46, no. 1, pp. 61–63, 2014.

[4] S. Mazziotti, F. Zimbaro, A. Pandolfo, S. Racchiusa, N. Settineri, and G. Ascenti, "Usefulness of contrast-enhanced ultrasonography in the diagnosis of renal pseudotumors," *Abdominal Imaging*, vol. 35, no. 2, pp. 241–245, 2010.

[5] G. Ascenti, G. Zimbaro, S. Mazziotti, M. Gaeta, S. Lamberto, and E. Scribano, "Contrast-enhanced power Doppler US in the diagnosis of renal pseudotumors," *European Radiology*, vol. 11, no. 12, pp. 2496–2499, 2001.

[6] S. Bhatt, G. MacLennan, and V. Dogra, "Renal pseudotumors," *American Journal of Roentgenology*, vol. 188, no. 5, pp. 1380–1387, 2007.

[7] G. M. Israel and M. A. Bosniak, "How I do it: evaluating renal masses," *Radiology*, vol. 236, no. 2, pp. 441–450, 2005.

[8] American College of Radiology Appropriateness Criteria, "Indeterminate renal mass," https://acsearch.acr.org/docs/69367/Narrative.

[9] G. Ascenti, A. Vanzulli, C. Catalano, and R. C. Nelson, *CT of the Retroperitoneum: From Conventional to Multi-Energy Imaging*, Springer-Verlag Italia, 2014.

[10] H. Malhi, E. G. Grant, and V. Duddalwar, "Contrast-enhanced ultrasound of the liver and kidney," *Radiologic Clinics of North America*, vol. 52, no. 6, pp. 1177–1190, 2014.

[11] G. Ascenti, S. Mazziotti, A. Mileto et al., "Dual-source dual-energy CT evaluation of complex cystic renal masses," *American Journal of Roentgenology*, vol. 199, no. 5, pp. 1026–1034, 2012.

[12] G. Ascenti, S. Mazziotti, G. Zimbaro et al., "Complex cystic renal masses: characterization with contrast-enhanced US," *Radiology*, vol. 243, no. 1, pp. 158–165, 2007.

[13] V. A. Sahni and S. G. Silverman, "Imaging management of incidentally detected small renal masses," *Seminars in Interventional Radiology*, vol. 31, no. 1, pp. 9–19, 2014.

[14] A. Jonson, A. N. Rubinowitz, P. G. Mutalik, and G. M. Israel, "Can high-attenuation renal cysts be differentiated from renal cell carcinoma at unenhanced CT?" *Radiology*, vol. 243, no. 2, pp. 445–450, 2007.

[15] C. Farrell, S. L. Noyes, M. Tourojman, and B. R. Lane, "Renal angiomyolipoma: preoperative identification of atypical fat-poor AML," *Current Urology Reports*, vol. 16, no. 3, article 12, 2015.

[16] F. U. Kay and I. Pedrosa, "Imaging of solid renal masses," *Radiologic Clinics of North America*, vol. 55, no. 2, pp. 243–258, 2017.

[17] K. Sasiwimonphan, N. Takahashi, B. C. Leibovich, R. E. Carter, T. D. Atwell, and A. Kawashima, "Small (<4 cm) renal mass: differentiation of angiomyolipoma without visible fat from renal cell carcinoma utilizing MR imaging," *Radiology*, vol. 280, no. 2, article 653, 2016.

[18] S. W. Hakim, N. Schieda, T. Hodgdon, M. D. F. McInnes, M. Dilauro, and T. A. Flood, "Angiomyolipoma (AML) without visible fat: ultrasound, CT and MR imaging features with pathological correlation," *European Radiology*, vol. 26, no. 2, pp. 592–600, 2016.

[19] J. J. Park and C. K. Kim, "Small (<4 cm) renal tumors with predominantly low signal intensity on T2-weighted images: differentiation of minimal-fat angiomyolipoma from renal cell carcinoma," *American Journal of Roentgenology*, vol. 208, no. 1, pp. 124–130, 2017.

[20] K. Ishigami, A. R. Jones, L. Dahmoush, L. V. Leite, M. G. Pakalniskis, and T. J. Barloon, "Imaging spectrum of renal

oncocytomas: a pictorial review with pathologic correlation," *Insights into Imaging*, vol. 6, no. 1, pp. 53–64, 2015.

[21] M. H. Maurer, K. H. Härmä, and H. Thoeny, "Diffusion-weighted genitourinary imaging," *Radiologic Clinics of North America*, vol. 55, no. 2, pp. 393–411, 2017.

[22] Y. Mytsyk, Y. Borys, I. Komnatska, I. Dutka, and I. Shatynska-Mytsyk, "Value of the diffusion-weighted MRI in the differential diagnostics of malignant and benign kidney neoplasms—our clinical experience," *Polish Journal of Radiology*, vol. 79, pp. 290–295, 2014.

[23] G. Low, G. Huang, W. Fu, Z. Moloo, and S. Girgis, "Review of renal cell carcinoma and its common subtypes in radiology," *World Journal of Radiology*, vol. 8, no. 5, pp. 484–500, 2016.

[24] V. F. Muglia and A. Prando, "Renal cell carcinoma: histological classification and correlation with imaging findings," *Radiologia Brasileira*, vol. 48, no. 3, pp. 166–174, 2015.

[25] G. Ascenti, M. Gaeta, C. Magno et al., "Contrast-enhanced second-harmonic sonography in the detection of pseudocapsule in renal cell carcinoma," *American Journal of Roentgenology*, vol. 182, no. 6, pp. 1525–1530, 2004.

[26] G. Ascenti, G. Zimbaro, S. Mazziotti, M. Gaeta, N. Settineri, and E. Scribano, "Usefulness of power Doppler and contrast-enhanced sonography in the differentiation of hyperechoic renal masses," *Abdominal Imaging*, vol. 26, no. 6, pp. 654–660, 2001.

[27] G. Ascenti, G. Zimbaro, S. Mazziotti et al., "Doppler power with contrast media in the characterization of renal masses," *Radiologia Medica*, vol. 100, no. 3, pp. 168–174, 2000.

[28] A. Mileto, D. Marin, M. Alfaro-Cordoba et al., "Iodine quantification to distinguish clear cell from papillary renal cell carcinoma at dual-energy multidetector CT: a multireader diagnostic performance study," *Radiology*, vol. 273, no. 3, pp. 813–820, 2014.

[29] A. Mileto, D. Marin, J. C. Ramirez-Giraldo et al., "Accuracy of contrast-enhanced dual-energy MDCT for the assessment of iodine uptake in renal lesions," *American Journal of Roentgenology*, vol. 202, no. 5, pp. W466–W474, 2014.

[30] G. Ascenti, A. Mileto, B. Krauss et al., "Distinguishing enhancing from nonenhancing renal masses with dual-source dual-energy CT: Iodine quantification versus standard enhancement measurements," *European Radiology*, vol. 23, no. 8, pp. 2288–2295, 2013.

[31] G. Ascenti, B. Krauss, S. Mazziotti et al., "Dual-energy computed tomography (DECT) in renal masses. nonlinear versus linear blending," *Academic Radiology*, vol. 19, no. 10, pp. 1186–1193, 2012.

[32] S. K. Kang, A. Zhang, P. V. Pandharipande, H. Chandarana, R. S. Braithwaite, and B. Littenberg, "DWI for renal mass characterization: systematic review and meta-analysis of diagnostic test performance," *American Journal of Roentgenology*, vol. 205, no. 2, pp. 317–324, 2015.

[33] A. M. Hotker, Y. Mazaheri, A. Wibmer et al., "Use of DWI in the differentiation of renal cortical tumors," *American Journal of Roentgenology*, vol. 206, no. 1, pp. 100–105, 2016.

Hindawi
BioMed Research International
Volume 2017, Article ID 5716835, 9 pages
https://doi.org/10.1155/2017/5716835

*Review Article*

# Abdominal Hernias, Giant Colon Diverticulum, GIST, Intestinal Pneumatosis, Colon Ischemia, Cold Intussusception, Gallstone Ileus, and Foreign Bodies: Our Experience and Literature Review of Incidental Gastrointestinal MDCT Findings

**G. Di Grezia,[1] G. Gatta,[2] R. Rella,[2] D. Donatello,[2] G. Falco,[3] R. Grassi,[4] and R. Grassi[2]**

[1]*Radiology Department, Sea Hospital, Naples, Italy*
[2]*Radiology Department, University of Campania Luigi Vanvitelli, Naples, Italy*
[3]*Breast Surgery Unit, IRCCS Arcispedale Santa Maria Nuova, Reggio Emilia, Italy*
[4]*Radiotherapy Department, University of Firenze, Florence, Italy*

Correspondence should be addressed to G. Di Grezia; graziella.digrezia@libero.it

Received 1 February 2017; Accepted 9 May 2017; Published 30 May 2017

Academic Editor: Luca Macarini



Incidental gastrointestinal findings are commonly detected on MDCT exams performed for various medical indications. This review describes the radiological MDCT spectrum of appearances already present in the past literature and in today's experience of several gastrointestinal acute conditions such as abdominal hernia, giant colon diverticulum, GIST, intestinal pneumatosis, colon ischemia, cold intussusception, gallstone ileus, and foreign bodies which can require medical and surgical intervention or clinical follow-up. The clinical presentation of this illness is frequently nonspecific: abdominal pain, distension, nausea, fever, rectal bleeding, vomiting, constipation, or a palpable mass, depending on the disease. A proper differential diagnosis is essential in the assessment of treatment and in this case MDCT exam plays a central rule. We wish that this article will familiarize the radiologist in the diagnosis of this kind of incidental MDCT findings for better orientation of the therapy.

## 1. Background

A large number of incidental gastrointestinal findings can be observed during abdominal MDCT exam; they can be divided into benign, indeterminate, and worrisome [1]; even if the most frequent are benign ones, there are several conditions such as abdominal hernias, giant colon diverticulum, GIST, intestinal pneumatosis, colon ischemia, cold intussusception, gallstone ileus, and foreign bodies that represent a clinical medical emergency, and because of that a strait clinical and surgical attention may be needed (Table 1).

## 2. Abdominal Hernias

Abdominal herniation is a condition characterized by different etiology, types, symptomatology, and treatment. It can be classified into congenital and acquired based on its etiology and into internal and external types [1]; some authors also include diaphragmatic types [2].

Abdominal hernias can be asymptomatic or symptomless and although in many cases the treatment of choice is a surgery intervention, the therapy should be personalized and because of that it is important to take into account complications and recurrences [3].

*Internal hernias* are the protrusion of the intestine through a mesenteric or peritoneal gap within the border of the peritoneal cavity. They can be congenital or acquired; in this second category we can include postinflammatory and traumatic postsurgical herniation, such as after liver transplantation or gastric bypass in bariatric surgery.

Despite the lack of incidence, they can be often misdiagnosed with a 50% mortality in case of strangulation [4]. In relation to the location, they can be distinguished in paraduodenal, through Winslow foramen, intersigmoid, pericecal,

Table 1: MDCT mayor criteria in differential diagnosis of incidental gastrointestinal findings.

| | |
|---|---|
| Abdominal hernias | Internal<br>Left: encapsulated bowel loops at duodenojejunal junction between the stomach and pancreas to the left of the ligament of Treitz or between the transverse colon and left adrenal gland<br>Right: encapsulated loops laterally and inferiorly to the descending duodenum associated with a small-bowel nonrotation; the SMA; and vein drain posteriorly<br>External: bowel dilation and mesangial thickening. A CT scan, followed by oral iodinated contrast administration, is the best method to determine whether the sac content is intestinal and in this case to identify the intestinal type<br>Diaphragmatic: segmental diaphragm nonvisualization, intrathoracic herniation of viscera, "collar sign," and peridiaphragmatic active contrast extravasation |
| Giant colon diverticulum | Cavity filled with gas, fluid, or stool, with a thin regular wall and no contrast enhancement except in the presence of inflammation; wall may contain calcifications in case of chronic inflammation |
| Gastrointestinal stromal tumors (GIST) | Mass with a soft tissue density with central areas of lower density if necrosis is present and occasionally appear as fluid-fluid levels. Torricelli-Bernoulli sign. (PET) avid tumors |
| Intestinal pneumatosis | Lung window is a low-density linear or bubbly pattern or combination of both and gas in the bowel wall. Abdominal CT scanning with or without contrast enhancement can show the morphology, distension, and thickness of bowel loops |
| Colon ischemia | Bowel wall thickening (8 mm), thumb-printing, and pericolonic stranding with or without ascites |
| Cold intussusception | Bowel-within-bowel and intestinal origin of underlying masses, the site and the intestinal tract involved, mesenteric vascular impairment, involvement of perivisceral fat, surrounding tissue, and locoregional lymph nodes |
| Gallstone ileus | Ectopic gallstone, SBO, abnormal gall bladder with complete air collection, presence of air-fluid level, or fluid accumulation with irregular wall |
| Foreign bodies | Shape, size, location, and depth of the impacted foreign body and the surrounding tissue can be visualized. IV contrast is not recommended |

transmesenteric, and retroanastomotic; in our personal data 48 out of 84 patients that present to our observation had right or left paraduodenal type (57%) so in line with literature this kind of hernias is the most frequent [5].

*2.1. MDCT Findings.* In left-sided paraduodenal hernia, MDCT can evidence encapsulated bowel loops at duodenojejunal junction between the stomach and pancreas to the left of the ligament of Treitz or between the transverse colon and left adrenal gland; often there is a small bowel obstruction with dilated loops and air-fluid levels; mesenteric vessels can be enlarged, stretched, and displaced; the posterior stomach wall can move anteriorly, the duodenojejunal junction inferomedially, and the transverse colon inferiorly [6].

In right-sided paraduodenal hernia MDCT can show encapsulated loops laterally and inferiorly to the descending duodenum associated with a small bowel nonrotation; superior mesenteric vessels supply the herniated loops [7] (Figure 1).

*External hernias* are the prolapse of intestinal loops through congenital or acquired weakness, defects, or holes of the abdominal or pelvic wall. They include inguinal hernia, umbilical hernia, and femoral hernia. These can be asymptomatic but in some cases a sudden increase in intra-abdominal pressure can lead to a common surgical emergency known as incarcerated hernia.

*2.2. CT Findings.* At CT incarcerated hernia appears with bowel dilation and mesangial thickening. A CT scan, followed by oral iodinated contrast administration, is the best method to determine whether the sac content is intestinal and in this case to identify the intestinal type. MDCT scans can help in the detection of bowel strangulation [8] (Figure 2).

Based on our experience in the preoperative assessment, in fact, the identification of a saclike mass or a cluster of dilated small bowel loops located in an abnormal anatomic point is fundamental. At the same time the detection of stretched and displaced mesenteric vascular pedicle and converging vessels at the hernial orifice is vital.

*Diaphragmatic hernias (DH)* are defect or hole in the diaphragm that allows herniation of abdominal contents into the chest cavity. DH are defined as congenital or acquired defect in the diaphragm (Figure 3).

Congenital diaphragmatic hernia (CDH) is a rare and severe condition. These defects can range from small subcentimetric defects to complete diaphragmatic agenesis.

Three different types of CDH have been described, which include a posterolateral Bochdalek-type, an anterior Morgagni-type, and a central septum transversum-type or hiatal hernia.

The complications associated with CDH are pulmonary hypoplasia, gastric volvulus, rotational abnormalities, midgut

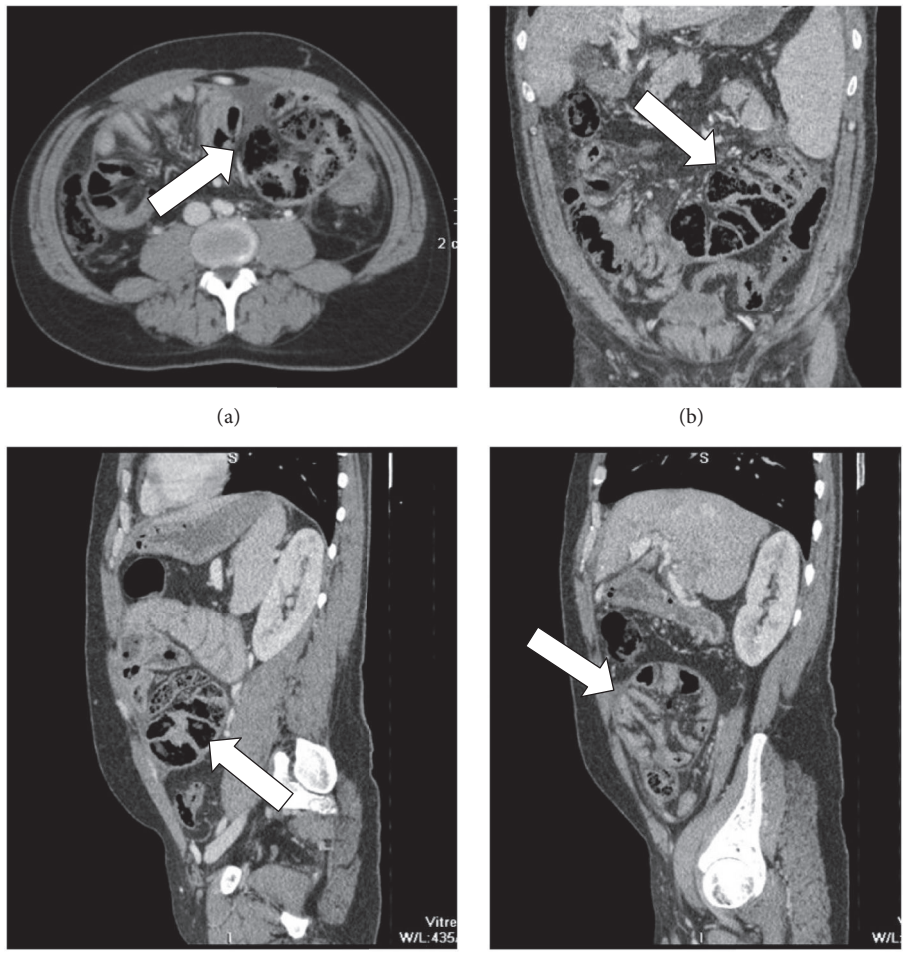

(a) (b)

(c) (d)

Figure 1: (a) Axial plane, (b) coronal reconstruction, (c, d) sagittal reconstruction of abdominal MDCT exam showing a case of internal hernia, a left side paraduodenal hernia (white arrow).

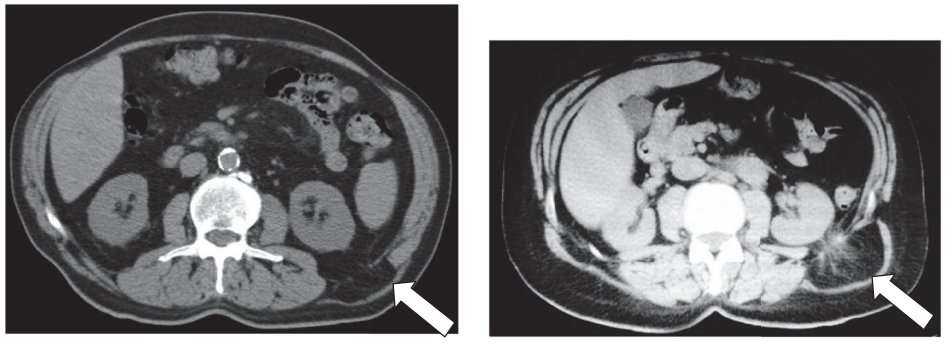

(a) (b)

Figure 2: (a, b) MDCT shows external left lumbar hernia (white arrow).

volvulus, hypoplasia of the left ventricle with a left-sided hernia or pleural effusions caused by right-sided involvement, and bilateral renal hypertrophy [9].

*2.3. US, Chest X-Ray, and CT Findings.* In our personal cases (15 patients) during the prenatal period we detected that US has a high sensitivity in the detection of CDH. In the neonatal and infantile periods, a chest radiograph permits an accurate diagnosis. The classic radiographic appearance is a left hemithorax filled with bowel loops with a right-sided mediastinal shifting and no bowel gas is evident in the abdomen [10].

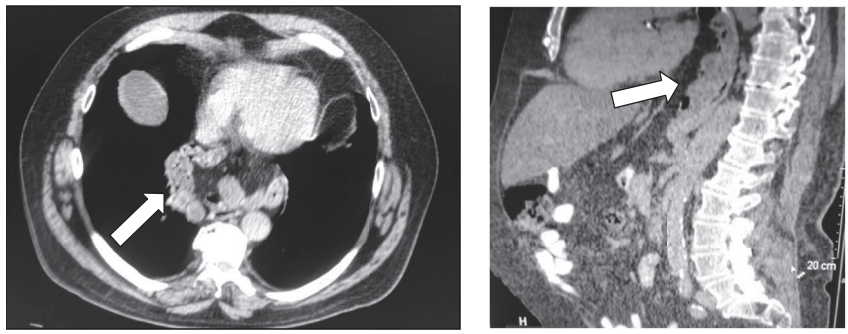


(a) (b)

Figure 3: (a) Axial plane and (b) sagittal reconstruction of abdominal MDCT exam showing a case of mixed paradiaphragmatic hernia (white arrow).

Acquired diaphragmatic hernias can occur for traumatic or iatrogenic causes. Depending on the location and size of the defect, retroperitoneal or intra-abdominal organs and tissues can prolapse into thoracic cavity due to the negative intrathoracic pressure.

CT has been reported to have a sensitivity of 14–82%, with a specificity of 87%. Spiral CT has increased sensitivity, 71–100%, with higher sensitivity on the left than on the right. CT findings indicative of rupture include direct visualization of injury, segmental diaphragm nonvisualization, intrathoracic herniation of viscera, "collar sign," and peridiaphragmatic active contrast extravasation [11–13].

## 3. Giant Colon Diverticulum

Giant colon diverticulum (GCD) is a rare manifestation of diverticular diseases and is characterized by a large diverticular mass (4 cm in size or larger), in communication with colonic lumen, usually filled with stool and gas. The majority (>90%) arises from the sigmoid colon but it can occur in any part of the colon [14].

Different theories have been proposed to explain the development of GCD but the exact etiology remains unknown. One hypothesis is that it can be caused by a unidirectional ball-valve mechanism through a tiny communicating diverticular neck, which causes air entrapment and gradual enlargement of the diverticulum. Another hypothesis is that GCD is secondary to the action of gas-forming organisms or a true congenital duplication during an anomalous embryologic development [15].

GCD can be divided into three types, based on their histopathological pattern: Type 1: pseudodiverticula (22%); Type 2: inflammatory diverticula (66%); Type 3: true diverticula (12%) [16].

Our patients present with not common symptoms like fever, nausea, vomiting, and rectal bleeding. Other symptoms include constipation and abdominal palpable masses.

The most common complication is peritonitis, caused by the perforation of the GCD, followed by abscess formation, intestinal obstruction, volvulus, and infarction. Rarely, a carcinoma might develop from the diverticular mucosa.

*3.1. CT Findings.* At CT, the diverticulum appears as a cavity filled with gas, fluid, or stool, with a thin regular wall and no contrast enhancement except in the presence of inflammation. The wall may contain calcifications in case of chronic inflammation [17].

The definitive treatment for a GCD is surgery through resection of the involved segment with primary anastomosis.

## 4. Gastrointestinal Stromal Tumors (GIST)

Gastrointestinal stromal tumors (GIST) are uncommon mesenchymal tumors arising from the interstitial cells of Cajal, which express KIT protein-CD117 on immunohistochemistry.

GIST occur not only anywhere along the gastrointestinal tract (GIT), but also in the mesentery, omentum, and retroperitoneum.

The clinical findings are usually site-specific. Lesions in the stomach, small bowel, or colon may present with gastrointestinal bleed in the form of hematemesis, melena, or occult blood in stools; lesions in the esophageal tract presents with dysphagia, but many patients present with vague symptoms, such as nausea, vomiting, abdominal discomfort, weight loss, or early satiety [18].

*4.1. CT Findings.* Although abdominal US is often the primary imaging technique used in the investigation of a patient with abdominal pain or mass we use CT as the modality of choice. It is used to characterize the lesion, to evaluate the extension, and to assess the presence or absence of metastasis. Contrast enhanced CT is also used for monitoring the response to therapy and performing follow-up in case of recurrence [19].

Tumors are usually of varying density and show patchy enhancement after intravenous contrast. Typically the mass has a soft-tissue density with central areas of lower density if necrosis is present and occasionally appears as fluid-fluid levels. Enhancement is typically peripherical and calcification is uncommon. A deep crescent-shaped ulceration demonstrating an internal air-fluid level may be referred to as the Torricelli-Bernoulli sign. This sign can be used to identify ulcerating neoplasms of the GI. Lymph node enlargement

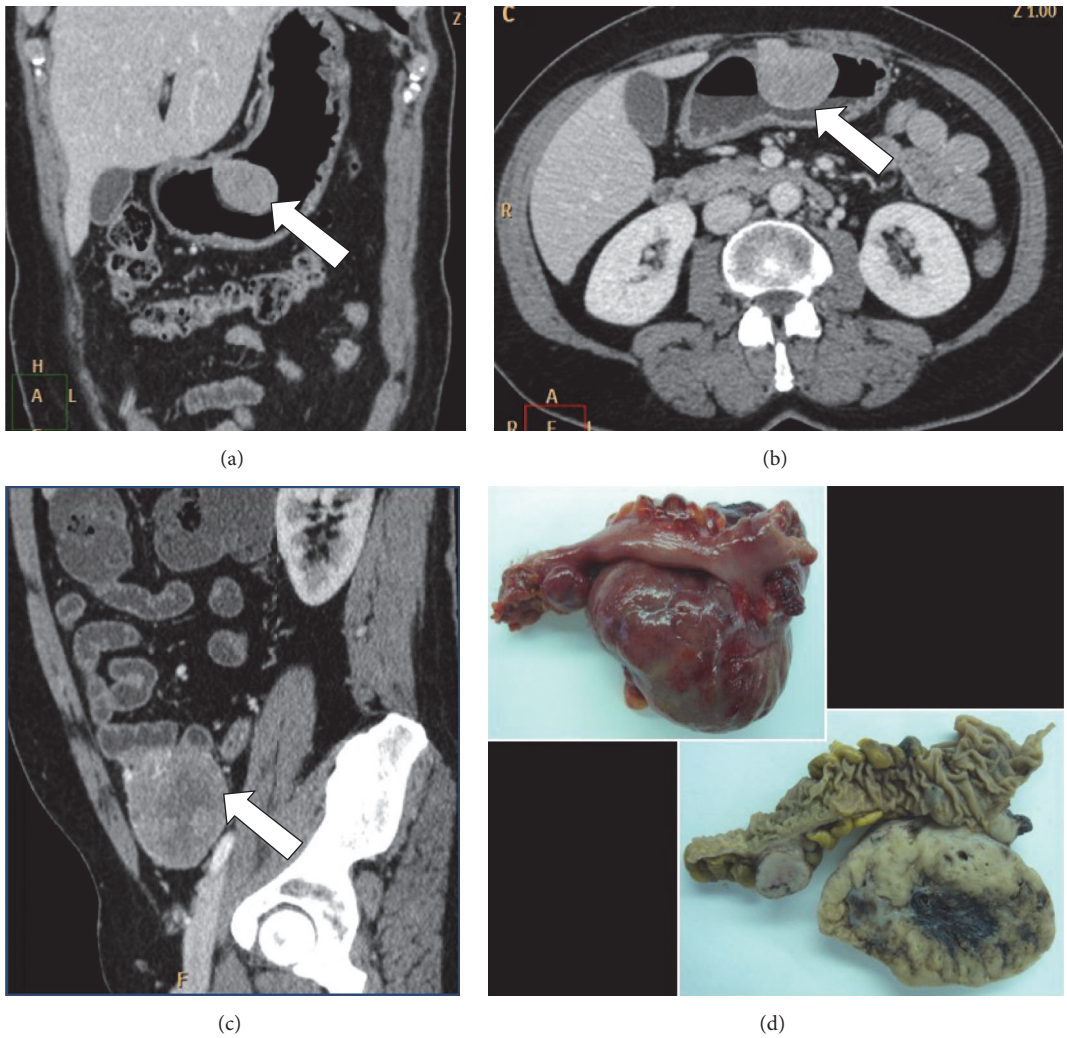


Figure 4: (a) Coronal reconstruction, (b) axial plane, and (c) sagittal reconstruction of abdominal MDCT exam showing cases of gastric GIST (a, b), small bowel neoplasia (c) (white arrow), and postsurgical appearance of the lesions (d).

is not a feature. Metastases or direct invasion into adjacent organs may be seen in more aggressive lesions.

GIST are positron emission tomography (PET) avid tumors because the receptor tyrosine kinase increases the glucose transport protein signaling. PET is useful in revealing small metastases which would not otherwise be seen on CT [20]. GIST is resistant to a standard chemo- and radiotherapy and has been treated with an advanced molecular targeting therapy or radical surgical excision [21] (Figure 4).

## 5. Intestinal Pneumatosis

Intestinal pneumatosis (IP), also referred to as intestinal emphysema, pneumatosis coli, or pneumatosis cystoides intestinalis, is a rare radiological finding, characterized by gas tracks along the bowel wall, appearing as either linear (submucosal) or rounded cystic collections (subserosal) that occurs in wide spectrum of clinical disorder [22]. The small intestine (42%) is most commonly involved followed by colon (36%), with involvement of both in 22% [23]. PI has been divided into two groups: primary and secondary.

Primary IP (15% of cases) is a benign idiopathic condition in which multiple thin-walled cysts develop in the submucosa or subserosa of the colon. Usually, this form has no associated symptoms, and it is often called pneumatosis cystoides intestinalis [24].

The secondary group (85% of cases) is associated with obstructive and necrotic gastrointestinal disease or with obstructive pulmonary disease.

The pathophysiology of IP has been debated and two main theories have been proposed in the literature. A mechanical theory hypothesizes that gas dissects into the bowel wall from either the intestinal lumen or the lungs via the mediastinum due to some mechanism causing increased pressure or direct trauma. A bacterial theory suggests that gas-forming bacilli enter the submucosa through mucosal rents or increased mucosal permeability and produce gas within the bowel wall.

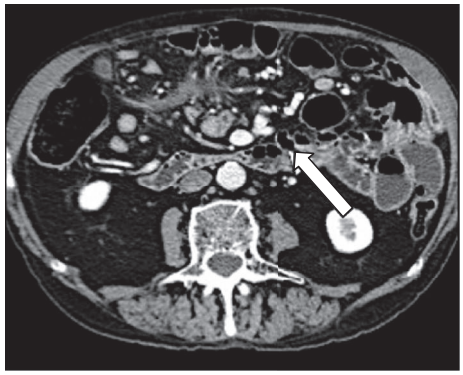

Figure 5: MDCT exam shows small bowel parietal pneumatosis (white arrow).

*5.1. CT Findings.* Computed tomography (CT) is more sensitive than conventional abdominal radiography in the detection of this condition and in the evaluation of extension and complications. The radiological characteristic of IP at CT scan using a lung window is a low-density linear or bubbly pattern or combination of both and gas in the bowel wall. Abdominal CT scanning with or without contrast enhancement can show the morphology, distension, and thickness of bowel loops. CT scans depict additional details, such as morphologic changes, including mural wall thickening, dilatation, abnormal or absent wall enhancement, mesenteric stranding, edema or hemorrhage, vascular engorgement, ascites, and portomesenteric gas, and are helpful in determining the cause of IP (Figure 5).

## 6. Colon Ischemia

Colon ischemia (CI) is a clinical condition that results when blood flow to the colon is reduced to a level insufficient to maintain cellular metabolic function. This process implicates that colonocytes become acidotic and dysfunctional, lose their integrity, and, ultimately, die [25].

The initial and most intense ischemic changes are always in the colonic mucosa. Ischemic change will subsequently extend from the mucosa to the serosa.

The diagnosis of CI is usually established in the presence of symptoms including sudden cramping, mild, and abdominal pain; an urgent desire to defecate; and passage within 24 h of bright red or maroon blood or bloody diarrhea.

CI is often classified according to the underlying cause. Nonocclusive ischemia develops because of low blood pressure or constriction of the vessels feeding the colon; occlusive ischemia indicates that a blood clot or other blockage has cutoff blood flow to the colon.

*6.1. CT Findings.* CT with intravenous and oral contrast is the most helpful in the initial assessment of the patient with abdominal pain to assess the distribution and phase of colitis. It can exclude other causes of abdominal pain, suggest a location and source of ischemia, and identify complications associated with more-advanced disease [26]. The diagnosis of CI can be suggested based on CT findings such as bowel wall thickening (8 mm), thumb-printing, and pericolonic stranding with or without ascites.

Most cases of CI resolve spontaneously and do not require specific therapy, and surgical intervention should be considered in the presence of CI accompanied by hypotension, tachycardia, and abdominal pain without rectal bleeding; for pan-colonic CI; and in the presence of gangrene (Figure 6).

## 7. Cold Intussusception

Intussusception is the prolapse of a bowel loop with its mesenteric fold into the lumen of a contiguous segment causing intestinal obstruction. Majority of the intussusceptions are ileocolic, while the remaining are of the ileoileal or the colocolic types [27].

Based on canalization and his consequence, intussusception is classified into three different types: cold intussusception; incomplete and reversible hot intussusception; and complete and irreversible hot intussusception.

Cold intussusception is incidental and asymptomatic with no sign of bowel obstruction such as abdominal pain and obstructive symptoms.

*7.1. CT Findings.* Abdominal CT with mdc with bowel distension by enteroclysis is the most sensitive radiological technique to identify intussusception. CT scans defines the presence (bowel-within-bowel) and intestinal origin of underlying masses, the site and the intestinal tract involved, mesenteric vascular impairment, involvement of perivisceral fat, surrounding tissue, and locoregional lymph nodes.

There are three patterns of intussusception that are expression of different stages of the same disease: the target-like pattern (early intussusception with only minimal obstruction and no sign of ischemia); the reniform-pattern (bilobed density with peripheral high attenuation and lower attenuation centrally); and the sausage-shape pattern (alternating areas of low and high attenuation related to the bowel wall, mesenteric fat and fluid, intraluminal fluid, contrast material, or air) [28] (Figure 7).

## 8. Gallstone Ileus

Gallstone ileus is an uncommon cause of a mechanical small bowel obstruction (SBO) due to impaction of one or more large gallstones within the GI tract. Biliary-enteric fistula is the major pathologic mechanism of gallstone ileus. The gallstone enters the GI tract through a fistula between a gangrenous gallbladder and the GI tract. Occasionally a stone may enter the intestine through a fistulous communication between the common bile duct and the GI tract [29]. It is a rare complication of chronic cholecystitis and the most common site of entry by erosion is thought to be to the duodenum.

The clinical manifestations of gallstone ileus are variable and depend on the site of obstruction but are frequently nonspecific with intermittent symptoms of nausea, vomiting, abdominal distension, and abdominal pain.

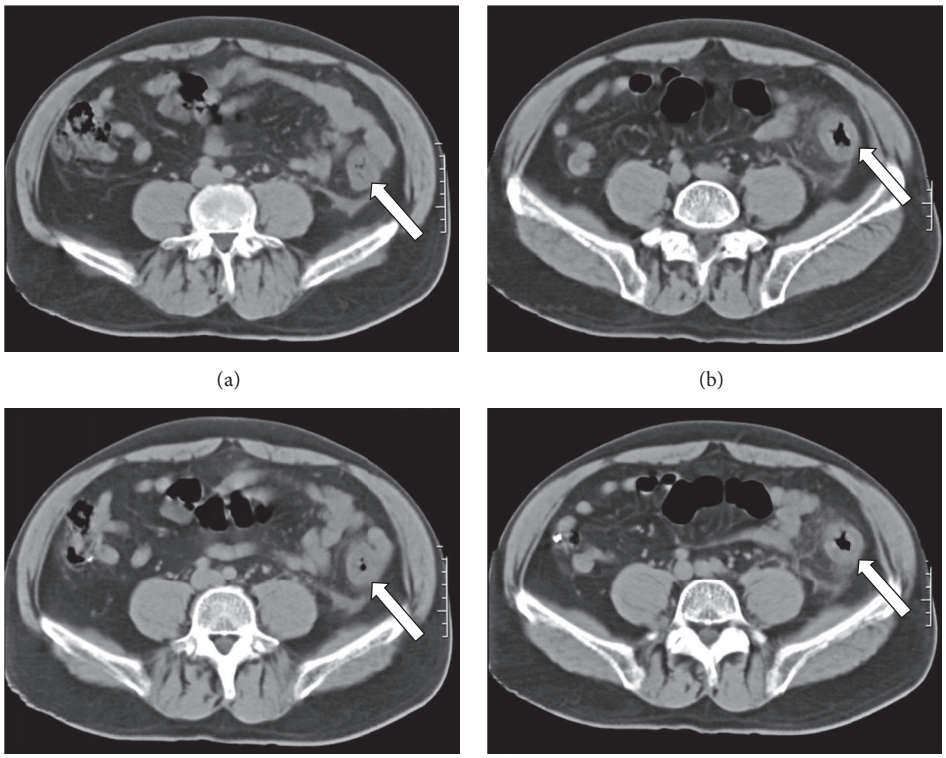

(a) (b)

(c) (d)

Figure 6: Colon ischemia axial images of MDCT showing bowel wall thickening corresponding to left colon (white arrow).

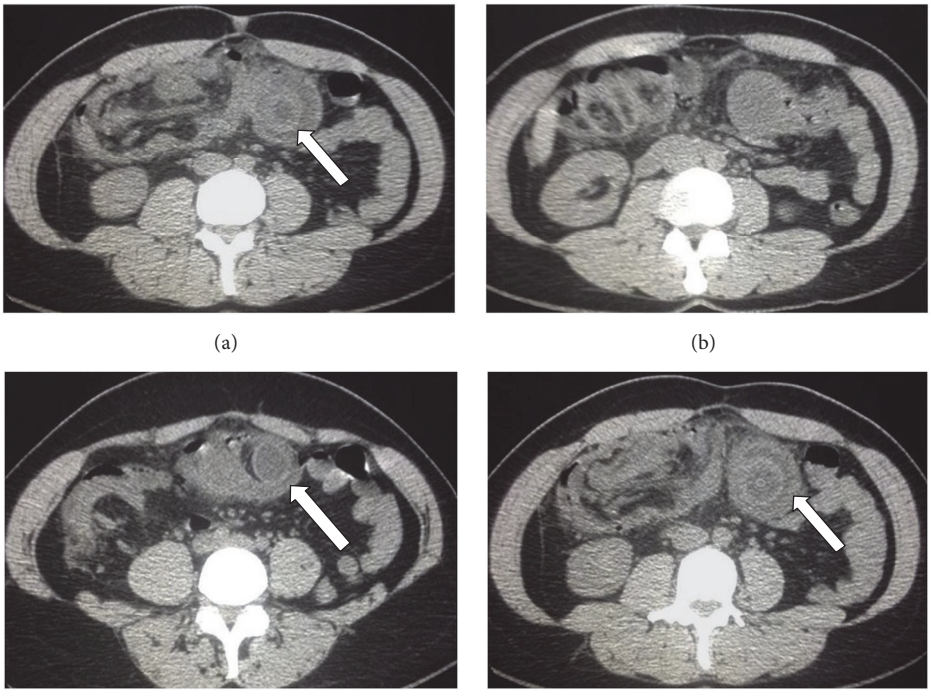

(a) (b)

(c) (d)

Figure 7: Cold intussusception axial images of MDCT showing the bowel pulled inward into itself (white arrow).

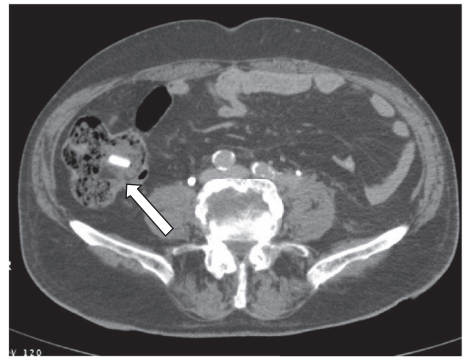

Figure 8: Axial images of MDCT show gallstone ileus (white arrow) in a typical location, the terminal ileum.

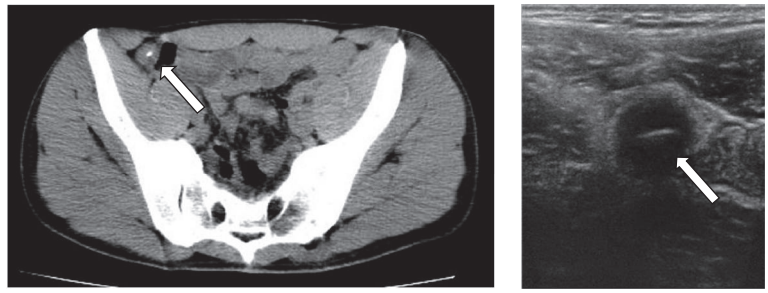

(a) (b)

Figure 9: Axial images of MDCT (a) show a foreign body in a small bowel loop (white arrow), also detected in abdominal ultrasonography (b).

*8.1. Abdominal X-Ray and CT Findings.* Classically the findings on abdominal radiographs are mechanical bowel obstruction, pneumobilia, and an ectopic gallstone within bowel lumen (Rigler's triad). Contrast enhanced CT evaluation of acute SBO offers prompt and rapid diagnosis of gallstone ileus before operation. The diagnostic criteria of gallstone ileus on CT are as follows:

(1) SBO;

(2) ectopic gallstone; either rim-calcified; or total-calcified;

(3) abnormal gall bladder with complete air collection, presence of air-fluid level, or fluid accumulation with irregular wall [30].

CT also has the capability to estimate size of ectopic gallstone, which renders decision-making in management strategy.

The main therapeutic goal is relief of intestinal obstruction by extraction of the offending gallstone [31] (Figure 8).

## 9. Foreign Bodies

Foreign bodies are any object that originates outside of the human body. Foreign bodies may be ingested, inserted into a body cavity, or deposited into the body by a traumatic or iatrogenic injury. The majority of foreign body ingestions occur in pediatric population [32].

Most true foreign bodies can be identified radiographically; however, radiography does not always reliably detect radiolucent foreign bodies, especially fish bones. Even when fish bones are sufficiently radiopaque to be visualized on radiographs, large soft-tissue masses and fluid can obscure the minimal calcium content of the bone, particularly in obese patients. The use of a barium swallow is not recommended because of the risk of aspiration and because coating of the foreign body and esophageal mucosa with contrast interferes with endoscopic visualization.

CT scan is significantly superior to radiography, with a sensitivity from 90% to 100% and a specificity of 93.7% to 100%. With CT, the shape, size, location, and depth of the impacted foreign body and the surrounding tissue can be visualized [33].

The use of IV contrast agent has been long established for the diagnosis of foreign body related complication such as abscess, peritonitis, or fistula formation. Knowledge of these parameters is very important in the management of ingested foreign bodies. The majority of foreign objects pass without intervention and endoscopic removal and surgery are reserved for long, sharp, toxic, or pointed object (Figure 9).

## Abbreviations

MDCT: Multidetector CT
GIST: Gastrointestinal stromal tumor
DH: Diaphragmatic hernia
CDH: Congenital diaphragmatic hernia
GCD: Giant colon diverticulum

CI: Colon ischemia
IP: Intestinal pneumatosis
SMA: Superior mesenteric artery.

## Conflicts of Interest

The authors declare that they have no conflicts of interest.

## References


[1] S. Waqas, J.-O. Johnson, N. Salastekar, K. K. Maddu, and F. Khosa, "Incidental findings detected on abdomino-pelvic multidetector computed tomography performed in the acute setting," *American Journal of Emergency Medicine*, vol. 32, no. 1, pp. 36–39, 2014.

[2] F. Lassandro, F. Iasiello, and N. L. Pizza, "Abdominal hernias: radiological features," *World Journal of Gastrointestinal Endoscopy*, vol. 3, no. 6, pp. 110–117, 2011.

[3] A. Kohler and G. Beldi, Recurrence after hernia surgery: Complication or natural course?

[4] B. D. Newsom and J. S. Kukora, "Congenital and acquired internal hernias: unusual causes of small bowel obstruction," *The American Journal of Surgery*, vol. 152, no. 3, pp. 279–285, 1986.

[5] N. Takeyama, T. Gokan, Y. Ohgiya et al., "CT of internal hernias," *Radiographics*, vol. 25, no. 4, pp. 997–1015, 2005.

[6] A. Blachar and M. P. Federle, "Internal hernia: an increasingly common cause of small bowel obstruction," *Seminars in Ultrasound CT and MRI*, vol. 23, no. 2, pp. 174–183, 2002.

[7] D. Mathieu, A. Luciani, and Germand Group, "Internal abdominal herniations," *American Journal of Roentgenology*, vol. 183, no. 2, pp. 397–404, 2004.

[8] X. F. Yang and J. L. Liu, "Acute incarcerated external abdominal hernia," *Annals of Translational Medicine*, vol. 2, no. 11, 110 pages, 2014.

[9] J. Haroon and R. S. Chamberlain, "An evidence-based review of the current treatment of congenital diaphragmatic hernia," *Clinical Pediatrics*, vol. 52, no. 2, pp. 115–124, 2013.

[10] J. A. Tovar, "Congenital diaphragmatic hernia," *Orphanet Journal of Rare Diseases*, vol. 7, no. 1, article 1, 2012.

[11] Saladyga Anne T., MD Acquired Diaphragmatic Hernias Workup.

[12] A. Reginelli, G. Di Grezia, G. Gatta et al., "Role of conventional radiology and MRi defecography of pelvic floor hernias," *BMC Surgery*, vol. 13, supplement 2, article s53, 2013.

[13] A. Faggian, M. E. Alabiso, N. Serra et al., "Entero-colpodefecography vs supine entero-MRI: Which one is the best tool in the differentiation of enterocele, elytrocele and edrocele?" *Journal of Biological Regulators and Homeostatic Agents*, vol. 27, no. 3, pp. 861–868, 2013.

[14] A. S. Abdelrazeq, A. E. Owais, M. I. Aldoori, and I. D. Botterill, "A giant colonic diverticulum presenting as a "phantom mass": a case report," *Journal of Medical Case Reports*, vol. 3, article no. 29, 2009.

[15] G. Nigri, N. Petrucciani, G. Giannini et al., "Giant colonic diverticulum: Clinical presentation, diagnosis and treatment: Systematic review of 166 cases," *World Journal of Gastroenterology*, vol. 21, no. 1, pp. 360–368, 2015.

[16] R. McNutt, D. Schmitt, and W. Schulte, "Giant colonic diverticula-three distinct entities - report of a case," *Diseases of Colon and Rectum*, vol. 31, no. 8, pp. 624–662, 1988.

[17] P. Sassani, H. M. Singh, D. Gerety, and M. A. Abbas, "Giant colonic diverticulum: endoscopic, imaging, and histopathologic findings," *The Permanente Journal*, vol. 12, no. 1, pp. 47–49, 2008.

[18] S. Sripathi, K. V. Rajagopal, R. K. Srivastava, and A. Ayachit, "CT features, mimics and atypical presentations of gastrointestinal stromal tumor (GIST)," *Indian Journal of Radiology and Imaging*, vol. 21, no. 3, pp. 176–181, 2011.

[19] D. M. King, "The radiology of gastrointestinal stromal tumours (GIST)," *Cancer Imaging*, vol. 5, no. 1, pp. 150–156, 2005.

[20] A. Rammohan, J. Sathyanesan, K. Rajendran et al., "A gist of gastrointestinal stromal tumors: a review," *World Journal of Gastrointestinal Oncology*, vol. 5, no. 6, pp. 102–112, 2013.

[21] A. Werewka-Maczuga, T. Osiński, R. Chrzan, M. Buczek, and A. Urbanik, "Characteristics of computed tomography imaging of gastrointestinal stromal tumor (GIST) and related diagnostic problems," *Polish Journal of Radiology*, vol. 76, no. 3, pp. 38–48, 2011.

[22] J. H. Wang, A. Furlan, D. Kaya, S. Goshima, M. Tublin, and K. T. Bae, "Pneumatosis intestinalis versus pseudo-pneumatosis: review of CT findings and differentiation," *Insights into Imaging*, vol. 2, no. 1, pp. 85–92, 2011.

[23] C. Braumann, C. Menenakos, and C. A. Jacobi, "Pneumatosis intestinalis—a pitfall for surgeons?" *Scandinavian Journal of Surgery*, vol. 94, no. 1, pp. 47–50, 2005.

[24] J. Theisen, P. Juhnke, H. Stein, and J. Siewert, "Pneumatosis cystoides intestinalis coli," *Surgical Endoscopy*, vol. 17, no. 1, pp. 157-158, 2003.

[25] L. J. Brandt, P. Feuerstadt, G. F. Longstreth, and S. J. Boley, "American College of Gastroenterology. ACG clinical guideline: epidemiology, risk factors, patterns of presentation, diagnosis, and management of colon ischemia (CI)," *American Journal of Gastroenterology*, 2015.

[26] R. F. Thoeni and J. P. Cello, "CT imaging of colitis," *Radiology*, vol. 240, no. 3, pp. 623–638, 2006.

[27] O. Catalano, "Transient small bowel intussusception: CT findings in adults," *British Journal of Radiology*, vol. 70, no. 836, pp. 805–808, 1997.

[28] F. Somma, A. Faggian, N. Serra et al., "Bowel intussusceptions in adults: the role of imaging," *Radiologia Medica*, vol. 120, no. 1, pp. 105–117, 2014.

[29] J.-W. Chou, C.-H. Hsu, K.-F. Liao et al., "Gallstone ileus: report of two cases and review of the literature," *World Journal of Gastroenterology*, vol. 13, no. 8, pp. 1295–1298, 2007.

[30] C.-Y. Yu, C.-C. Lin, R.-Y. Shyu et al., "Value of CT in the diagnosis and management of gallstone ileus," *World Journal of Gastroenterology*, vol. 11, no. 14, pp. 2142–2147, 2005.

[31] C. M. Nuño-Guzmán, M. E. Marín-Contreras, M. Figueroa-Sánchez, and J. L. Corona, "Gallstone ileus, clinical presentation, diagnostic and treatment approach," *World Journal of Gastrointestinal Surgery*, vol. 8, no. 1, pp. 65–76, 2016.

[32] T. B. Hunter and M. S. Taljanovic, "Foreign bodies," *Radiographics*, vol. 23, no. 3, pp. 731–757, 2003.

[33] M. Birk, P. Bauerfeind, P. H. Deprez et al., "Removal of foreign bodies in the upper gastrointestinal tract in adults: European Society of Gastrointestinal Endoscopy (ESGE) clinical guideline," *Endoscopy*, vol. 48, pp. 489–496, 2016.

Hindawi
BioMed Research International
Volume 2017, Article ID 8740635, 7 pages
https://doi.org/10.1155/2017/8740635

*Research Article*

# Incidental Paratracheal Air Cysts on Thoracic CT and Their Association with Chronic Inflammatory Lung Disease

**Ha Yeon Kim,[1] Kyung Hee Lee,[1] Yeo Ju Kim,[1] Ha Young Lee,[1] Ga Ram Kim,[1] Yong Sun Jeon,[1] Jung Soo Kim,[2] Young Sam Kim,[3] and Jun Ho Kim[1]**

[1]*Department of Radiology, Inha University Hospital, Inha University School of Medicine, Inhang-ro 27, Jung-gu, Incheon, Republic of Korea*
[2]*Department of Internal Medicine, Inha University Hospital, Inha University School of Medicine, Inhang-ro 27, Jung-gu, Incheon, Republic of Korea*
[3]*Department of Thoracic Surgery, Inha University Hospital, Inha University School of Medicine, Inhang-ro 27, Jung-gu, Incheon, Republic of Korea*

Correspondence should be addressed to Jun Ho Kim; jhkim7227@gmail.com

Received 27 January 2017; Accepted 5 March 2017; Published 15 March 2017

Academic Editor: Arnaldo Scardapane



*Purpose*. To determine the association between the progression of upper lung fibrosis and paratracheal air cysts (PACs) size. *Materials and Methods*. The thoracic CT images of 4573 patients were reviewed for the prevalence, size, and location of PACs and their communication with trachea. In addition, the presence of upper lung fibrosis, emphysema, and bronchiectasis was evaluated in patients with PACs and compared with a control group without PACs. Upper lung fibrosis was analyzed using a fibrosis score system. *Results*. The prevalence of PACs was 6.8%. Communication with tracheal lumen was demonstrated by 31.5% of patients with PACs. The prevalence of fibrosis, emphysema, and bronchiectasis in patients with PACs were 67.5%, 21.9%, and 28.3%, respectively. The prevalence of fibrosis was significantly different in the two groups by univariable and multivariable analysis (odds ratio = 2.077, $P < 0.001$). 140 patients with fibrosis among PAC group underwent a previous or follow-up CT; the prevalence with increase in PAC sizes was higher in patients with increase in fibrosis score than those without it (66.2% versus 17.3%, $P < 0.001$). *Conclusions*. PACs appear to be highly related to upper lung fibrosis and moderately related to bronchiectasis. In patients with fibrosis, PAC sizes tended to increase with the progression of upper lung fibrosis.

## 1. Introduction

Paratracheal air cysts (PACs) are small air collections and are usually detected incidentally by thoracic computed tomography (CT) [1–4]. The incidence of PACs in the general population has been reported to be from 0.75% to 8.1% [3, 5–7].

Most PACs are asymptomatic, but rarely, they are the cause of recurrent infections, chronic cough, right side recurrent laryngeal nerve paralysis, and difficult intubation [3, 4, 7]. PACs are usually located on the right side of tracheal area at the level of the thoracic inlet [2, 4, 6, 8]. Histological findings show that PACs are lined with ciliated columnar epithelia and often communicate with tracheal lumen [5, 6]. PACs and tracheal diverticula are considered similar entities [5]. Tracheal diverticula develop by mucosal herniation through weak points in the trachea due to increased intrathoracic pressure [1, 4, 5].

Some authors have suggested that obstructive lung diseases, such as chronic obstructive pulmonary disease (COPD) and bronchiectasis, are associated with the presence of PACs, but results are debated [1, 2, 6, 7]. In a recent study, it was proposed that upper lung fibrosis could cause traction of the tracheal wall and result in cyst formation [4]. We also considered that upper lung fibrosis might be associated with both development and morphologic changes of PACs. In addition, we previously noticed that pulmonary fibrosis usually accompanies obstructive lung disease in clinical practice [4]. However, little information is available regarding this relationship, and it has not been determined which disease is more associated with the presence of PACs. In fact, no

published study has addressed the relation between changes in PAC morphology and degree of upper lung fibrosis [4].

The primary purpose of this study was to determine the incidence and CT features of PACs. The secondary purpose was to explore the relation between PACs and underlying pulmonary disease including upper lung fibrosis, bronchiectasis, and emphysema and to evaluate the association between progression of upper lung fibrosis and PACs size.

## 2. Materials and Methods

This retrospective study was approved by the hospital ethics committee on human studies at our institution.

*2.1. Patients and CT Imaging Technique.* Between January 2014 and June 2014, routine thoracic CT was performed on 4573 patients for different reasons, such as health check-up, pulmonary disease, trauma, lung cancer follow-up, or detection of metastasis.

CT scans were performed using a 16-slice MDCT scanner (Siemens SOMATOM Sensation 16) or a 64-slice MDCT scanner (GE LightSpeed VCT). Thoracic CT scanning was performed from the lower part of the neck to adrenal glands. Axial section data were reconstructed at a thickness of 3 mm using a 3 mm slice interval for the SOMATOM Sensation 16 or at a thickness of 2.5 mm using a 2.5 mm slice interval for the LightSpeed VCT, respectively. All images were processed with standard mediastinal (width, 350 HU; level 20 HU) and lung (width, 1500 HU; level −700 HU) window settings.

*2.2. Image Analysis.* Two radiologists with 8 years (reader 1) and 3 years (reader 2) of experience dedicated to thoracic CT imaging served as independent readers. In cases of disagreement between the two reviewers, consensus was reached by discussion.

PACs were defined as air-attenuations in paratracheal soft tissue with or without communication with tracheal lumen and without communication with lung parenchyma or esophagus. PACs were evaluated based on location (right, left, and bilateral), number (single or multiple), presence of communication with tracheal lumen, and longest diameter on axial CT scans with a lung setting window. In cases with multiple cysts, the largest cyst was included in the statistical analysis.

In all patients with PACs, the presence of fibrosis, emphysema, and bronchiectasis was evaluated. Fibrosis was evaluated in both upper lungs. Upper lung range was defined from apex to carina. To perform detailed analysis, we use the fibrosis scoring system with minimal changes. Four features were included; (1) ground glass opacities, (2) irregular pleural margin, (3) reticular opacities and fibrosis, and (4) honeycombing.

Ground glass opacity was defined as a hazy area of increased attenuation in the lung with preserved bronchial and vascular markings. Irregular pleural margin was defined as pleural thickening with prominent subpleural consolidation opacities. Reticular opacities were defined as a collection of innumerable areas of small linear opacity. Honeycombing was defined as the presence of cystic airspaces measuring 3–10 mm in diameter with 1–3 mm thick walls [9, 10].

Extent of these feature was measured using scoring systems in each upper lung; 0, none; 1, 1–10%; 2, 11–25%; 3, 26–50%; 4, 51–75%; and 5, 76–100% [10]. Scores were summed to calculate fibrosis scores (range 0–20) for each upper lung. Total fibrosis scores were calculated by summing the fibrosis scores of both upper lungs. Using this method minimum and maximum possible total fibrosis scores were 0 and 40, respectively.

The presences of emphysema and bronchiectasis in both lungs (ranging from apices to bases of lower lobes) were evaluated. Emphysema was defined as areas of decreased attenuation with no walls or discrete walls. Bronchiectasis was diagnosed based on bronchial dilatation relative to an adjacent pulmonary artery, lack of bronchial tapering, and visualization of bronchi in lung periphery.

Patients with PACs were classified according to the availability of a previous or follow-up CT. We selected two CT scans with the longest interscan interval. In each of the two scans chosen, the diameter of the largest PAC was measured and upper lung fibrosis score was determined.

We selected 311 patients, matched for age and gender using computer software, as a control group with no PAC. The presences of fibrosis, emphysema, and bronchiectasis in controls were determined as described above.

*2.3. Statistical Analysis.* Student's $t$-test was used to analyze continuous variables and Fisher's exact test or the chi-squared test was used to identify correlations among categorical variables. The Cochran-Armitage test was used to assess linear trends regarding PAC prevalence according to decade of life. Multivariable logistic regression analyses were performed to determine and obtain odds ratios (ORs) of factors affecting the presence and increases in the sizes of PACs. Correlation with fibrosis progression scores and PAC size changes were determined using Spearman's correlation coefficients (rho). The analysis was conducted using SPSS statistical software package (version 19.0, Chicago, IL) and dBSTAT for Windows (version 5.0, Seoul, Korea). $P$ values of $< 0.05$ were considered statistically significant.

## 3. Results

PACs were detected in 311 of the 4573 (6.8%) study subjects, that is, in 184 of 2735 males (6.72%) and in 127 of 1838 females (6.9%), which showed that the prevalence of PACs was not associated with gender ($P = 0.81$). Mean age of the 311 patients with PACs was 63.44 years (±13.55, range 18–107). A list of PAC prevalence against age in decades is presented in Table 1. A plot shows its prevalence increased significantly with age ($P < 0.001$).

Three hundred and eleven patients without PACs were selected as a control group, 184 men and 127 women. Mean age of the control group was 63.45 years (±14.39, range 22–96).

Mean greatest PAC diameter was $5.93 \pm 0.21$ mm (median 5.00, range 1–22). Most were located in the right lateral side of the trachea (307 of 311, 98.7%); 3 cases were located in the left side (1.9%), and in 1 case of PACs was bilateral. 42 of 311 (13.5%) patients had more than one PAC and 1 patient had

Table 1: The prevalence of PACs by decades of life.

| Decade of life | Number of subjects | Number of PACs | Prevalence (%) |
|---|---|---|---|
| 0~19 | 82 | 2 | 2.4 |
| 20~29 | 113 | 3 | 2.65 |
| 30~39 | 265 | 5 | 1.88 |
| 40~49 | 654 | 35 | 5.35 |
| 50~59 | 1081 | 74 | 6.84 |
| 60~69 | 1034 | 94 | 9.09 |
| 70~79 | 828 | 53 | 6.4 |
| 80~89 | 452 | 41 | 9.07 |
| 90~109 | 64 | 4 | 6.25 |
| Total | 4573 | 311 | 6.8 |

PACs = paratracheal air cysts.

Table 2: Cyst characteristics.

| PACs ($n$ = 311) | |
|---|---|
| Right paratracheal | 307 (98.7%) |
| Left paratracheal | 3 (1.0%) |
| Both paratracheal | 1 (0.3) |
| Multiple | 42 (13.5%) |
| Communication | 98 (31.5%) |
| Size (mm), mean ± SD | 5.93 ± 0.21 |

*Note*. Data are presented as numbers (percentages) of patients.
SD = standard deviation.

multiple PACs located bilaterally with respect to the trachea. 98 of 311 (31.5%) PACs communicated with tracheal lumen (Table 2).

Of the 311 patients with PACs, 210 had upper lung fibrosis (67.5%), 61 had emphysema (21.9%), and 88 had bronchiectasis (28.3%). In the control group, 125 patients had upper lung fibrosis (40.2%), 54 had emphysema (17.4%), and 53 had bronchiectasis (17.0%). Intergroup differences were significant for upper lung fibrosis ($P < 0.001$) and bronchiectasis ($P < 0.001$). The prevalence of fibrosis in patients with PACs was 2.921 (odds ratio, 2.921; 95% CI, 2.077–4.106) times higher than in controls (Table 3).

Of the 311 patients with PACs, 129 of the 184 men (70.1%) and 81 of the 127 women (63.8%) had upper lung fibrosis. No significant differences were observed between genders with respect to the prevalence of upper lung fibrosis ($P = 0.268$). 69 of 98 (70.4%) patient with PACs and tracheal communication had upper lung fibrosis, and 141 of the 213 (66.2%) without communication had upper lung fibrosis, which was not significantly different ($P = 0.46$).

The fibrosis scores of patients with PACs ranged from 1 to 22 and their mean score was 3.53 ± 3.10. In the control group, fibrosis scores ranged from 1 to 15 and the mean score was 3.35 ± 2.34. No significant difference was observed between the fibrosis scores of patients with or without PACs ($P = 0.50$).

Among 210 patients with upper lung fibrosis, 140 had follow-up CT scans. The mean intervening period was 42.67 months. During this time, upper lung fibrosis scores increased in 56 patients. The mean score change in theses group was 2.57 ± 2.16 points (range 1–13). Of these 56 patients, 43 (76.8%) showed an increase in longest PAC diameter, and the mean diameter increase was 1.73 ± 1.85 mm (range 1–9). In 84 patients without a change in upper lung fibrosis score, 22 (26.2%) showed an increase in longest PAC diameter. 43 of 65 (66.2%) with increased PAC diameter showed progression of upper lung fibrosis (Figure 1), and 17.3% (13 of 75) of those that did not show an increase in diameter showed progression of upper lung fibrosis, and this difference was significant ($P < 0.001$). After adjusting for age, sex, and time to follow-up CT scan, progression of upper lung fibrosis was found to be significantly associated with an increase in PAC size ($P < 0.001$; odds ratio, 8.785; 95% CI, 3.897–19.084) (Table 4). Of the 311 patients with PACs, 15 patients did not have PACs by previous CT. Thirteen of these 15 patients (86.7%) had upper lung fibrosis, and 11 of those 13 patients (84.6%) showed progression of fibrosis (Figure 2).

The correlation between progression of fibrosis score and PAC size change was not significant by Spearman's correlation analysis ($P = 0.216$).

## 4. Discussion

PACs are almost detected incidentally on thoracic CT scans and in most cases are asymptomatic [2]. Previous studies have reported that the prevalence of PACs on CT scan ranges from 2.0% to 8.1% [1, 3–8]. In the present study, which involved the largest numbers of patients with PACs, the prevalence of PACs was 6.8%, which was not surprising, as PACs are not an uncommon finding on thoracic CT scans. This prevalence is higher than that reported by Unlu et al. (5.4%) [4], who used a thicker CT slice, but lower than those reported by Boyaci et al. (8.0%) [7] and Bae et al. (8.1%) [6], who both used a high resolution multidetector CT unit with a slice thickness of 1 mm. Accordingly, it appears that prevalence of PACs as determined by thoracic CT may depend on slice thickness, which suggests that as CT technology evolves reported PAC prevalence will increase.

The etiology of PACs is still the subject of debate; Goo et al. suggested that PACs might be caused by the protrusion of tracheal mucosa through weak points in the trachea due to

Table 3: Demographics and the prevalence of upper lung fibrosis, emphysema, and bronchiectasis in patients with or without PACs.

| Variables | PAC+[a] ($n$ = 311) | PACs−[b] ($n$ = 311) | Univariable $P$ | Multivariable $P$ | Odds ratio (95% CI) |
|---|---|---|---|---|---|
| Age (mean ± SD) | 63.44 ± 13.55 | 63.45 ± 14.39 | 0.989 | 0.619 | |
| Sex | | | 1 | 0.795 | |
| Male | 184 (59.0%) | 184 (59.0%) | | | |
| Female | 127 (41.0%) | 127 (41.0%) | | | |
| Upper lung fibrosis | 210 (67.5%) | 125 (40.2%) | <0.001 | <0.001 | 2.921 (2.07–4.106) |
| Emphysema | 61 (21.9%) | 54 (17.4%) | 0.157 | 0.877 | |
| Bronchiectasis | 88 (28.3%) | 53 (17.0%) | 0.001 | 0.059 | |

*Note.* All data except $P$ values are presented as numbers (percentages) of patients.
PAC = paratracheal air cysts, CI = confidence interval, SD = standard deviation, and $n$ = number.
[a]Patients with PACs; [b]patients without PACs.

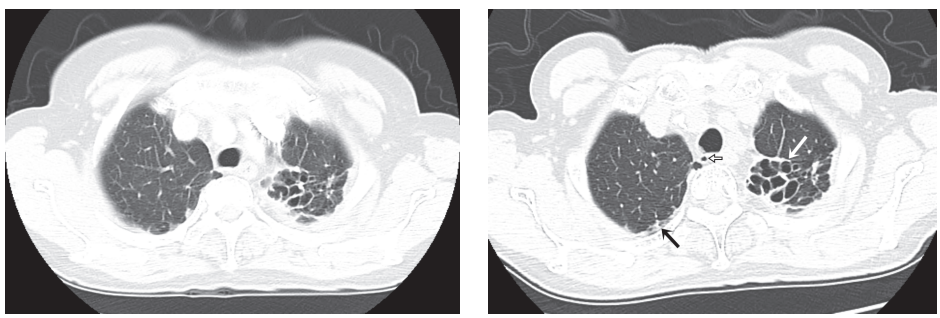

(a) (b)

Figure 1: (a) Axial CT scan shows fibrosis and irregular pleural thickening in a left upper lobe. No paratracheal air cyst is visualized. (b) CT scan obtained 57 months later shows a paratracheal air cyst at the right posterior side of the trachea (black line arrow). CT image shows subpleural irregularity in the right upper lobe (black arrow) and progression of fibrosis and bronchiectasis in the left upper lobe (white arrow). The total fibrosis score of both upper lungs increases from 5 to 7 points over the 57 months.

chronic inflammation or increased intraluminal pressure of trachea [5]. Previous reports have revealed that most PACs are located on the right side of trachea [1, 2, 4–8, 11]. Our findings concur as they were detected on the right side in 307 of the 311 (98.7%) patients. Because the esophagus and aortic arch are usually located on the left side of the trachea, the right side is relatively weaker in terms of withstanding intratracheal pressure, which probably explains reported findings [1, 2, 7].

In the present study, communication with the trachea was observed in 98 patients (31.5%), which is a lower rate than those reported previously (42.6% to 56.1%) [2, 4, 7]. The higher rates observed in these previous studies were probably due to the use of thin CT slices [2, 7] or multiplane analysis [4].

According to our findings, PACs showed a slight but nonsignificant female predominance, and the majority of previous studies have also indicated PACs are more prevalent in women [2, 3, 6–8].

In the present study, mean age of 311 patients with PACs was 63.44 years and the prevalence of PAC was found to peak in the 7th decade of life. Furthermore, we found a positive correlation between age and the presence of PACs ($P < 0.001$). Several authors have examined the relation between the prevalence of PACs and age [1, 6–8]. Boyaci et al. reported a negative correlation between the two [7], but only a small number of subjects were included in this study. In addition, all of the studies conducted, including that by Boyaci et al., reported the prevalence of PACs peaked in the 6th decade [1, 6–8]. These findings suggest that PACs probably do not have a congenital etiology. In a recent report, the prevalence of PACs in pediatric patients (1.3%) was lower than in adults [12], which also suggested the underlying mechanism probably involves an acquired etiology.

Several authors have suggested bronchial diverticula are related to COPD and smoking-related lung diseases [13–16]. Others have suggested that the development of PACs, which is similar to subcarinal or bronchial diverticula, is associated with chronic inflammation and obstructive lung disease (including COPD), upper lung fibrosis, and bronchiectasis [4, 7, 17, 18]. However, these suggested associations remain controversial. Goo et al. [5] and Polat et al. [1] reported that the presence of PACs indicates the presence of obstructive lung disease and possibly emphysema. In addition, Boyaci et al. suggested that the presence of PACs was a significant association with bronchiectasis [7]. In a recent study, it was reported that the prevalence of PACs was associated with upper lobe pulmonary fibrosis [4]. Unlu et al. found the incidence of PACs was significantly associated with upper

Table 4: Factors associated with an increase in PAC size.

| Variables | Not increase in size of PACs ($n$ = 75) | Increase in size of PACs ($n$ = 65) | Univariable $P$ | Multivariable $P$ | Odds ratio (95% CI) |
|---|---|---|---|---|---|
| Age (mean ± SD) | 64.63 ± 11.93 | 66.22 ± 13.45 | 0.460 | 0.901 | |
| Sex | | | | | |
| Male | 49 (65.3%) | 40 (61.5%) | 0.642 | 0.829 | |
| Female | 26 (34.7%) | 25 (38.5%) | | | |
| Progression of upper lung fibrosis | 13 (17.3%) | 43 (66.2%) | <0.001 | <0.001 | 8.785 (3.897–19.084) |
| Follow-up interval (month) | 32 (15–46) | 42 (24.5–71) | 0.018 | 0.512 | |

*Note.* All data except $P$ values are presented as numbers (percentages) of patients.
PAC = paratracheal air cysts, CI = confidence interval, SD = standard deviation, and $n$ = number.

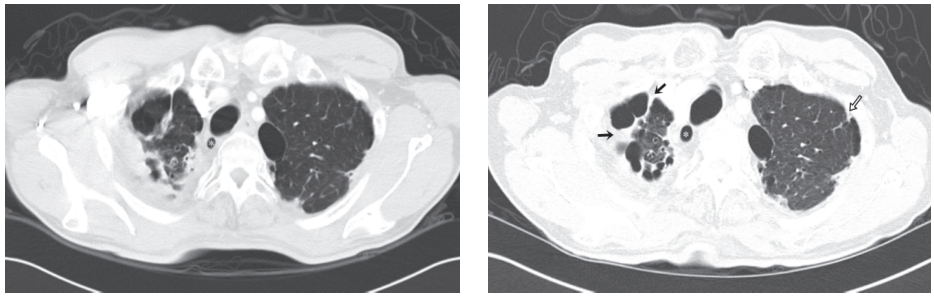

(a) (b)

Figure 2: (a) Axial CT scan shows a paratracheal air cyst (∗) and fibrosis with volume decrease in a right upper lung and subpleural fibrosis in a left upper lung. (b) CT scan obtained 32 months later shows an increase in PAC size. In addition, fibrosis had thickened (arrow) and the volume of the right upper lobe has reduced. Subpleural fibrosis is more prominent in the left upper lung (black line arrow). The total fibrosis score of both upper lungs increased from 9 to 12 points over the 32 months.

lobe fibrosis and suggested upper lobe fibrosis contributes to the formation of PACs and that the coexistence of emphysema and fibrosis increases the possibility of the presence of PACs [4]. They also found bronchiectasis was related to the presence of PACs [4]. However, other studies found no relation between emphysematous pulmonary change and the presence of PACs [2, 3, 6–8]. Previous studies have reported controversial results about relationships between PACs and pulmonary diseases. In our study, the presence of PACs was found to be significantly associated with upper lung fibrosis and bronchiectasis, but not with emphysema. Of these two diseases found to be significantly associated with the presence of PACs, only upper lung fibrosis was found to be associated by univariable and multivariable analyses. Bronchiectasis showed a borderline association with PACs ($P = 0.059$) by multivariable analysis. In the present study, upper lung fibrosis was found to be correlated more strongly with the presence of PACs than bronchiectasis or emphysema.

In our study, fibrosis rates of upper lungs are 67.5% in patients with PACs and 40.2% in control group, and this result is higher than rates previously reported by Unlu et al. (45.8%, 19.5%, resp.) [4]. There are several possible reasons for this. First, South Korea is still tuberculosis endemic country and seven times higher than the average incidence of Organisation for Economic Cooperation and Development member countries [19]. The sequelae of tuberculosis represent fibrotic response such as parenchymal bands, apical pleural thickening, or volume loss of the upper lobes [20]. Second, since fibrosis grading system can be applied, it was possible to include our study subjects with delicate fibrosis, compared with previous study [4]. Finally, the use of thin slice CT could affect the rate of upper lung fibrosis as the prevalence of reported PAC. Therefore, the rate of upper lung fibrosis will increase by using CT with thinner slice thickness such as 1 mm or 0.625 mm more than that of our study in both control and PACs groups.

Unlu et al. suggested a significant correlation exists between communication and the presence of upper lobe fibrosis in patients with PACs [4], and in the present study this association was higher for patients with PACs and fibrosis, although no significant difference was found between these patients and nonfibrotic group (70.4% versus 66.2%, resp.).

In some previous studies, grading systems were used to analyze relationships between the presence or morphologic features of PACs and the severities of emphysema or bronchiectasis [6, 7]. In another study, focus was placed on the association between the presence of fibrosis and PACs [4]. In the present study, we modified a previously described semiquantitative fibrosis scoring system to evaluate the presence and progression of lung fibrosis [21] and to determine whether increases in PAC sizes and the progression of upper lobe fibrosis are relevant. Although the mean fibrosis score

of patients with PACs was higher than those without PACs, no significant difference was found (3.53 ± 3.10 versus 3.35 ± 2.34, resp.). However, we did find a significant relationship between the progression of fibrosis and an increase in PAC size by both univariable and multivariable analysis. The incidence rate in patients that exhibited upper lung fibrosis progression was 2.921 times higher in those that showed an increase in PAC size than in those that did not. Our results tend to support PACs have an acquired etiology, that is, probably mucosal herniation due to difficulties in expiration associated with chronic inflammation, and indicate upper lung fibrosis contributes to the development of PACs. In the present study, there were 15 newly developed PACs during intervening period. High rates of the presence (86.7%) and progression of upper lung fibrosis (84.6%) with newly developed PACs also suggested that fibrosis play an important role in the occurrence of PACs.

This study had several limitations. First, it is limited by its retrospective nature. In particular, histopathological and bronchoscopic results were not obtained because PACs are an incidental CT finding. Second, diagnoses of upper lung fibrosis, bronchiectasis, and emphysema were based on CT alone and were not confirmed by histopathologic results and pulmonary function tests. Third, because our study group included patients with variable symptoms that underwent thoracic CT, it might be argued that our results better represent the general population. On the other hand, our study subjects better reflected daily practice.

## 5. Conclusions

PACs were found to be positively correlated with age and to show a slight female preponderance. The presence of PACs and upper lung fibrosis were observed to be highly related, and we also observed a borderline association between the presence of PACs and bronchiectasis. In addition, the increase of PAC sizes and the progression of upper lung fibrosis were a significant correlation.

## Ethical Approval

An appropriate institutional review board approved the study (for studies involving human subjects or animals).

## Disclosure

The study sponsor had no involvement in the conduct of the study or in the writing of the article.

## Conflicts of Interest

The authors declare that there are no conflicts of interest regarding the publication of this paper.

## Acknowledgments

This work was supported by Inha University Research Grant.

## References

[1] A. V. Polat, M. Elmali, R. Aydin, A. Ozbay, C. Celenk, and N. Murat, "Paratracheal air cysts: prevalence and correlation with lung diseases using multi-detector CT," *Journal of Medical Imaging and Radiation Oncology*, vol. 58, no. 2, pp. 144–148, 2014.

[2] H.-M. Cheng, P.-Y. Chang, K.-H. Chiang, H.-W. Huang, and C.-C. Lee, "Prevalence and characteristics of paratracheal air cysts and their association with emphysema in a general population," *European Journal of Radiology*, vol. 81, no. 10, pp. 2673–2677, 2012.

[3] J. E. Buterbaugh and W. K. Erly, "Paratracheal air cysts: A common finding on routine CT examinations of the cervical spine and neck that may mimic pneumomediastinum in patients with traumatic injuries," *American Journal of Neuroradiology*, vol. 29, no. 6, pp. 1218–1221, 2008.

[4] E. N. Unlu, E. G. Balbay, M. Boran, M. A. Sungur, A. Buyukkaya, and A. A. Safak, "Is there a relationship between paratracheal air cysts and upper lobe fibrosis?" *Journal of Computer Assisted Tomography*, vol. 40, no. 2, pp. 256–260, 2016.

[5] J. M. Goo, J.-G. Im, J. M. Ahn et al., "Right paratracheal air cysts in the thoracic inlet: clinical and radiologic significance," *American Journal of Roentgenology*, vol. 173, no. 1, pp. 65–70, 1999.

[6] H.-J. Bae, E.-Y. Kang, H. S. Yong et al., "Paratracheal air cysts on thoracic multidetector CT: incidence, morphological characteristics and relevance to pulmonary emphysema," *British Journal of Radiology*, vol. 86, no. 1021, 2013.

[7] N. Boyaci, D. Sen Dokumaci, E. Karakas, F. Yalcin, and A. G. Oney Kurnaz, "Paratracheal air cysts: prevalence and relevance to pulmonary emphysema and bronchiectasis using thoracic multidetector CT," *Diagnostic and Interventional Radiology*, vol. 21, no. 1, pp. 42–46, 2015.

[8] J. S. Kim, A.-Y. Kim, and Y. Yoon, "Paratracheal air cysts using low-dose screening chest computed tomography: clinical significance and imaging findings," *Japanese Journal of Radiology*, vol. 29, no. 9, pp. 644–648, 2011.

[9] K. Oda, H. Ishimoto, K. Yatera et al., "High-resolution CT scoring system-based grading scale predicts the clinical outcomes in patients with idiopathic pulmonary fibrosis," *Respiratory Research*, vol. 15, no. 1, article 10, 2014.

[10] N. Enomoto, H. Kusagaya, Y. Oyama et al., "Quantitative analysis of lung elastic fibers in idiopathic pleuroparenchymal fibroelastosis (IPPFE): comparison of clinical, radiological, and pathological findings with those of idiopathic pulmonary fibrosis (IPF)," *BMC Pulmonary Medicine*, vol. 14, no. 1, article 91, 2014.

[11] A. Oikonomou, P. Mintzopoulou, A. Tzouvelekis et al., "Pulmonary fibrosis and emphysema: is the emphysema type associated with the pattern of fibrosis?" *World Journal of Radiology*, vol. 7, no. 9, pp. 294–305, 2015.

[12] M. K. Lee, E. Y. Kim, Y. M. Jeong, J. H. Kim, and H.-Y. Choi, "Paratracheal air cysts are uncommon findings in the pediatric population," *Japanese Journal of Radiology*, vol. 34, no. 8, pp. 579–584, 2016.

[13] A. Tanrivermis Sayit, M. Elmali, D. Saglam, and C. Celenk, "The diseases of airway-tracheal diverticulum: a review of the literature," *Journal of Thoracic Disease*, vol. 8, no. 10, pp. E1163–E1167, 2016.

[14] S. Han, E. Dikmen, S. Aydin, and O. Yapakci, "Tracheal diverticulum: a rare cause of dysphagia," *European Journal of Cardio-thoracic Surgery*, vol. 34, no. 4, pp. 916–917, 2008.

[15] E. J. Soto-Hurtado, L. Peñuela-Ruíz, I. Rivera-Sánchez, and J. Torres-Jiménez, "Tracheal diverticulum: a review of the literature," *Lung*, vol. 184, no. 6, pp. 303–307, 2006.

[16] R. Polverosi, A. Carloni, and V. Poletti, "Tracheal and main bronchial diverticula: the role of CT," *Radiologia Medica*, vol. 113, no. 2, pp. 181–189, 2008.

[17] Y. Oshiro and S. Murayama, "Subcarinal air cysts: multidetector computed tomographic findings," *Journal of Computer Assisted Tomography*, vol. 34, no. 3, pp. 402–405, 2010.

[18] T. Higuchi, N. Takahashi, M. Shiotani, H. Maeda, and N. Yoshimura, "Characteristics and CT features of subcarinal air collections/main bronchial diverticula," *European Radiology*, vol. 20, no. 1, pp. 95–99, 2010.

[19] J. H. Kim and J.-J. Yim, "Achievements in and challenges of tuberculosis control in South Korea," *Emerging Infectious Diseases*, vol. 21, no. 11, pp. 1913–1920, 2015.

[20] H. Y. Kim, K.-S. Song, J. M. Goo, J. S. Lee, K. S. Lee, and T.-H. Lim, "Thoracic sequelae and complications of tuberculosis," *RadioGraphics*, vol. 21, no. 4, pp. 839–858, 2001.

[21] D. Assayag, S. Kaduri, M. Hudson, A. Hirsch, and M. Baron, "High resolution computed tomography scoring systems for evaluating interstitial lung disease in systemic sclerosis patients," *Rheumatology: Current Research*, supplement 1, article 003, 2012.